

Development, structure, and maintenance of *C. elegans* body wall muscle*

Kathrin Gieseler¹, Hiroshi Qadota², and Guy M. Benian^{2§}

¹Institute NeuroMyoGene, CNRS UMR5310, INSERM U1217, Universite Claude Bernard Lyon 1, 69622 Villeurbanne, France

² Department of Pathology, Emory University, Atlanta, GA 30322

Table of Contents

1.	Introduction.....	2
2.	Transcriptional network regulating muscle differentiation.....	5
3.	Building muscle adhesion complexes (M-lines and dense bodies).....	7
3.1.	Introduction.....	7
3.1.1.	Identification of M-line and dense body components.....	7
3.1.2.	Assembly of integrin adhesion complexes.....	8
3.2.	Differential localization of M-line and dense body proteins.....	12
3.3.	Dynamics of muscle adhesion proteins.....	13
3.4.	Multiple protein complexes link integrin to myosin in thick filaments at the M-line.....	14
3.5.	M-line proteins and paramyosin.....	15
3.6.	Novel methods to study muscle proteins and phenotypes.....	15
3.7.	Nuclear functions for muscle adhesion proteins?.....	18
3.8.	Newly identified muscle components—ready for further analysis.....	20
4.	Regulation of the assembly and maintenance of the sarcomere by chaperones and proteases.....	21
4.1.	Chaperones.....	21
4.1.1.	UNC-45—discovery of a conserved myosin head chaperone.....	21
4.1.2.	UNC-23, a chaperone regulator.....	24
4.1.3.	HSP-25.....	24
4.2.	The ubiquitin/proteasome system and calpains.....	25
4.2.1.	The ubiquitin/proteasome system.....	25
4.2.2.	Calpains are required for the proper assembly and maintenance of muscle adhesion complexes.....	25
5.	Roles of giant kinases in regulation of contraction and sarcomere organization.....	26
5.1.	Introduction.....	26
5.2.	Twitchin: the structure of the kinase domain and question of its activation.....	27
5.3.	TTN-1: a twitchin/titin hybrid in the I-band.....	29
5.4.	UNC-89: a scaffold for multiple proteins at the M-line.....	30
6.	New insights into dystrophin function from <i>C. elegans</i>	33
6.1.	Structure and localization of the DYS-1 protein.....	33
6.2.	The function of DYS-1 and the DGC in cholinergic transmission and calcium homeostasis.....	34
6.3.	The function of DYS-1 in dense body and sarcolemma integrity.....	36
6.4.	How does the <i>hlh-1(cc561)</i> mutation contribute to muscle degeneration?.....	38
7.	Conclusion.....	39
8.	Table 1 and Table 2.....	39
9.	Acknowledgements.....	44
10.	References.....	44

*Edited by Michel Labouesse. Last revised June 25, 2016. Published August 23, 2016. This chapter should be cited as: Gieseler, K., Qadota, H., and Benian, G.M. Development, structure, and maintenance of *C. elegans* body wall muscle (August 23, 2016), WormBook, ed. The *C. elegans* Research Community, WormBook, doi/10.1895/wormbook.1.81.2, <http://www.wormbook.org>.

§To whom correspondence should be addressed: E-mail: pathgb@emory.edu

Abstract

In *C. elegans*, mutants that are defective in muscle function and/or structure are easy to detect and analyze since: 1) body wall muscle is essential for locomotion, and 2) muscle structure can be assessed by multiple methods including polarized light, electron microscopy (EM), Green Fluorescent Protein (GFP) tagged proteins, and immunofluorescence microscopy. The overall structure of the sarcomere, the fundamental unit of contraction, is conserved from *C. elegans* to man, and the molecules involved in sarcomere assembly, maintenance, and regulation of muscle contraction are also largely conserved. This review reports the latest findings on the following topics: the transcriptional network that regulates muscle differentiation, identification/function/dynamics of muscle attachment site proteins, regulation of the assembly and maintenance of the sarcomere by chaperones and proteases, the role of muscle-specific giant protein kinases in sarcomere assembly, and the regulation of contractile activity, and new insights into the functions of the dystrophin glycoprotein complex.

1. Introduction

The nematode *Caenorhabditis elegans* has long been used to study muscle development, organization and function (Waterston, 1988; Moerman and Fire, 1997; the WormBook chapter [Sarcomere assembly in *C. elegans* muscle](#)). *C. elegans* has striated and non-striated muscles. Non-striated muscles include 20 pharyngeal muscle cells, 2 stomatointestinal muscles, one anal depressor muscle, one anal sphincter muscle, 8 vulval muscles, 8 uterine muscles, and 10 contractile gonadal sheath cells (<http://www.wormatlas.org/hermaphrodite/musclenonstriated/mainframe.htm>). Most studies, however, have been performed on the 95 striated body wall muscle cells. These muscles are the functional equivalents of vertebrate skeletal muscles. The overall structure, composition, and function of the muscle basic functional unit, the sarcomere, is highly conserved between nematodes and vertebrates. Functional body wall muscle is required for the sinusoidal movement on semi-solid surfaces or the c-shaped thrashing of *C. elegans* in liquid. The optical transparency of the nematode allows visualization of muscle structure by polarized light microscopy, or fluorescence microscopy using GFP tagged proteins in live animals. Self-fertilization allows propagation of mutants that are unable to mate. Powerful forward and reverse genetics allows isolation and analysis of mutants in individual muscle components. All of these advantages have permitted research using *C. elegans* to make landmark discoveries for muscle in general, some of which are listed in **Table 1**, Section 8.

As in vertebrates, each sarcomere is composed of myosin containing thick filaments associated with an M-line, and actin containing thin filaments associated with a Z-disk analog named the dense body. The pulling of actin filaments by myosin heads generates force. To generate movement, the produced force needs to be transduced outside the muscle cell. In vertebrates, this force transduction is ensured by: 1) anchoring sarcomeres to the sarcolemma by specific muscle adhesion complexes, called costameres, that link Z-disks to the extracellular matrix (ECM) (Ervasti, 2003: PMID 12556452; Samarel, 2005: PMID 16284104); 2) by having all the myofibrils in a given cell mechanically linked by intermediate filaments; and 3) by the anchoring of the muscle ends through tendons to the bones. In *C. elegans*, M-lines and dense bodies directly perform the attachment of sarcomeres to the muscle membrane and the underlying basement membrane (**Figure 1**). These integrin based protein complexes thus share functional similarity with both the vertebrate Z-disk/ M-line and the costamere. In addition, the muscles are linked via fibrous organelles in the hypodermis to the underlying cuticle, the exoskeleton of the nematode (Cox and Hardin, 2004: PMID 15090594). Contractile filaments form a layer anchored to the distal sarcolemma of each cell (Figure 1). The striation observed by microscopy corresponds to the repetition of myosin-enriched A bands and actin-enriched I bands in alignment. While vertebrates exhibit cross-striated muscles, striation in *C. elegans* muscles appears slightly oblique with respect to the longitudinal axis of the muscle cell with which it forms an angle of 5.9° (MacKenzie and Epstein, 1980: PMID 7193096) (Figure 1).

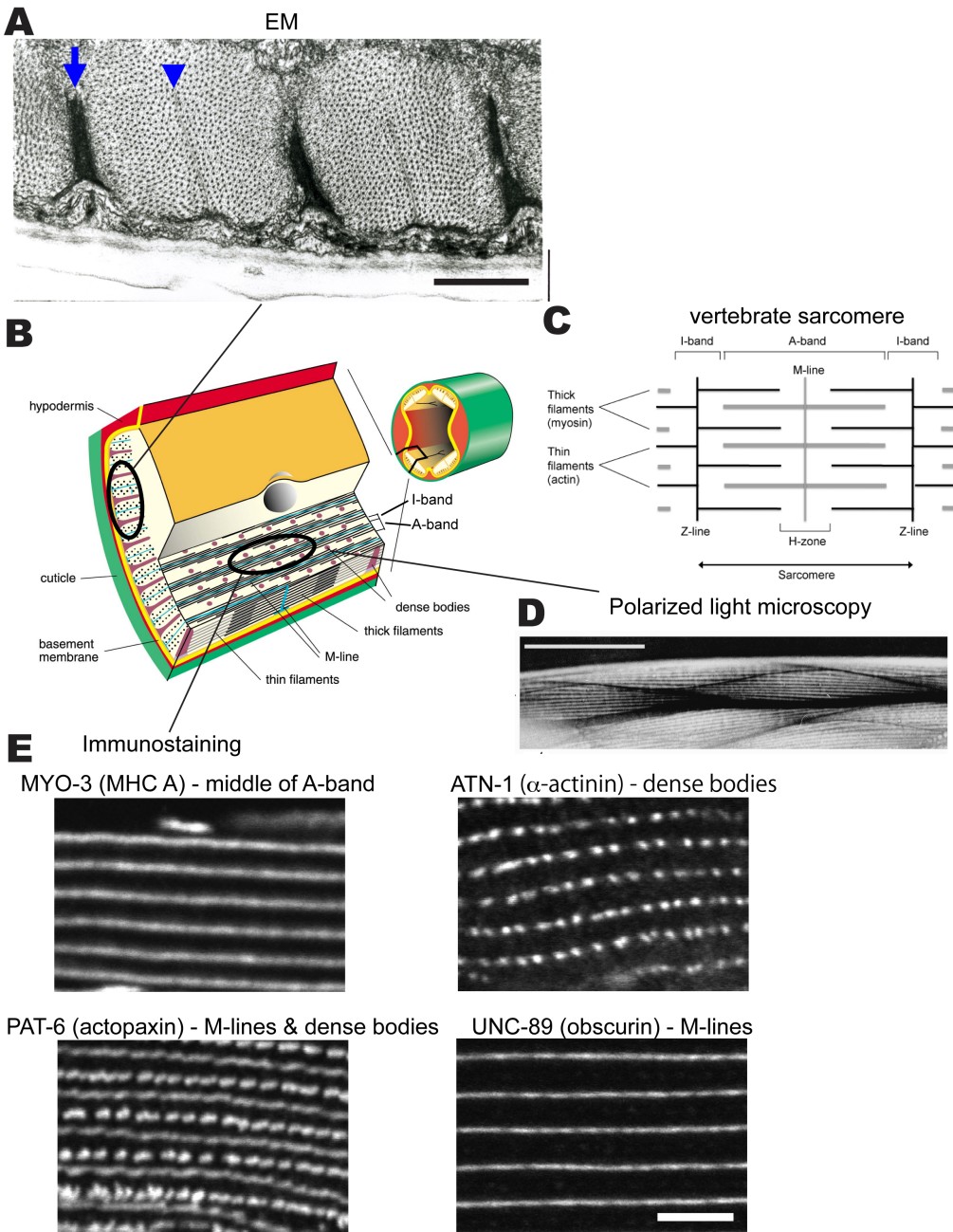


Figure 1. The body wall muscle of *C. elegans*. (A) Transmission electron microscopy (EM) of a cross-section of a body wall muscle cell showing two full sarcomeres. An arrow points to a dense body and an arrowhead points to an M-line. The largest black dots are cross sections of thick filaments in the A-bands; the smallest dots are cross sections of thin filaments in the I-bands (surrounding the dense bodies). Note that all the dense bodies and the M-lines are anchored to the muscle cell membrane, which sits on top of a basement membrane, a thin hypodermis, and thick cuticle. A diagonal line indicates how the EM view is related to the drawing in (B). Scale bar, 1 μ m. (B) The small drawing on the right shows a cross-section through an adult worm emphasizing that the body wall muscle consists of four quadrants. Each quadrant consists of interlocking pairs of mononuclear spindle-shaped cells (23 or 24 per quadrant). In the enlargement, note that the myofilament lattice is limited to one side of the cell rather than filling the entire cross-sectional area as in a vertebrate striated muscle cell. Several planes of section are depicted, one of which emphasizes the muscle's striated organization with typical A-bands containing thick filaments organized around M-lines, and overlapping thin filaments probably attached to Z-disk-like structures called dense bodies. The sarcomere, which is defined as the repeating distance from one dense body to the next dense body is approximately 12 μ m in adult muscle. Note that the plane of section parallel to the page is the plane viewed when an animal crawls on agar or is placed on a slide and examined by light microscopy (note the lines to the polarized light view in (D) and immunostaining views in (E)). (C) A drawing of a typical sarcomere in vertebrate striated muscle. The sarcomere, which is defined as the repeating distance from one Z-line to the next Z-line is typically 2.2-2.5 μ m. (D) Polarized light microscopy on a live nematode of portions of two muscle quadrants, each containing interlocking pairs of spindle shaped cells. The parallel white lines are A-bands, which alternate with parallel dark lines that are I-bands. Scale bar, 10 μ m. (E) Immunofluorescent localizations of several sarcomeric proteins in adult muscle, MYO-3 (myosin heavy chain A, MHC A) localized to the middle of the A-bands; ATN-1 (α -actinin) localized to dense bodies; UNC-89 (obscurin) localized to M-lines; and PAT-6 (actopaxin) localized to both M-lines and dense bodies. Scale bar, 10 μ m.

Most body wall muscle cells develop during embryogenesis. At hatching 81 muscle cells have formed; 14 muscle cells develop post-embryonically (Krause, 1995: PMID 7748176; Moerman and Fire, 1997: PMID 21413235). At the L1 larval stage muscle cells are 2 sarcomeres wide (Figure 2). During larval development new sarcomeres are added, resulting in adult cells that contain up to 10 sarcomeres in mid-body body wall muscle cells and smaller numbers of sarcomeres in body wall muscle cells at the ends of the animal (see WormBook chapter [Sarcomere assembly in *C. elegans* muscle](#)) (Figure 2). M lines and dense bodies also increase in size during post-embryonic development. In adult muscles, the layer of the contractile apparatus, which is approximately 1.5 μm thick, is parallel to the hypodermis and the cuticle. Cellular organelles such as the nucleus, mitochondria, endoplasmic reticulum, ribosomes, etc. are localized in the deeper part of the muscle cell (Figure 1 and Figure 2).

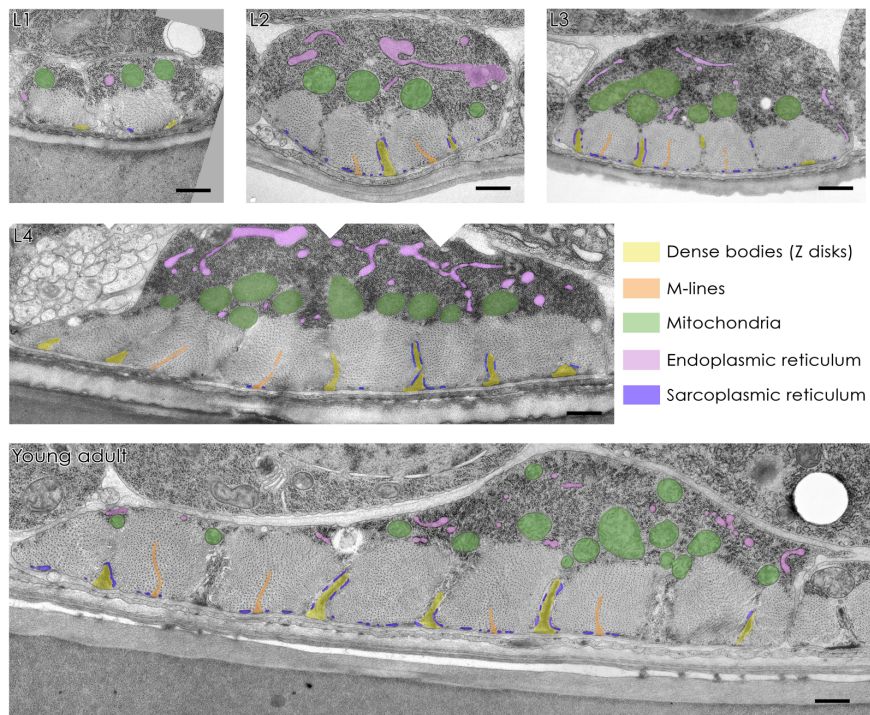


Figure 2. Muscle development observed by transmission EM. Electron micrographs are representative of muscle cells from wild type L1, L2, L3, and L4 larvae and young adults. All images were identically orientated with the cuticle at the bottom. Pseudo coloring indicates dense bodies (yellow), M-lines (orange), mitochondria (green), endoplasmic reticulum (pink), and sarcoplasmic reticulum (blue) localized around the dense bodies. Scale bars correspond to 0.5 μm in L1 to L4, and 0.2 μm in young adults. Figure adapted by N. Brouilly et al., 2015: PMID 26358775.

Some striking differences between nematodes and vertebrates make striated body wall muscles of adult *C. elegans* a tissue of choice to analyze cellular processes such as proteotoxicity, autophagy and mitophagy, mitochondrial biology, signaling pathways involving cell adhesion complexes, aging, and muscle degeneration. *C. elegans* muscles lack satellite cells (muscle stem cells) and therefore muscle regeneration. In adult worms, body wall muscles are totally post-mitotic, do not fuse and remain mononucleated. The adult worm possesses 95 diamond-shaped body wall muscle cells, which form a single layer of cells and are arranged in four longitudinal bands of two mutually offset rows of cells, named quadrants, running from head to tail. (<http://wormatlas.org/hermaphrodite/musclesomatic/MusSomaticframeset/html>). Together, these properties allow bypassing the complexities that arise from the syncytial nature of skeletal muscle of vertebrates.

Finally, it should be noted that, for practical reasons, we could not cover all of the interesting and important topics in nematode muscle. One major topic that is missing in our review is the role of actin regulatory proteins (e.g., UNC-60B (ADF/cofilin), UNC-78 (AIP1)) in sarcomere assembly and function. However, this subject has been expertly covered in a recent review by Ono (2014: PMID 25125169). We also do not discuss the effects of micro/zero gravity on muscle structure and function. Our review is primarily focused on sarcomere assembly and maintenance, rather than on the regulation of contractility. We do not fully discuss the role of K⁺ channels such as UNC-93/SUP-9/SUP-10, or BK channels, or Ca⁺⁺ channels, although we do discuss the possible role of twitchin (UNC-22) in regulating contractility.

2. Transcriptional network regulating muscle differentiation

The 81 body wall muscle cells present in L1 larvae at hatching are derived from 4 of 5 founder blastomeres: one from AB, 28 from MS, 32 from C, and 20 from D. The germline founder cell, P4, does not produce any muscle cells. The D lineage produces exclusively body wall muscle cells, but other founder lineages produce multiple cell fates. Maternal factors that determine founder cell fate affect numerous body wall muscle cells. In *skn-1* mutants, 28 body wall muscle cells that derived from MS are absent, but body wall muscle cells from C and D lineages are not affected (Bowerman et al., 1992: PMID 1547503; Bowerman et al., 1997: PMID 9367437). *pal-1* mutants lack the body wall muscle cells from C and D lineages, but those from MS lineage are not affected (Hunter and Kenyon, 1996: PMID 8861906; Ahringer, 1997: PMID 9367442).

Embryonic development is controlled by maternally expressed genes initially, but then there is a switch to control by zygotically expressed genes (Baugh and Hunter, 2006: PMID 17182863). In the C and D lineages at least, *pal-1* initially acts as a maternal factor for body wall muscle cell fate (Hunter and Kenyon, 1996: PMID 8861906; Edgar et al., 2001: PMID 11133155). *pal-1* encodes a Caudal-related homeobox transcription factor (Hunter and Kenyon, 1996: PMID 8861906) and the maternal function of *pal-1* is determination of C and D lineages; zygotically expressed *pal-1* is directly involved in muscle differentiation. Over-expression of *pal-1* triggers robust muscle cell differentiation in the absence or reduced levels of POP-1 (TCF), the downstream transcriptional factor of Wnt/MAP kinase signaling. In the presence of high levels of POP-1 (TCF), over-expression of *pal-1* produces robust hypodermal cells (Fukushige and Krause, 2005: PMID 15772130).

Myogenic regulatory factors (MRFs), first characterized in mammalian muscle, have also been characterized by genetic and molecular biological approaches in *C. elegans* (Moerman and Fire, 1997: PMID 21413235). *hlh-1* encodes the *C. elegans* ortholog of MyoD and is the single MRF-related factor in *C. elegans*. Its alternative name, HLH-1, derives from having a basic helix-loop-helix domain (Krause et al., 1990: PMID 2175254). *hlh-1* is expressed zygotically in embryonic body wall muscle precursor cells from about the 90 cell stage (Krause et al., 1990: PMID 2175254). *hlh-1* null mutants stop development at the L1 larval stage with paralysis and severe morphological defects, suggesting essential roles of HLH-1 in development. However, in *hlh-1* null mutant animals, the 81 embryonic body wall muscle cells are produced (Chen et al., 1992: PMID 1314423; Chen et al., 1994: PMID 8050369). These observations suggest that *hlh-1* is important for development but not essential for myogenic differentiation, and that one or more other factors are involved in muscle differentiation. Ectopic expression experiments revealed that HLH-1 is a potent myogenic factor (Fukushige and Krause, 2005: PMID 15772130). When *hlh-1* is ubiquitously expressed by a heat shock promoter in early embryos almost all cells adopt a muscle cell fate. Interestingly, although the cells that follow the muscle fate express many muscle markers, including structural attachment components (e.g., PAT-3 (b-integrin) and UNC-89 (obscurin)), there is no sarcomere assembly. The authors suggest that since the conversion to muscle fate abolishes other tissue fates, sarcomere assembly might require the presence of other tissues (e.g., the hypodermis) (Fukushige and Krause, 2005: PMID 15772130).

Over-expression of *pal-1*, which encodes maternal and zygotic factor functions in the C and D lineages, also converts embryonic cells to the muscle cell fate, and this conversion is not dependent on *hlh-1*, also suggesting that other factors independent from *hlh-1* are involved in muscle differentiation (Fukushige and Krause, 2005: PMID 15772130). Microarray data suggest that two additional transcriptional factors, UNC-120 and HND-1, are involved in body wall muscle differentiation (Fukushige et al., 2006: PMID 17142668). First, *unc-120* encodes a serum response factor (SRF)-related protein, and is induced by PAL-1 and HLH-1 (Dichoso et al., 2000: PMID 10882527; Baugh et al., 2005: PMID 15892873; Fukushige et al., 2006: PMID 17142668). Second, HND-1, which is closely related to mammalian HAND family basic helix-loop-helix proteins, is induced by PAL-1, but not by HLH-1 (Mathies et al. 2003: PMID 12756172; Fukuhige et al., 2006: PMID 17142668). Ectopic expression of either *unc-120* or *hnd-1* also results in cells adopting the muscle cell fate (albeit less efficiently than when *hlh-1* is ectopically expressed) including expression of muscle markers, suggesting that both transcriptional factors are also myogenic. Cells adopting a muscle cell fate occur by ectopic expression of HND-1 even in an *hlh-1* null mutant background.

Muscle cell fates can also be induced by ectopic expression of UNC-120, and although this does not require *hlh-1*, the presence of *hlh-1* increases the expression of muscle cell markers in these cells. An *hlh-1*, *hnd-1*, *unc-120* triple mutant produces no body wall muscle cells in embryos, suggesting that these three transcriptional factors are required together for body wall muscle differentiation (Fukushige et al., 2006: PMID 17142668). Genetic analysis revealed that *hlh-1* and *hnd-1* are redundant, and that *hlh-1* and *unc-120* cooperate and maintain their expression until the late embryonic stage (Figure 3A). The PAL-1 protein directly binds to upstream enhancer regions of *hlh-1* and *unc-120* and activates their expression (Lei et al., 2009: PMID

19261701). The binding of HLH-1 to an upstream enhancer region of the *hh-1* gene makes the positive auto-regulation of *hh-1* possible (Krause et al., 1994; PMID 7958441) (Figure 3B). Target genes for HLH-1 have been identified; 2,753 by ChIP-seq, and 1,032 by ChIP-Chip (Lei et al., 2010; PMID 21209968). An overlapping set of 569 target genes was identified by both methods. Future analysis of these genes will hopefully clarify the transcriptional network that is regulated by HLH-1. It is interesting to note that Meissner et al. (2009; PMID 19557190) identified a total of 3,577 genes expressed in body wall muscle by SAGE (Serial Analysis of Gene Expression) and microarray data. Among the 2,753 genes identified as targets of HLH-1 by ChIP-seq, 880 genes are found in the Meissner set; among the 1,032 genes identified as targets of HLH-1 by ChIP-chip, 282 are found in the Meissner set. Among the 569 genes identified by both ChIP methods, 194 are also found in the 3,577 genes identified by Meissner et al. (2009; PMID 19557190).

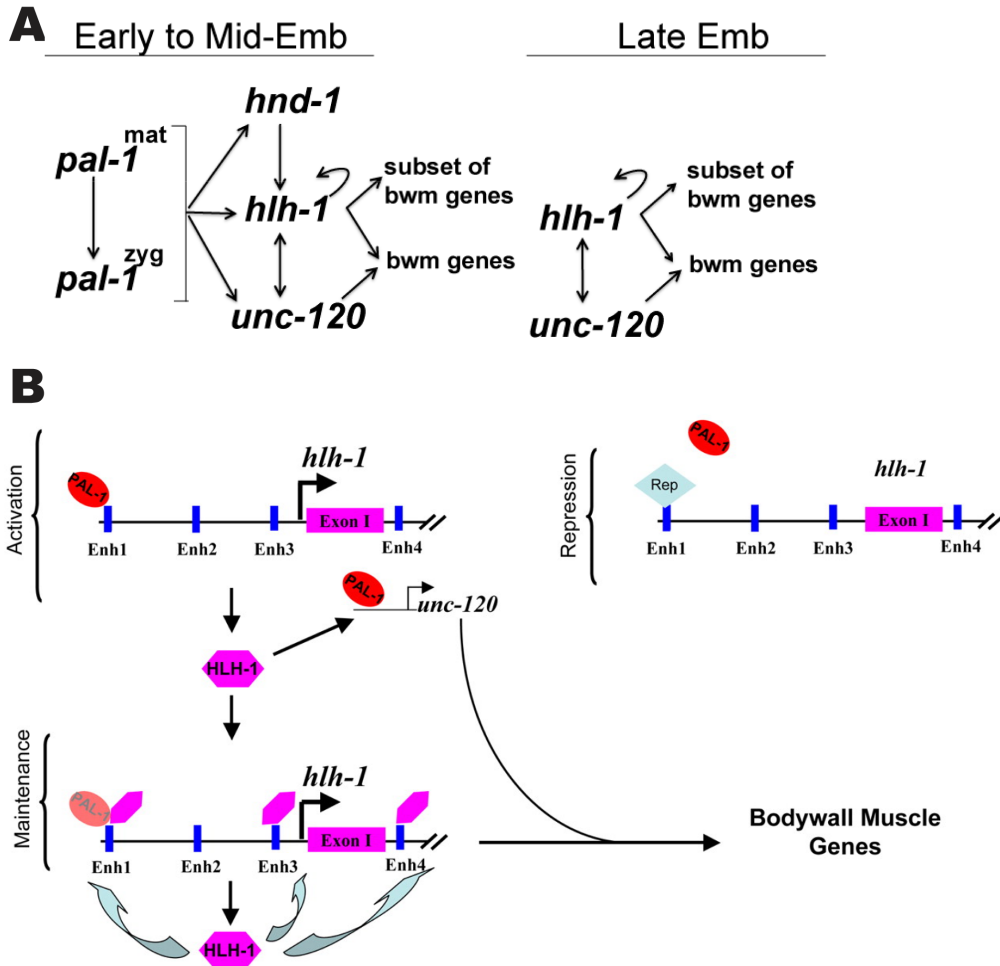


Figure 3. Transcriptional regulation of body wall muscle cells in the C and D founder cell lineages of *C. elegans* embryos. (A) Arrows indicate genetic relationships. Maternal and zygotic PAL-1 activates expression of HLH-1, UNC-120, and HND-1. All three transcription factors are involved in cell fate determination of body wall muscle. HLH-1 and UNC-120 continue to express until late embryonic stage. (Adapted, with permission, from Fukushige et al., 2006; PMID 17142668). (B) A model for activation of muscle-expressing genes by PAL-1. PAL-1 binds to enhancer regions of *hh-1* and possibly *unc-120*. HLH-1 binds to multiple enhancer regions of *hh-1* itself, resulting in positive auto-regulation. HLH-1 also binds to an enhancer region of *unc-120* and activates its expression. (Adapted, with permission, from Lei et al., 2009; PMID 19261701).

In addition to being expressed in embryos, *hh-1* continues expression in mature body wall muscle cells including in adults (Krause et al., 1994; PMID 7958441; our unpublished results). This suggests that HLH-1 has a role in promoting the continued development of larval and adult muscle, and perhaps even maintenance of adult muscle.

In vertebrate muscle differentiation, MRFs cooperate with other transcription factors, such as MEF-2 and Twist. In *C. elegans*, the MEF-2 ortholog is not essential for myogenesis (Dichoso et al., 2000; PMID 10882527). However, it should be noted that MEF-2, like UNC-120, is related to SRF and it could be that nematodes became reliant on UNC-120 (SRF), whereas other animals became reliant on MEF-2. The *C. elegans*

Twist homolog, HLH-8, is expressed in mesodermal tissues (M cell lineage) (Harfe et al., 1998: PMID 9716413). *hlh-8* null mutants have egg-laying and defecation defects. Corresponding to this phenotype, in *hlh-8* null mutants sex muscle and defecation muscles are not formed properly: vulval muscles are missing, and 5% of the animals have fewer, and 60% have extra sex myoblasts. In *hlh-8* nulls, although the overall organization of body wall muscle is normal, the number of postembryonic body wall muscle cells is different: 15% of the animals have extra body wall muscle cells (96-100 cells), and 80% have fewer body wall muscle cells (86-94 cells) (Corsi et al., 2000: PMID 10769229).

3. Building muscle adhesion complexes (M-lines and dense bodies)

3.1. Introduction

3.1.1. Identification of M-line and dense body components

The first success in identifying muscle attachment components came from an immunological approach. Francis and Waterston (Francis and Waterston, 1985: PMID 2413045; Francis and Waterston, 1991: PMID 1860880) used protein fractions enriched in nematode body wall muscle components to generate a battery of monoclonal antibodies and then determined their staining patterns in nematodes and their Western blot reactivity. These monoclonal antibodies recognized many components of muscle and hypodermis attachment structures, and the extracellular matrix.

Identification of the genes involved began with the identification of *myo-3*, the gene encoding body wall muscle myosin heavy chain A (MHC A) (Waterston, 1989: PMID 2583106). Body wall muscle contains two myosin heavy chain isoforms, MHC A and MHC B (Epstein et al., 1974: PMID 4453018; Miller et al., 1983: PMID 6352051). These isoforms form homodimers (Schachat et al., 1978: PMID 82486) and are differentially localized in the 10 mm long adult thick filaments, with MHC A lying in the central 2 mm, and MHC B lying in the polar 4 mm of the thick filament (Miller et al. 1983: PMID 6352051). *unc-54*, which encodes myosin heavy chain B (MHC B), was first identified genetically (Epstein et al., 1974: PMID 4453018) while the other 3 myosin heavy chain genes expressed in muscle, including *myo-3*, were first identified through sequence homology (Miller et al., 1986: PMID 2422655). *unc-54* null mutant animals show reduced movement at all stages and as adults are unable to move on an agar surface. Although duplication and two-fold overexpression of *myo-3*, was identified as a suppressor (called *sup-3*) of *unc-54* null animals (Riddle and Brenner, 1978: PMID 669254; Maruyama et al., 1989: PMID 2575705), the loss-of-function phenotype for *myo-3* was not known. The two genes, *unc-54* and *myo-3* are of equivalent size, and while many alleles of *unc-54* had been identified, none had been identified for *myo-3*. This led [Bob Waterston](#) to wonder if *myo-3* loss-of-function (lof) might be lethal. He designed a screen for lethal mutations linked to *sma-1*, as *myo-3* had been localized close to this gene by *in situ* hybridization (Albertson, 1985: PMID 4054096). He obtained multiple lethal mutants that arrested at different developmental stages, two of which bore similarity to certain *unc-54* dominant alleles when homozygous. Both of the candidate mutations failed to complement and sequencing revealed point mutations in the *myo-3* gene (Waterston, 1989: PMID 2583106). The *myo-3* mutant embryos stopped elongation at the 2-fold stage and showed greatly reduced or no movement in the eggshell although other aspects of development including pharyngeal pumping and cuticle deposition were normal; the embryos hatched, remained in a folded state, did not move, and died.

Soon after the discovery of the *myo-3* phenotype, it was shown that strong loss-of-function alleles for the *unc-45* gene display a similar embryonic lethal phenotype (Venolia and Waterston, 1990: PMID 2245914). Using two of the aforementioned antibodies developed by Francis and Waterston (1985: PMID 2413045), which recognize proteins localized to the base of dense bodies, Barstead and Waterston (1989: PMID 2498337) screened an expression library, and pulled out cDNAs specifying *C. elegans* vinculin, encoded by the *deb-1* gene. After placing *deb-1* on the genetic map, a screen was conducted for loss-of-function mutations (Barstead and Waterston, 1991: PMID 1907975). Two mutants in *deb-1* were shown to be embryonic lethal and displayed the same phenotype that was first identified for loss-of-function mutations in the *myo-3* gene (Waterston, 1989: PMID 2583106).

The phenotype of loss-of-function alleles consistent with a null state for *myo-3*, *unc-45* and *deb-1* is “Pat”, which is an abbreviation for paralyzed and arrested at two-fold embryonic stage. During normal nematode embryonic development there is both an expansion of cell number and morphogenesis in which the initially football-shaped embryo elongates 4-fold, going through stages that are named according to length, 1.5-fold, 2-fold, and 3-fold, before hatching from the eggshell. At the ~1.5-fold stage, embryonic muscle contraction begins and the embryos continue to move within the eggshell throughout the remainder of embryogenesis. Pat

embryos do not move in the eggshell at the 1.5-fold stage (or later) and arrest development at the 2-fold stage. Other aspects of development continue and the embryo hatches as an abnormal “jack knife”-appearing L1 larva and dies.

3.1.2. Assembly of integrin adhesion complexes

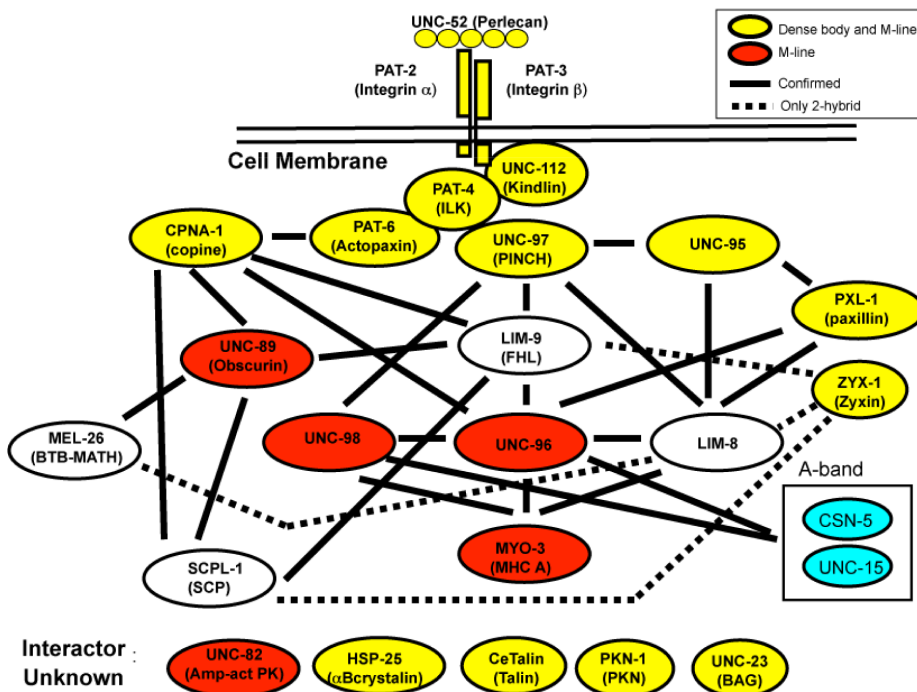
Encouraged by findings of Pat phenotypes for *myo-3*, *deb-1*, and *unc-45*, Williams and Waterston (1994: PMID 8106547) conducted a genome-wide screen and identified 13 additional genes with a Pat mutant phenotype, and new alleles of *deb-1* and *myo-3*. Three classes of Pat mutants were isolated, based on severity of paralysis in the eggshell: severe Pat mutants were similar to the original *myo-3* and *deb-1* mutants; “Mild Pat” mutants (*pat-11*, *pat-12*), in which movement began at the 1.5 fold stage but did not show the vigorous movement at the 2 fold stage; and “Lat” mutants (late paralysis, arrested elongation at two fold) (*let-2*, *emb-9*), in which movement began at the 1.5 fold stage and continued vigorously, as in wild type, through the 2 fold stage. The Pat genes were placed into five classes (I to V in lessening severity), based on the localization and organization of myosin and actin. Class I genes (*unc-52*, *unc-112*, *pat-2*, *pat-3*) showed no localization of myosin or actin near the sarcolemma (lack of “polarization”). Class II genes (*pat-4*, *pat-6*, *pat-11*) showed polarization but no organization of myosin or actin into thick or thin filaments. Class III genes (*deb-1*, *pat-8*, *pat-9*, *pat-12*) showed both normal polarization and thick filaments but no thin filaments. Class IV genes (*lev-11*, *pat-5*, *pat-10*) showed normal polarization and normal thick and thin filaments. Class V consisted of one gene, *myo-3*, and showed normal polarization, normal thin filaments, but no thick filaments. At the time this study was completed, a number of the gene products had been identified: *unc-52* encodes the ECM protein perlecan (Rogalski et al., 1993: PMID 8393416), *pat-3* encodes b-integrin (Gettner et al., 1995: PMID 7744961), and *deb-1* encodes vinculin (Barstead and Waterston, 1989: PMID 2498337). In addition, there was unpublished data cited noting that *pat-2* was likely to encode a-integrin (Gettner et al., 1995: PMID 7744961; see also WormBase [pat-2](#) page). Therefore, the authors proposed that because class I genes have the most severe effects and encode components of the ECM and sarcolemma, sarcomere assembly proceeds from the outside to the inside, initiated by molecules localized at the cell surface at future dense bodies and M-lines. This excellent model was verified by studying the temporal appearance of adhesion and sarcomere components during embryonic muscle development (Hresko et al., 1994: PMID 8106548), and by the subsequent cloning and mutant analysis of the other Pat genes, primarily by the laboratories of [Don Moerman](#) and [Ben Williams](#) (summarized in [Sarcomere assembly in C. elegans muscle](#)).

The other major phenotypic class of muscle-affecting mutant genes is the “Unc” (uncoordinated) class of 40 genes. Mutations in any of these genes result in slow moving or paralyzed adult worms (Waterston et al., 1980: PMID 7190524; Zengel and Epstein, 1980: PMID 7348600). There are a total of 111 Unc genes, but 71 of these genes primarily affect the nervous system, not muscle. For a number of muscle *unc* genes (*unc-45*, *unc-52*, *unc-97*, and *unc-112*), the phenotype of hypomorphic alleles is Unc, and the phenotype of null alleles is Pat. *unc-112* encodes the nematode ortholog of mammalian Kindlins (Rogalski et al., 2000: PMID 10893272; Qadota et al., 2014: PMID 24692564), *pat-4* encodes integrin linked kinase, ILK (Mackinnon et al., 2002: PMID 12015115), and *pat-6* encodes the nematode ortholog of actopaxin (Lin et al., 2003: PMID 12781130). *unc-97* encodes the *C. elegans* ortholog of PINCH (Hobert et al., 1999: PMID 9885243), and the null state for *unc-97* is also Pat (Norman et al., 2007: PMID 17662976). All the above-mentioned *pat* and *unc* gene products, except for *unc-45*, have been localized to both dense bodies and M-lines by GFP fusions (Hobert et al., 1999: PMID 9885243; Rogalski et al., 2000: PMID 10893272; Mackinnon et al., 2002: PMID 12015115: Lin et al., 2003: PMID 12781130), and also in some cases by specific antibodies (Gettner et al., 1995: PMID 7744961; Mullen et al., 1999: PMID 10512861; Lin et al., 2003: PMID 12781130; Hikita et al., 2005: PMID 16055082; Miller et al., 2006: PMID 17158957; Qadota et al., 2012: PMID 22761445; Warner et al., 2013: PMID 23283987).

Yeast two hybrid (Y2H) assays and binding experiments using purified proteins have demonstrated that class I and II Pat gene products interact with each other (Figure 4). Based on what is known about their mammalian orthologs, it is likely that UNC-52 (perlecan) associates with PAT-2 (a-integrin) and PAT-3 (b-integrin) at the extracellular surface of muscle cells (Figure 5). Inside the muscle cell, the cytoplasmic tail of PAT-3 associates directly with UNC-112 (Qadota et al., 2012: PMID 22761445), and PAT-4 associates with UNC-112 (Mackinnon et al., 2002: PMID 12015115), PAT-6 (Lin et al., 2003: PMID 12781130), and UNC-97 (Mackinnon et al., 2002: PMID 12015115; Norman et al., 2007: PMID 17662976). The UNC-112/PAT-4/PAT-6/UNC-97 complex has been confirmed by co-immunoprecipitation (Qadota et al., 2014: PMID 24692564). UNC-52, PAT-2, PAT-3, UNC-112, PAT-4, PAT-6, and UNC-97 are found at the base of both M-lines and dense bodies.

A

At M-lines

**B**

At dense bodies

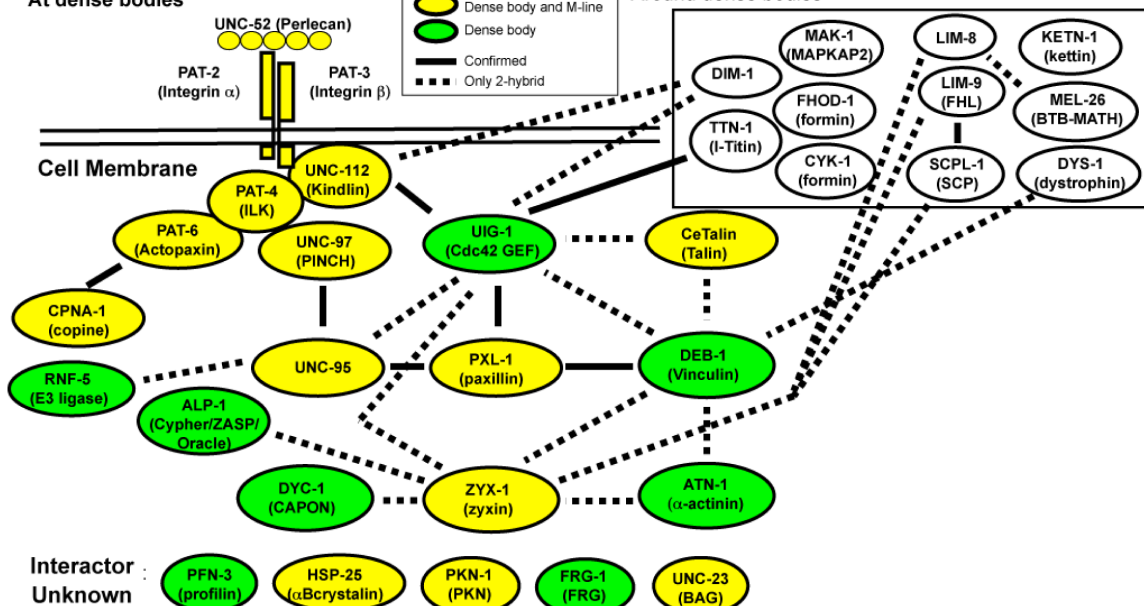


Figure 4. Networks of interacting proteins found at integrin adhesion sites in body wall muscle of *C. elegans*. Yellow denotes proteins that are localized to both M-lines and dense bodies; red denotes proteins that are localized only to M-lines; green denotes proteins localized only to dense bodies; white (or clear) denotes proteins that are found around or between dense bodies, and in some cases, also to M-lines; blue indicates proteins that are localized to the A-band. In parentheses are the names of the human orthologs or homologs. Most of the interactions were first identified by Y2H screens or assays, and then confirmed by in vitro binding using purified recombinant proteins, localized by antibodies and/or GFP fusions, and genetic analysis. Black lines indicate confirmed interactions; dotted lines indicated interactions only suggested by Y2H results. At M-lines, these interactions create a physical linkage from the muscle cell membrane (via integrins) to MHC A in thick filaments. At dense bodies, beginning also with integrins, there is a similar linkage of multiple proteins, presumably to actin in thin filaments, via DEB-1 and ATN-1. A few of the interactions (MEL-26 to LIM-8; UNC-95 to LIM-8; CeTalin (TLN-1) to UIG-1; CeTalin to DEB-1; DEB-1 to ATN-1; UIG-1 to TTN-1; UNC-112 to DIM-1; UIG-1 to DIM-1) are unpublished ([H. Qadota, D.G. Moerman, G.M. Benian, unpublished data](#)).

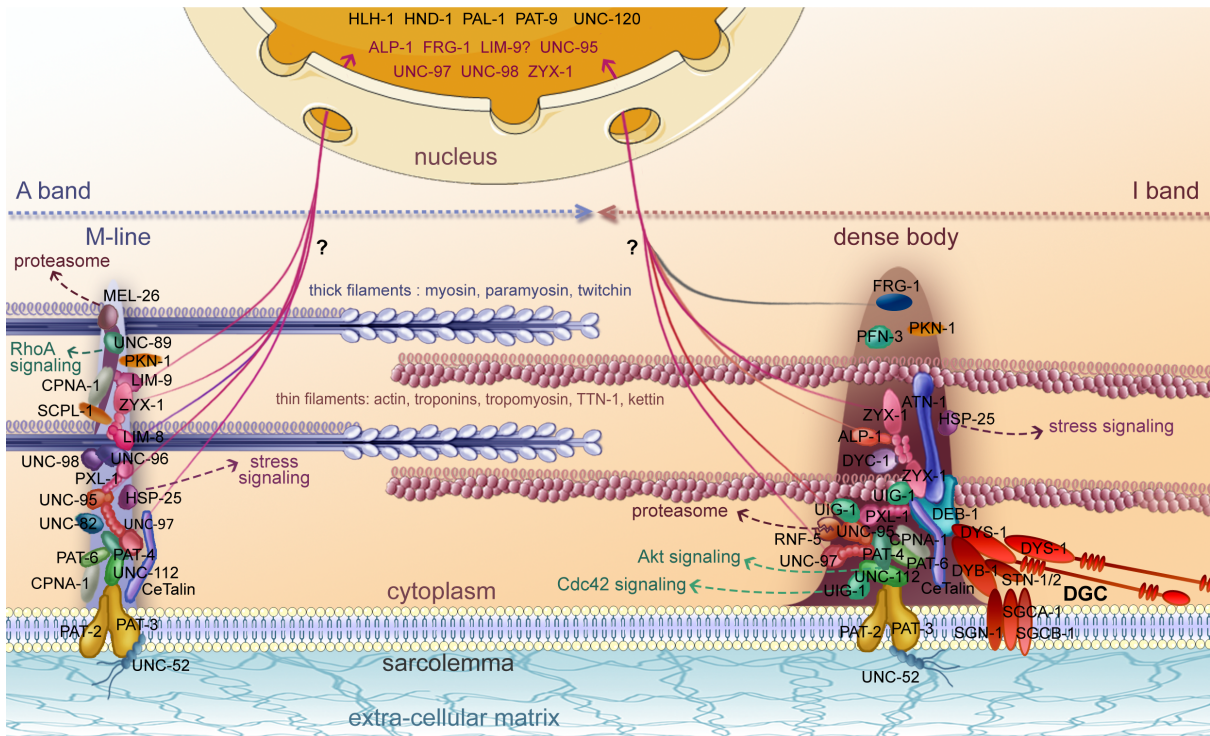


Figure 5. Molecular composition of the sarcomere in body wall muscles.

The cartoon shows a schematic representation of part of a sarcomere. Thin filaments (pink) are mainly composed of actin (ACT-1 to 4), tropomyosin (LEV-11), troponin C (PAT-10), troponin I (TNT-1 to 3), and troponin T (MUP-2). Kettin (KETN-1), and TTN-1 are likely associated to thin filaments. Thick filaments (blue) contain myosin heavy chains A (MYO-3) and B (UNC-54), paramyosin (UNC-15), and twitchin (UNC-22). Thick filaments are likely cross-linked at the M-line, and thin filaments are probably anchored to the dense body. The main proteins associated to dense bodies and M-lines are indicated along with some of the protein interactions summarized in Figure 4. The bases of dense bodies and M-lines are composed of α - (PAT-2) and β - (PAT-3) integrin dimers (yellow). Integrin anchors dense bodies and M-lines to the sarcolemma and likely interact with perlecan (UNC-52) at the outside of muscle cells. Some dense body and M-line associated proteins are linked to signaling pathways: UNC-89 to RhoA signaling, UIG-1 to Cdc42 signaling, HSP-25 to stress signaling, UNC-112 to Akt signaling, and MEL-26 and RNF-5 to the ubiquitin proteasome system. ALP-1, FRG-1, UNC-95, UNC-97, UNC-98, ZYX-1, and most likely LIM-9, possibly shuttle from the dense body and/or the M-line into the nucleus. Several transcriptional regulators are permanently present in the nucleus: HLH-1, HND-1, PAL-1, PAT-9, and UNC-120. Dystrophin (DYS-1) and the Dystrophin Glycoprotein Complex (DGC, red) localize close to the dense body. By the interaction of its C-terminal end with DEB-1, DYS-1 may link the DGC to the dense body. The DGC is composed of dystrobrevin (DYB-1), α - and β -sarcoglycans (SGCA-1 and SGCB-1), δ/γ -sarcoglycan (SGN-1) and syntrophins (STN-1 and -2). This figure was adapted by [C. Lecroisey](#) from Lecroisey, 2010.

Three additional proteins have been localized at both M-lines and dense bodies: ZYX-1 (zyxin) (Lecroisey et al., 2008: PMID 18094057; Lecroisey et al., 2013: PMID 23427270; discussed below), HSP-25 (abcrystallin) (Ding and Candido, 2000: 10734099), and CeTalin (Moulder et al., 1996: PMID 8856663). CeTalin is now called TLN-1, and is also known as UNC-35 ([WormBase](#)). Although the effect of *unc-35* mutations on body wall muscle structure and function have not been reported, the fact that at least one allele (*e259*) (Brenner, 1974: PMID 4366476) leads to an Unc phenotype indicates the importance of this protein in muscle. Some of the M-line-specific proteins (UNC-89, UNC-98, UNC-96, UNC-82) are described below.

In addition to DEB-1 (vinculin) (Barstead and Waterston, 1989: PMID 2498337; discussed above), dense-body specific proteins include: ATN-1 (a-actinin) (Barstead et al., 1991: PMID 1756579), UIG-1 (Cdc42 GEF) (Hikita et al., 2005: PMID 16055082), and ALP-1 (ALP/Enigma) (McKeown et al., 2006: PMID 16278882). ATN-1 was identified by homology to vertebrate a-actinin and its gene placed on the genetic map (Barstead et al., 1991: PMID 1756579); it is the sole a-actinin gene in *C. elegans*. An *atn-1* null mutant (Moulder et al., 2010: PMID 20850453) shows abnormally short and broad dense bodies by EM, but most of the I-bands are normally ordered and, as shown by phalloidin staining, display some abnormal accumulations of F-actin near the sarcolemma. Despite these abnormalities, the *atn-1* null mutant has a remarkably mild locomotion defect: it shows normal locomotion in liquid (swimming/thrashing) but has less ability to bend maximally, consistent with a defect in the transmission of muscle contraction (discussed below). UIG-1 was identified as a binding partner for UNC-112 from a Y2H screen (Hikita et al., 2005: PMID 16055082). UIG-1 shows Cdc42-specific guanine nucleotide exchange activity in vitro. GFP::UIG-1 localizes to dense bodies; a *uig-1* intragenic deletion mutant shows abnormal adult muscle structure by polarized light. Figure 4 and Figure 5 represent a more complete picture of proteins residing at both M-lines and dense bodies, or specifically at one of the

structures. Nevertheless, this is a tentative picture that is likely simplified, based on what is known for vertebrate adhesion complexes (Zaidel-Bar and Geiger, 2010: PMID 20410370). Some details about the proteins shown in Figure 5 and discussed in the text, including human homologs/orthologs, location in the sarcomere, interacting partners, phenotypes of mutants, and key references are given in 2, Section 8.

Localization of UNC-112 to muscle integrin adhesions requires PAT-4 (Mackinnon et al., 2002: PMID 12015115). PAT-4 (ILK) kinase domain binds to the N-terminal half of UNC-112 (Mackinnon et al., 2002: PMID 12015115). UNC-112 N- and C-terminal halves interact, and UNC-112, but not PAT-4, interacts directly with the cytoplasmic tail of PAT-3 (Qadota et al., 2012: PMID 22761445). Biochemical, genetic, and cell biological data (Qadota et al., 2012: PMID 22761445; Qadota et al., 2014: PMID 24692564) suggest the following model for this requirement: UNC-112 exists in a closed form that interacts weakly with integrin, and an open form that interacts more strongly with integrin, and conversion to the open active form is promoted by binding of PAT-4 (ILK) to UNC-112 (Figure 6A).

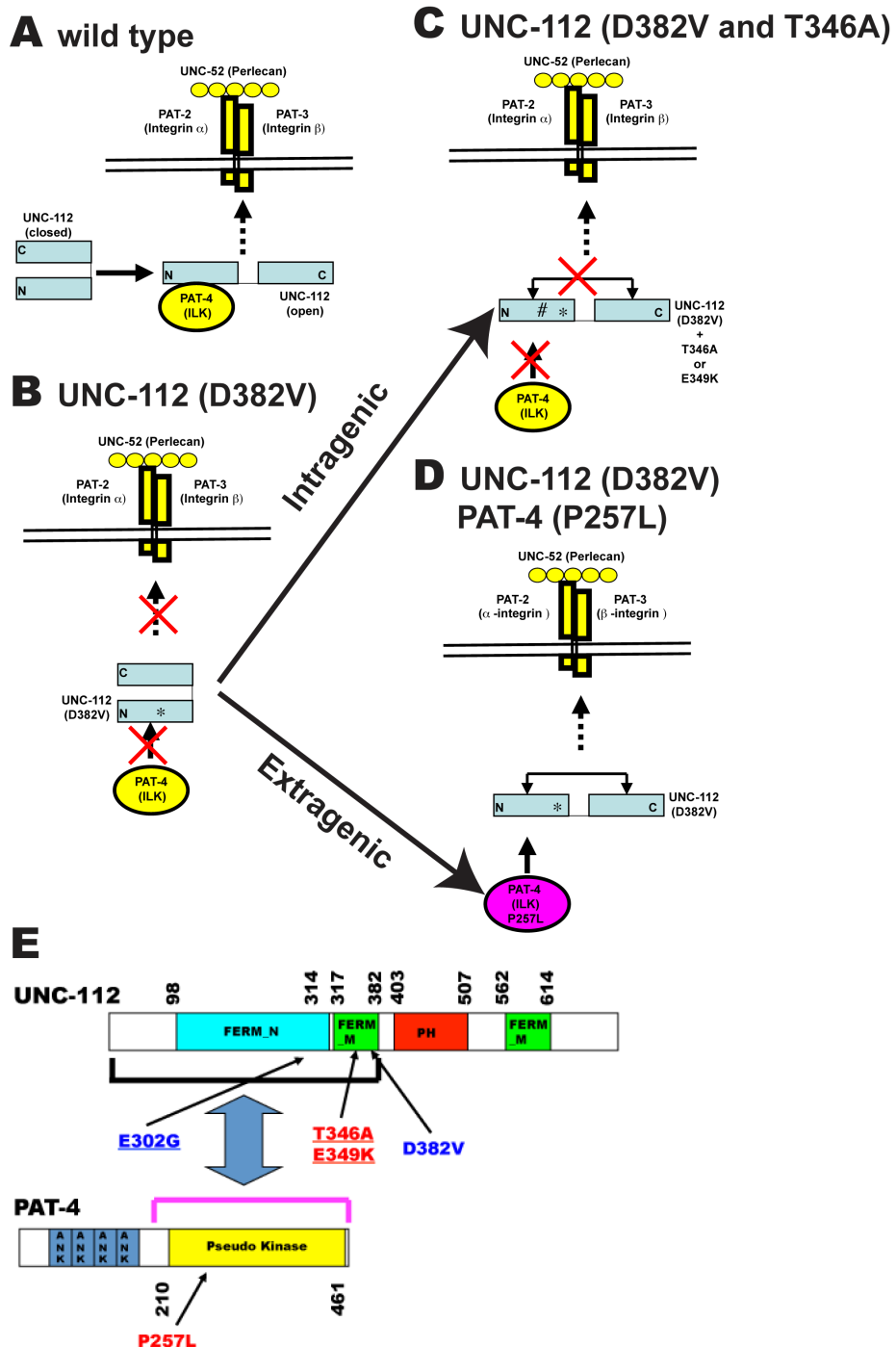


Figure 6. Conformational model for the interaction of UNC-112 with integrin, and key mutations supporting the model. (A) It is hypothesized that UNC-112 exists in two conformations, closed and open, and that only the open form can interact with the cytoplasmic tail of β -integrin at the base of adhesion sites in muscle. The conversion to the open active form is promoted by binding of UNC-112 to PAT-4. (B) UNC-112 D382V does not bind to PAT-4, and fails to localize to integrin adhesion sites in vivo. According to the model, this mutant form of UNC-112 is in a closed conformation. (C) In wild type UNC-112, the N- and C-terminal halves interact. However, UNC-112 T346A or UNC-112 E349K fails to show this interaction. UNC-112 containing both D382V and T346A (or D382V and E349K) does localize to adhesion sites in vivo. According to the model, this is because even without PAT-4 binding this mutant form of UNC-112 is in an open conformation able to bind to integrin. (D) PAT-4 P257L allows PAT-4 to bind to UNC-112 D382V. Co-expression of UNC-112 D382V and PAT-4 P257L allows for localization of UNC-112 D382V to adhesion sites in vivo. (E) Schematic representation of domains, mutation sites and interaction of UNC-112 with PAT-4. Domains of each protein, indicated by colored rectangles were predicted by PFAM, with boundaries indicated by residue numbers. The black and purple brackets denote the minimal regions that are required for interaction of UNC-112 with PAT-4, respectively. In UNC-112, the D382V and E302G mutations each prevent UNC-112 from interacting with PAT-4; the T346A and the E349K mutations each prevent interaction of the N-terminal half of UNC-112 with the C-terminal half of UNC-112, and in the presence of D382V or E302G, act as intragenic suppressors to permit binding of these mutant forms of UNC-112 to PAT-4. In PAT-4, P257L is one of 9 mutations lying within the pseudo kinase domain that act as extragenic suppressors of UNC-112 D382V, allowing this mutant form of UNC-112 to interact with PAT-4. Underlined residues are conserved in human kindlins and ILK. The original genetic mutations in *unc-112* and *pat-4* are not shown. (Updated, with permission, from Qadota et al. 2012: PMID 22761445; Qadota and Benian, 2014: PMID 24808865).

To obtain evidence for this model in vivo, UNC-112 and PAT-4 non-binding mutant forms and their suppressor mutations were isolated (Figure 6E). This was accomplished by error-prone PCR mutagenesis followed by Y2H screening, and confirmation using in vitro binding assays with recombinant proteins. UNC-112 D382V and UNC-112 E302G cannot bind to PAT-4 (Figure 6E). When UNC-112 D382V is expressed in worms, it does not localize to integrin adhesion sites in striated muscle, suggesting that PAT-4 binding is required for UNC-112 localization to these sites (Figure 6B). Using the same mutagenesis/Y2H methods, two classes of suppressor mutations (Figure 6E) for D382V were isolated. One class consists of intragenic suppressors in UNC-112: T346A and E349K mutations block the interaction of UNC-112 N- and C-terminal halves. UNC-112 (D382V and T346A (or E349K)) cannot bind to PAT-4. However, UNC-112 (D382V and T346A (or E349K)) can localize to integrin adhesion sites in worms, suggesting that a change of UNC-112 to an “open” conformation is essential for association with integrin (Figure 6C). The second class consists of extragenic suppressors, and these are missense mutations in PAT-4. Each of the nine PAT-4 suppressor mutant proteins can bind to UNC-112 D382V (one of nine is P257L) (Figure 6E). In the presence of PAT-4 P257L, UNC-112 D382V can localize to integrin adhesion sites in vivo (Figure 6D). Using the crystal structure of human ILK (Fukuda et al., 2009: PMID 20005845), an homology model of PAT-4 was generated, and this shows that all nine mutations affect residues that may form a binding surface for UNC-112, and lie on a different surface from that which binds to α -parvin (PAT-6). Confirmation of this model awaits a crystal structure of UNC-112 and/or the UNC-112/PAT-4 complex. Currently, however, a crystal structure of any kindlin (like UNC-112) is not available.

3.2. Differential localization of M-line and dense body proteins

As is apparent in Figure 4 and Figure 5, the same proteins are located at the base of both dense bodies and M-lines, and these are the earliest proteins to associate in the assembly process, as shown by immunostaining during embryonic muscle development (Hresko et al., 1994: PMID 8106548). However, a mystery is what determines whether a dense body or an M-line will be built upon this same “foundation”? Certainly, this involves the recruitment of dense body-specific and M-line-specific proteins, but it is not known how this occurs. Dense body-specific proteins include DEB-1 (vinculin) (Barstead and Waterston, 1989: PMID 2498337; discussed above), ATN-1 (α -actinin) (Barstead et al., 1991: PMID 1756579), UIG-1 (Cdc42 GEF) (Hikita et al., 2005: PMID 16055082), and ALP-1 (ALP/Enigma) (McKeown et al., 2006: PMID 16278882; discussed below). M-line specific proteins include UNC-89, UNC-98, UNC-96, and UNC-82 (discussed below). One way to approach this problem might be to conduct screens for mutants in which a GFP-tagged protein that is normally present only at the dense body or the M-line, is found at both structures, or the opposite structure.

It should be noted that the various components of M-lines and dense bodies are not uniformly distributed throughout these structures. At both M-lines and dense bodies, because UNC-112 interacts with the cytoplasmic tail of PAT-3 (β -integrin), UNC-112 and its associated proteins (PAT-4, UNC-97, and PAT-6) are located close to the outer muscle cell membrane. For example, a confocal z-series shows that UNC-52 (perlecan) and PAT-6 (actopaxin), via antibodies, and UNC-112::GFP, are located close to the cell membrane (Warner et al., 2013: PMID 23283987). This also seems to be true for UNC-95, which interacts with UNC-97 (Qadota et al., 2007: PMID 17761533), and DIM-1 (Ig domain protein) (Rogalski et al., 2003: PMID 12663531). At dense bodies, DEB-1 (vinculin) is clearly near the muscle cell membrane whereas ATN-1 (α -actinin) is clearly located in the major and deeper region of dense bodies (Francis and Waterston, 1985: PMID 2413045). The ATN-1 (α -actinin) binding protein, ALP-1, is localized to the deeper portion of dense bodies,

similar to ATN-1 (Han and Beckerle, 2009: PMID 19261811). Interestingly, ZYX-1 is located in the middle of dense bodies, consistent with its interaction with both DEB-1 (vinculin) and ATN-1 (α -actinin) as demonstrated by Y2H assays (Lecroisey et al., 2013: PMID 23427270). By a z-series of confocal images, UNC-89 (Warner et al., 2013: PMID 23283987) is located throughout the depth of the M-line, from near the outer muscle cell membrane to deep into the myofilament lattice. CPNA-1 is found at all three levels of dense bodies (membrane proximal, middle, and deep), but at M-lines, CPNA-1 is found near the muscle cell membrane, absent from the middle, and then reappears deep in the lattice. However, this may reflect either absence in the middle portion of the M-line, or that CPNA-1 epitopes are masked by other proteins in this region (Warner et al., 2013: PMID 23283987).

There are also a number of proteins that are found around and between dense bodies (as indicated in Figure 4). These include LIM-8, LIM-9 (FHL-2) (Qadota et al., 2007: PMID 17761533), the formin family members FHOD-1 and CYK-1 (Mi-Mi et al., 2012: PMID 22753896), MEL-26 (Wilson et al., 2012: PMID 22621901), DIM-1 (Rogalski et al., 2003: PMID 12663531), and MAK-1 (MAPKAP kinase 2) (Matsunaga et al., 2015: PMID 25851606). TTN-1 (Forbes et al., 2010: PMID 20346955; see below) and KETN-1 (kettin, an invertebrate-specific actin-binding 427,000 Da protein comprised of 31 Ig domains) (Ono et al., 2006: PMID 16597697) are more evenly distributed throughout the I-band (except for dense bodies).

3.3. Dynamics of muscle adhesion proteins

GFP tagged proteins can be used to determine the real-time dynamic exchange of proteins in vivo. The first, and so far, most extensive study on the dynamics of sarcomeric proteins in *C. elegans* has been reported by Ghosh and Hope (2010: PMID 20226563). The authors used Fluorescence Recovery After Photobleaching (FRAP) to assess the mobility of six GFP tagged proteins, UNC-112 (kindlin), UNC-95, MYO-3 (MHC A), MUP-2 (troponin T), T03G6.3 (NPP6), and C46G7.2 (large isoform of α -filagrinin), in living transgenic young adult worms. After photobleaching, recovery of fluorescence is interpreted as replacement of bleached proteins with proteins that arrive from either a cytoplasmic pool, or are coming off from similar structures outside the bleached area; given the timescale of the typical experiment contribution from newly synthesized protein is negligible. The proteins studied showed a wide variation of exchange rates. Thin filament or I-band components, MUP-2 (troponin T) and T03G6.3 (NPP6) were fastest to recover, with $t_{1/2}$ of recovery of 2.5 min and 1.5 min, respectively. MYO-3 (MHC A), C46G7.2, and UNC-112 (kindlin) showed no recovery even after 15 min. UNC-95 showed an intermediate response, with about 50% recovering initially at a fast rate comparable to T03G6.3, and then maintaining that level up through 15 min (Ghosh and Hope, 2010: PMID 20226563). As noted by the authors, their results for the replacement of MUP-2 and MYO-3 are consistent with what has been reported thin filament and thick filament components in vertebrate and zebrafish skeletal muscles; rapid exchange for thin filament components, slow exchange for myosin. The authors suggest that the more dynamic proteins are peripheral components of complexes or filaments, whereas the less dynamic proteins are more central proteins with roles in anchorage. Their results with the M-line/dense body protein UNC-112, is certainly consistent with this interpretation (Ghosh and Hope, 2010: PMID 20226563).

More recently, the dynamics of ZYX-1 (zyxin) have been studied in living *zyx-1::gfp* transgenic worms (Lecroisey et al., 2013: PMID 23427270). FRAP experiments indicate that ZYX-1 is highly dynamic. When a region containing dense body and M-line ZYX-1::GFP was bleached, the average $t_{1/2}$ of recovery was 4.96 sec, with maximal recovery of 77.5% occurring after 70 sec. When nuclei were bleached, the average $t_{1/2}$ of recovery was 7.57 sec, with a maximum recovery of only 14.3% after 70 sec. The lower maximum recovery for nuclear ZYX-1::GFP suggests that a large percent (~86%) of ZYX-1 may be permanently localized to the nucleus. In contrast, the faster maximum recovery for muscle attachment complex ZYX-1 suggests that ZYX-1 is more peripheral and dynamic in these locations. Preliminary FRAP experiments on UNC-98::GFP have also been performed (R.K. Miller and [G.M. Benian](#), unpublished data). After photobleaching nuclear UNC-98::GFP, the $t_{1/2}$ of recovery was 163 sec; after photobleaching a line of 4 dense bodies, the $t_{1/2}$ of recovery was 25 sec. However, after photobleaching the M-line, the fluorescence did not even reach half of its original level during the 725 sec monitoring period. These results suggest that nuclear UNC-98 may be more stable than nuclear ZYX-1, and that although UNC-98 is very stably associated with the M-line, it is only peripherally or transiently associated with the dense body (see comment above that endogenous UNC-98, may be localized to the M-line, not the dense body).

The fast recovery rates of the nematode integrin adhesion complex proteins ZYX-1, dense body-associated UNC-98, and UNC-95 is consistent with FRAP results obtained for integrin, tensin, talin, and ILK at the myotendinous junctions of *Drosophila* embryonic and larval muscles: each of these proteins had $t_{1/2}$ of less

than 100 sec (Yuan et al., 2009: PMID 20179102). Overall, FRAP experiments in *C. elegans* and *Drosophila* demonstrate that integrin adhesion structures show considerable turnover of their components. This turnover may play an important role in the maintenance of these structures, which are subjected to mechanical stress during muscle activity.

3.4. Multiple protein complexes link integrin to myosin in thick filaments at the M-line

unc-95, *unc-96*, and *unc-98* were first identified by Zengel and Epstein (1980: PMID 7348600) from a screen for mutants that are defective in muscle function and structure. *unc-96* and *unc-98* mutants are slower moving than wild type, and by polarized light microscopy display a moderately disorganized myofilament lattice and birefringent “needle-like” structures at the ends of their body wall muscle cells. These “needles” correspond to accumulations of proteins that contain paramyosin, but not actin, myosin, UNC-89, or α -actinin (Mercer et al., 2003: PMID 12808046; Mercer et al., 2006: PMID 16790495; Miller et al., 2008: PMID 18256289). UNC-98 is a 310-residue polypeptide containing four C2H2 Zn finger domains and several predicted nuclear localization and nuclear export signal sequences (NLS and NES) (Mercer et al., 2003: PMID 12808046). Antibodies to UNC-98 localize to M-lines. However, in transgenic animals, UNC-98::GFP localizes to M-lines, dense bodies, and muscle cell nuclei. *unc-98* mutant animals, when rescued with a wild type copy of the gene, show localization of anti-UNC-98 antibodies to M-lines, dense bodies, and nuclei. Deletion derivatives of UNC-98::GFP in transgenic worms demonstrated that the N-terminal 110 residues of UNC-98 are necessary and sufficient for nuclear localization, and that all four Zn fingers are sufficient for localization to M-lines and dense bodies (Mercer et al., 2003: PMID 12808046). Using an UNC-98 bait to screen a collection of Y2H clones representing known M-line and dense body proteins, interaction with UNC-97 (PINCH) was identified and confirmed by in vitro binding using purified proteins. Binding requires the first two LIM domains of the five LIM-domain protein UNC-97, and all four C2H2 Zn fingers of UNC-98 (Mercer et al., 2003: PMID 12808046).

unc-96 encodes 408 and 418 residue polypeptides by alternative splicing, and these proteins lack recognizable domains (Mercer et al., 2006: PMID 16790495). Antibodies to UNC-96 localize to M-lines (Mercer et al., 2006: PMID 16790495). The strongest mutant allele of *unc-96*, *sfl8*, is not Pat embryonic lethal, and yet is presumably a null mutant as it is a nonsense mutation and no protein can be detected by Western blot. Intriguingly, either a decreased (by loss-of-function mutation) or an increased level (by over-expression under the control of a heat shock promoter) of UNC-96 results in disorganization of thick filaments (Qadota et al., 2007: PMID 17761533). Apparently, the level of UNC-96 must be tightly controlled to obtain proper organization of thick filaments. By both genetic and biochemical criteria, UNC-96 and UNC-98 interact with each other. Protein accumulations at the ends of the muscle cells contain the UNC-98 protein in *unc-96* mutants, and contain the UNC-96 protein in *unc-98* mutants (Mercer et al., 2006: PMID 16790495).

unc-95 was identified at the molecular level by Broday et al. (2004: PMID 15210732). *unc-95* mutants are slow moving and have disorganized muscle structure. Immunostaining with various antibodies shows that thick and thin filaments and dense bodies are disorganized (Broday et al. 2004). UNC-95 is a 350-residue polypeptide with a single LIM domain near its C-terminus, a region predicted to have coiled-coil structure and a NLS sequence (Broday et al., 2004: PMID 15210732). In transgenic nematodes, UNC-95-GFP localizes to M-lines, dense bodies, muscle cell-cell boundaries, and nuclei in adult body wall muscle. UNC-95::GFP is also expressed in embryonic muscle, and by the 3-fold stage is localized to muscle attachment sites (dense bodies and M-lines) and nuclei. Antibodies to UNC-95 clearly label M-lines, dense bodies and cell-cell boundaries, but not nuclei in adult body wall muscle (Qadota et al., 2007: PMID 17761533).

Genetic, cellular, and biochemical evidence support a model in which UNC-98 links integrin-associated proteins to myosin in thick filaments at M-lines (Miller et al., 2006: PMID 17158957) (Figure 4A). As noted above, UNC-97 (PINCH), a member of a conserved four-protein complex associated with integrin, interacts with UNC-98 (Mercer et al., 2003: PMID 12808046). The N-terminal 110 residues of UNC-98 interact with the C-terminal portion of myosin heavy chain A (MHC A) that resides in the middle of thick filaments in the proximity of M-lines (Miller et al., 2006: PMID 17158957). Although vertebrate costameres are usually regarded to reside at the level of Z-disks, some components of focal adhesions, including $\alpha\beta$ integrin have also been found at M-lines (McDonald et al., 1995: PMID 7593298). Thus, these data for *C. elegans* muscles suggest the possibility of a similar mechanism of linkage between integrins and myosin thick filaments at the M-lines of peripheral myofibrils of vertebrate muscle. UNC-97, in addition to interacting with UNC-98, also interacts with LIM-8, LIM-9, and UNC-95 (Qadota et al., 2007: PMID 17761533). These proteins are involved in three additional linkages from UNC-97 to myosin: 1) from UNC-97 to LIM-8 to myosin, 2) from UNC-97 to LIM-9

to UNC-96 to myosin, and 3) from UNC-97 to UNC-95 to LIM-8 to myosin. LIM-8 is a novel LIM domain-containing protein. LIM-9 is the nematode homolog of mammalian FHL-2 (four and a half LIM domain protein 2). UNC-96 and LIM-8 also bind to the C-terminal portion of MHC A (to a slightly different portion of MHC A that binds to UNC-98) (Figure 4A). These interactions were first identified by Y2H and then confirmed by in vitro binding assays using purified proteins. By antibody staining, LIM-8, LIM-9, and UNC-95 localize, at least partially, to M-lines. The fact that UNC-96, UNC-98, and LIM-8 interact with C-terminal portions of the myosin rod is consistent with models for the M-line in which the shafts of thick filaments are cross-linked.

3.5. M-line proteins and paramyosin

In addition to a structural role for UNC-96 and UNC-98 at the M-line, these proteins interact with paramyosin (UNC-15) to promote paramyosin's incorporation into thick filaments (Mercer et al., 2006: PMID 16790495; Miller et al., 2008: PMID 18256289). Paramyosin is an invertebrate-specific “headless myosin” that is primarily an a-helical coiled-coil rod and is 36-38% identical in sequence to the rod domains of myosin heavy chains (Kagawa et al., 1989: PMID 2754728). In *C. elegans* body wall muscle, the myosins and a portion of paramyosin are organized around a tubular core consisting of paramyosin and filagenins in a specific geometry (Deitiker and Epstein, 1993: PMID 8408214; Epstein et al., 1995: PMID 7577237; Muller et al., 2001: PMID 11162112). In *C. elegans*, paramyosin is encoded by a single gene, *unc-15*. Loss-of-function *unc-15* mutants are severely paralyzed and display disorganized body wall muscle (Waterston et al., 1977: PMID 564970). *unc-15* null mutants have shorter hollow-appearing thick filaments (MacKenzie and Epstein, 1980: PMID 7193096).

The birefringent needles observed in the body wall muscle of *unc-96* and *unc-98* mutants contain paramyosin located outside the thick filaments (Mercer et al., 2006: PMID 16790495; Miller et al., 2008: PMID 18256289). By genetic and biochemical criteria, paramyosin interacts with UNC-96 and UNC-98 (Mercer et al., 2006: PMID 16790495; Miller et al., 2008: PMID 18256289). By both Y2H analysis and ELISAs using purified proteins, UNC-98 interacts with paramyosin residues 31-693, whereas UNC-96 interacts with a separate region of paramyosin, residues 699-798. Although UNC-96 and UNC-98 affect, at least partially, the localization of paramyosin (some in accumulations, some in its normal A-band location), total paramyosin levels do not change in either *unc-96* or *unc-98* loss-of-function mutants (Miller et al., 2008: PMID 18256289). By Western blot, in the *unc-15* nonsense mutant *e1214*, the level of UNC-98 is diminished, and in *unc-15* missense mutants (*e1215* and *e73*, which form paramyosin aggregates), the level of UNC-98 is increased. The dependence of UNC-98, and possibly UNC-96, levels on the state of paramyosin might be due to a chaperone function of these proteins in response to aggregation of mutant paramyosin. In fact, there is growing evidence that molecular chaperones are crucial for muscle assembly and maintenance; this topic is discussed in detail in Section 4.

There are two more links between paramyosin and M-line proteins. First, is the connection of paramyosin to UNC-82. *unc-82* mutants have disorganized sarcomeres including mis-localization of thick filament and M-line components (Hoppe et al., 2010: PMID 19901071). Phenotypic analysis suggests that *unc-82* is required in embryonic muscle cells, as the cells, including the myofilaments, increase in size. In an *unc-82* null mutant, at the 1.5 fold stage of embryogenesis, the localization of MHC A, paramyosin, and UNC-89 are normal, but by the 2 fold stage, these proteins form aggregates, which become larger and more numerous at the 3 fold stage. Muscle contraction *per se* does not seem to be responsible for aggregate formation, as an *unc-54(s95);unc-82* double mutant, in which myosin activity is reduced, does not fully rescue the phenotype. UNC-82 is a 1600 residue polypeptide containing an N-terminal protein kinase domain homologous to human ARK5 (NUAK1) and SNARK (NUAK2) protein kinases, and simple repetitive sequences in the remainder of the protein. A rescuing UNC-82::GFP fusion protein localizes to M-lines throughout the depth of the myofilament lattice. UNC-82 is a candidate for a protein kinase that phosphorylates myosin heavy chains and paramyosin (Hoppe et al., 2010: PMID 19901071). A small N-terminal nonhelical segment of paramyosin is phosphorylated on serine by a thick filament-associated kinase (Dey et al., 1992: PMID 1324668; Schriefer and Waterston, 1989: PMID 2754733). This N-terminus contains multiple copies of the motif, S_S_A, which may be sites of phosphorylation. This S_S_A motif is also found in multiple copies in the C-terminal nonhelical tailpieces of MHC A and MHC B. Supporting the idea that UNC-82 phosphorylates paramyosin is the observation that more acidic isoelectric species of paramyosin are absent from extracts of *unc-82* mutants (Schriefer and Waterston, 1989: PMID 2754733).

Another link between paramyosin and M-line proteins is that the M-line protein UNC-89 interacts with paramyosin through its SH3 domain, and *unc-89* mutants that lack expression of UNC-89 isoforms containing the SH3 domain show aggregates of paramyosin (Qadota et al., 2016: PMID 27009202; see below).

3.6. Novel methods to study muscle proteins and phenotypes

Null mutants for many of the M-line and dense body proteins do not have defects in sarcomere organization, or even locomotion when observed by a conventional motility assay in which the number of times a worm moves back and forth (flexes) in liquid is counted (as described in Epstein and Thomson, 1974: PMID 4845659). One possibility for this lack of effect could be functional redundancy. The functional redundancy of PXL-1 and LIM-8 (described in more details below) provides an example: neither loss-of-function mutant by itself has a defect in body wall muscle structure or nematode locomotion, however, a *pxl-1; lim-8(RNAi)* animal is slow moving with disorganized sarcomeres (Warner et al., 2011: PMID 21633109). Another possibility is that some of these proteins may not have roles in muscle assembly or maintenance. Instead, the M-line, and especially the dense body, is a “way station” for proteins to “park” or “rest” before departing for a new location. This is a tempting idea, but there is no evidence for it currently.

Yet another possibility is that these proteins, located as they are at muscle focal adhesions, function in force transmission, but a more sensitive assay is needed to reveal this function (Qadota and Benian, 2010: PMID 20414365). The ability to maximally bend during backward movement (Figure 7A) can discriminate wild type from many of the mutants in various integrin adhesion site proteins. The first successful application of this assay was on a null mutant of the single a-actinin gene in the worm, *atn-1*. Homozygous null mutations in this gene yield animals with abnormally short and broad dense bodies, but surprisingly display normal movement on an agar surface and normal swimming in liquid (Moulder et al., 2010: PMID 20850453). In contrast, the more sensitive bending assay shows that this mutant has a reduced ability to bend (Moulder et al., 2010: PMID 20850453). When the assay was applied to mutants in 18 other genes encoding proteins that are located at M-lines and dense bodies, defective bending was found in 12 more (Nahabedian et al., 2012: PMID 22126736). Four of them, *unc-82*, *unc-89*, *unc-95*, and *unc-96* were previously described as having reduced motility. Thus, this assay can detect a locomotion defect in mutants that were previously recognized to have an adult “Unc” phenotype. Eight of the mutants were not previously known to have motility defects (*pkn-1*, *zyx-1*, *frg-1*, *alp-1*, *kin-32*, *pfn-3*, *lim-8*, and *dim-1*). Interestingly, one mutant gene, *scpl-1* (2 alleles tested), had greater ability to bend maximally. SCLP-1 is a CTD-type phosphatase found to interact with UNC-89 (Qadota et al., 2008a: PMID 18337465; see below).

Varkuti et al. (2012: PMID 22343723) reported a new and conserved actin binding site on the myosin head called the “activation loop” that is crucial for F-actin activation of myosin ATPase activity. In this same report, the authors describe a novel method for measuring worm motility, and a novel method for measuring the force exerted by single nematodes (Figure 7B). After verifying that a missense mutation in this activation loop affects myosin’s biochemical properties in vitro (with *Dicytostelium* and mouse myosins), the comparable mutation K525E was introduced into UNC-54 (MHC B), and a transgenic strain was created in which P_{unc-54::UNC-54_{K525E}::GFP} was introduced into an *unc-54* null background. These animals showed reduced locomotion as compared to wild type or transgenic animals in which the *unc-54* null was rescued with wild type UNC-54::GFP. Locomotion was measured by calculating velocities of worm tails in video recordings. To measure the ability of individual worms to generate force a clever method was devised in which a single worm was placed beneath the cantilever of an atomic force microscope (AFM), worms were exposed to a deforming force (a “push”), and the force the worm generates to escape from under the cantilever was measured. Force (μNewtons) vs. time (sec) show that wild type and the *unc-54* null mutant rescued by UNC-54::GFP generated ~30-50 μN, whereas UNC-54_{K525E::GFP} generated much less force (~15-18 μN). It would be informative to use this method to measure forces generated by other alleles of *unc-54* and many other Uncs as well.

Johari et al. (2013: PMID 23511608) used another innovative method to measure the force generated by individual wild-type nematodes (Figure 7C). This assay records the movement of a worm in a microfabricated array of soft polydimethylsiloxane (PDMS) micropillars in a chip (9 x 9 mm) and, from the displacement of the pillars, the force exerted by the worm is calculated using a modified form of the Timoshenko beam deflection theory. At any given time a single worm is in contact with 6-10 pillars, primarily depending on pillar spacing. Interestingly, the force varies depending on which position along the worm length is measured, with the maximum force exerted from the middle part of the worm body. This result agrees with theoretical analysis that predicted that maximum force is generated near the middle part of the body (Shen et al., 2012: PMID 22735527). The maximum force measured was 31.3 mN (this was obtained with pillars arranged in a hexagonal lattice; a lower maximum force of 18.9 mN was obtained with pillars arranged in a square lattice; in each case the pillar to pillar distance was 140 nm). The recordings could also be easily analyzed to derive speed, amplitude and wavelength. So far, there is only one report in which this method has been used to measure forces

exerted by muscle mutants: Etheridge et al. (2015: PMID 25491313) reported decreased peak forces from *unc-52ts* and *unc-112ts* adults at the restrictive temperature.

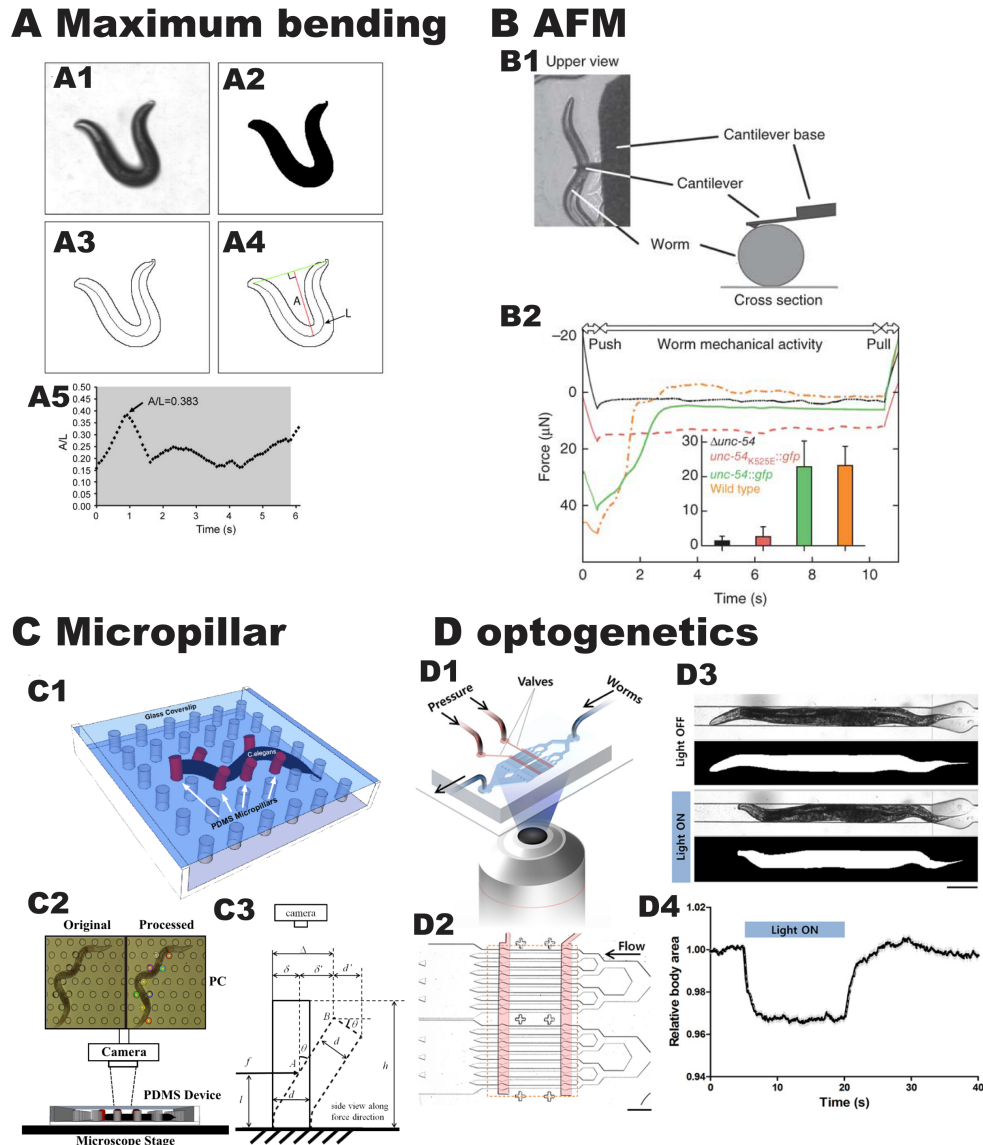


Figure 7. Recently reported methods to assess the locomotion and force generated by *C. elegans*. (A) Measurement of maximum bending amplitude (A/L) as a worm moves backwards. (A1) Frame from a video showing a deep bend of an adult during a reversal. (A2) Binary image of the frame from (A1). (A3) Outline of the animal and the corresponding midline spline used to determine the length of the animal. (A4) Measurement of the amplitude of the bend was made by measuring the longest perpendicular length, A, from a line connecting the head to the tail into the midline spline, of contour length L. The ratio of this value, A, to the contour length, L, was calculated (A/L). (A4) Time course of A/L values. Shortly before $t = 0$, the worm was tapped gently on the head to induce backwards movement. The grey region indicates the time the animal is in a reversal. Reproduced from Nahabedian et al. (2012: PMID 22126736) with permission. (B) The use of an atomic force microscope (AFM) to measure force generated by a single nematode. (B1) Schematic of how the experiment is setup. (B2) Representative force curves generated by four *C. elegans* strains. Animals were exposed to a deforming force (push), and their force-generating activities were measured (worm mechanical activity) until the retraction of the cantilever (pull). The inset shows the force production averages and error bars with standard deviations of 15–25 animals from each strain. Reproduced with permission from Varkuti et al. 2012: PMID 22343723. (C) Measurement of the force generated by single nematodes by measuring deflection of flexible micropillars. (C1) Drawing of an animal as it deflects an array of micropillars made from polydimethylsiloxane (PDMS). (C2) Experimental setup comprising the PDMS device on a microscope stage with a camera connected to a computer for recording worm videos. (C3) Schematic of the deflected pillar for *C. elegans* force measurement model. Reproduced with permission from Johari et al. (2013: PMID 23511608). (D) Use of optogenetics to measure the kinetics of muscle contraction and relaxation. (D1) Experimental setup that combines microfluidics, optogenetics and image processing. (D2) The microfluidic device has 16 parallel microchannels for simultaneous illumination and analysis of multiple animals trapped by pneumatically-controlled microvalves (red). (D3) Microscopic and segmented images of a wild-type worm trapped in a microchannel with (top) and without (bottom) the illumination of blue light. (D4) Temporal change in the body size of wild type animals that was calculated from the segmented images and normalized by average value in the first 5 seconds (s). The light was on for 15 s beginning at the 5 s time point. Data represent mean +/- standard error of the mean, $n = 88$. Reproduced with permission from Hwang et al. (2016: PMID 26822332).

Although the forces measured by the AFM (Atomic Force Microscopy) and micropillar methods are close (31-50 mN), they do not agree with measurements of forces exerted by single worms crawling on agar surfaces. For example, Rabets et al. (2014: 25418179), after measuring drag forces exerted on worms as they move along an agar surface, used “resistive force theory” to calculate the force generated by a single crawling worm as ~5 mN, an order of magnitude lower than the methods noted above. Using kinematic data and a hydrodynamic model based on lubrication theory, Shen et al. (2012: PMID 22735527) calculated a much lower bending force of 85-89 nN. The reasons for this wide variation in measured forces is not clear but may certainly depend on variation in methodology. The AFM method measures an “escape force”, the micropillar method measures deflection of pillars, but the other studies involved measurement or calculation of force on a wet viscoelastic agar gel. Moreover, various studies, using different methods, have reported that the bending force of individual worms in liquid is ~1-3 nN (Krajacic et al., 2012: PMID 22554893; Shen et al., 2012: PMID 22735527; Kuo et al., 2014: PMID 7748176). It is clear that nematodes generate much higher bending forces to crawl on a surface than to swim in liquid. Despite the method used, most of these methods have been used to distinguish wild type from mutants. It is hoped that more of this analysis will be reported for phenotyping muscle mutants in the future.

Multiple computer programs ([Nemo](#), [Worm Tracker 2.0](#), [Parallel worm tracker](#), [Multi Worm Tracker](#), The Tracker, etc.) for tracking and measuring crawling of *C. elegans* on a solid surface have been described (WormBook chapter [Keeping track of worm trackers](#)). There is also a program ([CeleST](#)) available for analyzing swimming (Restif et al., 2014: PMID 25033081). These programs quantify different aspects of locomotion such as posture, directional changes, curvature of the sinusoidal shape, and velocity. The programs have been used to analyze the locomotion of wild type and various mutants (e.g., Brown et al., 2013: PMID 23267063; Swierczek et al., 2011: PMID 21642964; Koren et al., 2015: PMID 25816290). However, the main focus of these studies has been on neuronal mutants, only a few muscle *uncs* have been analyzed. This type of analysis clearly has potential for understanding muscle gene function.

Due to the small size of *C. elegans* and consequent inability to isolate muscle cells or groups of muscle cells, it has not been possible to conduct measurements of muscle kinetics as is conducted on individual muscle fibers from vertebrate muscle. However, recently some kinetic parameters have been measured by optogenetically controlling muscle contraction of whole nematodes. In a report by Hwang et al. (2016: PMID 26822332) (Figure 7D), a worm strain was used in which channelrhodopsin-2 is expressed in cholinergic motor neurons. Illumination was used to induce contractions in body wall muscles. A measure of muscle contraction state is total body area normalized to the length of the animals. Using image processing, the change in body area vs. time when light is on and off was plotted.

Results were obtained for wild type and mutants in genes encoding 15 sarcomere proteins. Curve fitting with one phase decay and one-phase association models were used to calculate rate constants for contraction and relaxation, respectively. Many of the mutants were defective in these and related parameters. *unc-54(s74)* was the only mutant tested that showed a decrease in the rate of contraction. This is perhaps expected since *s74* is a missense mutation in the ATP binding site that is likely to result in reduced ATPase and motor velocity and a slower contraction/relaxation cycle (Moerman et al., 1982: PMID 7151169; Moerman and Fire, 1997: PMID 21413235). Increased relaxation rates observed in two of the mutants, *unc-27* and *unc-22*, might be explained from what is known or speculated about their roles in muscle activity. UNC-27 is one of four troponin I isoforms (Burkeen et al., 2004: PMID 14747334) and in vertebrate striated muscle troponin I is known to inhibit the interaction of myosin heads with thin filaments (Perry, 1999: PMID 10098965). *unc-22* encodes twitchin (see below), and both the loss-of-function twitching phenotype, and the presence of a protein kinase domain similar to myosin light chain kinase suggests a role for twitchin in regulating muscle contraction. Prior work in *Aplysia* and *Mytilus* suggested that twitchin inhibits the rate of relaxation (Probst et al., 1994: PMID 8078908; Siegman et al., 1998: PMID 9560285; Funabara et al., 2007: PMID 18055628). It is noteworthy that the rate constants for relaxation are increased by two *unc-22* alleles, *e66* and *e105*: *e66* leads to disorganized sarcomeres, whereas *e105* has normal organization of sarcomeres (Matsunaga et al., 2015: PMID 25851606). This suggests that twitchin has two separable functions, one structural and one regulatory.

3.7. Nuclear function for muscle adhesion proteins?

There is growing recognition that in mammalian striated muscle, a number of Z-disk and M-line proteins, including LIM domain proteins (e.g., MLP, FHL2), translocate to the nucleus in response to mechanical stimuli or extracellular signals, and once inside the nucleus, influence gene transcription (Lange et al., 2006: PMID ; Gautel, 2008: PMID 19181101). In *C. elegans*, some M-line and dense body proteins are also

found in the nucleus (ALP-1, FRG-1, UNC-95, UNC-97, UNC-98, ZYX-1). However, the functional significance of this nuclear localization is unknown. The most significant finding would be to show that proteins from the cell surface shuttle to the nucleus. As noted below, FRAP experiments indicate when either ZYX-1::GFP (Lecroisey et al., 2013: PMID 23427270) or UNC-98::GFP (R.K. Miller and [G.M. Benian](#), unpublished data) are bleached in the nucleus, the nuclear signal reappears, presumably from protein originating from the cytoplasm. However, whether this protein originates from near the cell surface (dense bodies and M-lines) or from cytoplasmic pools is unknown. A definitive experiment would be to use photoactivatable GFP tagged proteins, activate them at the cell surface and then monitor their possible appearance in the nucleus. Such an experiment has not been reported.

In transgenic worms, translational GFP fusions of full-length UNC-97 (Hobert et al., 1999: PMID 9885243), UNC-98 (Mercer et al., 2003: PMID 12808046), UNC-95 (Broday et al., 2004: PMID 15210732), and ZYX-1 (zyxin) (Lecroisey et al., 2008: PMID 18094057; Lecroisey et al., 2013: PMID 23427270) show localization to M-lines, dense bodies, and nuclei. However, antibodies developed to UNC-98 (Mercer et al., 2003: PMID 12808046), to UNC-97 (Miller et al., 2006: PMID 17158957), and to UNC-95 (Qadota et al., 2007: PMID 17761533), when used in immunofluorescent experiments, failed to localize to nuclei under normal conditions. Nevertheless, anti-UNC-98 reacted to nuclei when a non-standard fixation method was used, or when UNC-98 was overexpressed (Mercer et al., 2003: PMID 12808046). Additional support that endogenous UNC-98 and UNC-97 reside in nuclei was obtained during purification of native thick filaments reported in Miller et al., (2006: PMID 17158957): nuclear-enriched fractions contained UNC-98 and UNC-97 detectable by Western blot. In the Y2H system, when either UNC-98 (Mercer et al., 2003: PMID 12808046) or UNC-97 (Mackinnon et al., 2002: PMID 12015115) are fused to the GAL4 DNA binding domain, they can activate transcription, suggesting that UNC-98 and UNC-97 may activate transcription *in vivo*. By testing deletion derivatives of UNC-98::GFP, the N-terminal 110 residues of UNC-98 are sufficient for nuclear localization (Mercer et al., 2003: PMID 12808046). A similar approach by Norman et al., (2007: PMID 17662976) indicates that the LIM2 and LIM3 domains are required for nuclear localization of UNC-97 (PINCH).

Nuclear localization has also been found for the dense body proteins ALP-1 (McKeown et al., 2006: PMID 16278882) and FRG-1 (Liu et al., 2010: PMID 20215405). *alp-1* encodes four isoforms, one is ALP-like (ALP-1A), and three are Enigma-like (ALP-1B, -1C, -1D) (McKeown et al., 2006: PMID 16278882). Use of GFP translational fusions demonstrates a complex pattern of expression of genes encoding these proteins in embryos and adults, and localization to dense bodies and nuclei of muscle and hypodermal (epithelial) cells. In fact, ALP-1 is one of the few integrin adhesion site proteins showing strong localization to embryonic muscle (ALP-1A) and hypodermal cell (ALP-1B, C, D) nuclei. FRG-1 is the *C. elegans* ortholog of the human facioscapulohumeral muscular dystrophy region gene 1 (FRG1) (Liu et al., 2010: PMID 20215405). Antibodies to FRG-1 localize both to dense bodies, and to muscle cell nuclei, concentrated in the nucleoli. FRG-1 bundles F-actin *in vitro*. Overproduction of FRG-1 from the *myo-3* muscle specific promoter resulted in no obvious defects in muscle structure or nematode locomotion. However, when overexpressed from its own promoter, Liu et al. (2010: PMID 20215405) observed disruption of some muscle-muscle lateral junctions and/or absence of some muscle cells in the ventral but not dorsal musculature.

In contrast to most other Pat genes that encode components of the integrin adhesion sites, PAT-9 is exclusively localized to nuclei (Liu et al., 2012: PMID 22616817). This was determined by both antibodies to PAT-9 and use of a PAT-9::GFP translational fusion in transgenic animals. In addition to localizing to embryonic, larval, and adult body wall muscle cell nuclei, PAT-9 also localizes to germline nuclei of the syncytial gonad. Localization is confined to the DAPI poor, presumably nucleolar region. PAT-9 is a 470-residue long protein containing three C2H2 Zn fingers and one predicted nuclear localization sequence (NLS). This NLS was confirmed by transgenic experiments. Given that *pat-9*, like *deb-1*, is a class III Pat gene required specifically for the formation of actin filaments (Williams and Waterston, 1994: PMID 8106547), one hypothesis is that PAT-9 is a nuclear C2H2 zinc finger transcription factor that regulates the expression of genes critical for assembly of dense bodies or thin filaments. However, a yeast one-hybrid screen (Liu et al., 2012: PMID 22616817) showed that PAT-9 is bound to the promoters of five genes (*daf-3*, *tbx-2*, *cog-1*, *let-7*, and *mir-76*). Three of these five genes (*let-7*, *daf-3*, and *tbx-2*) are expressed in body wall muscle by promoter ([WormBase](#)) and/or SAGE analysis (Meissner et al., 2009: PMID 19557190). ChIP assays performed by Liu et al. (2012: PMID 22616817) confirmed that PAT-9 binds to the promoters of *tbx-2* and *daf-3*. An additional gene tested by ChIP was *frg-1*, which, as noted above, encodes a protein localized to dense bodies and muscle cell nuclei. PAT-9 was also found bound to the promoter of *frg-1*.

3.8. Newly identified muscle components—ready for further analysis

Two additional M-line and dense body proteins have recently been reported. These are PKN-1 (PKN) and PXL-1 (paxillin). PKN-1 is the *C. elegans* ortholog of protein kinase N (PKN), an effector of RhoA. The *pkn-1* promoter is expressed in body wall muscle, and a GFP::PKN-1 fusion protein localizes to M-lines and dense bodies (Qadota et al., 2011: PMID 21277858). An intragenic deletion of *pkn-1* or heat shock-induced overexpression of the protein kinase domain has normal sarcomere structure, but displays an unusual “loop Unc” phenotype, which has been reported in many mutants of neuronal genes. The results of mosaic analysis and body wall muscle over-expression of the kinase domain (using the *myo-3* promoter) suggest that this loopy phenotype is due to expression of PKN-1 in body wall muscle.

Warner et al. (2011: PMID 21633109) report that PXL-1 is the nematode ortholog of paxillin, a well-known component of integrin adhesion sites of vertebrates. The protein is expressed in both body wall and pharyngeal muscles. Based on antibody staining and a GFP fusion protein, PXL-1 localizes to dense bodies and M-lines in body wall muscle, and to ring-shaped structures near the sarcolemma in pharyngeal muscle corresponding to podosome-like sites of actin attachment. A *pxl-1* intragenic deletion mutant shows L1 arrest with paralyzed pharyngeal muscle and ultimately lethality, probably due to an inability to feed. The lethality can be rescued by expressing PXL-1 only in the pharynx. Rescued animals develop into adults that show normal locomotion and normal body wall muscle sarcomere organization. Therefore, PXL-1 is not required for the structure or function of body wall muscle. PXL-1 was found to interact with numerous proteins, including UNC-95. In body wall muscle of an *unc-95* null mutant, PXL-1 is mis-localized. In body wall muscle, *pxl-1* is likely to be redundant with a second LIM domain containing protein, LIM-8, since in the pharyngeally-rescued *pxl-1* deletion mutant, RNAi for *lim-8* results in slow moving animals with mildly disorganized sarcomeres. A *lim-8* null mutant has normally organized sarcomeres (Qadota et al., 2007: PMID 17761533).

Meissner et al. (2009: PMID 19557190) reported that an RNAi screen of ~3300 muscle-expressed genes identified 108 new genes that are important for sarcomere assembly and/or maintenance. Actually, two screens were performed, one for new Pat genes, and one for new genes that when knocked down result in abnormal sarcomere organization of adult muscle. In the Pat screen, four new Pat genes were discovered: T27B1.2, F31D5.3, T28B4.3, and F25B3.6. F31D5.3 was independently identified as a Pat gene and re-named *cpna-1* (Warner et al., 2013: PMID 23283987; see below). T27B1.2 was later identified as *pat-9* (Liu et al., 2012: PMID 22616817; see above). The second RNAi screen involved looking for defects in myosin localization in adults by using a GFP::MHC A expressing strain. Myosin mis-localization was observed for RNAi knockdown of 104 genes not previously known to be involved in myofibrillar organization. Many of these genes have human homologs for which little or nothing is known.

In a related study, Meissner et al. (2011: PMID 21611156), using transgenic animals expressing GFP-tagged proteins, determined the sub-cellular localization of 227 muscle-expressed proteins. For most of these, no previous information on sub-cellular localization was known. The authors described 14 different sub-cellular localization patterns within body wall muscle cells (e.g., thick and thin filaments plus or minus dense bodies; dense bodies, M-lines, and attachment sites; dense bodies and attachment sites; dense bodies, cytoplasm (plus or minus M-lines), nucleus; sarcoplasmic reticulum; nucleolus; nucleus; etc.). Localization patterns were obtained for 37 of the 108 new genes identified from their previous RNAi study (Meissner et al., 2009: PMID 19557190). The authors rightly point out that it is somewhat uncertain whether the location of a given protein determined by their study actually reflects the location of a given endogenous protein *in vivo*. This is because the proteins had the ~200 residue GFP molecule attached to their C-termini that could possibly interfere with normal localization and function. In addition, the transgenic approach used is an overexpression situation that could potentially result in mis-localization. Also, all of the proteins were expressed from a single muscle-specific promoter (from T05G5.1), not the genes' own promoter. It will be important to verify these locations by antibodies to endogenous proteins and/or the use of CRISPR to tag the endogenously expressed gene products.

Most recently, Etheridge et al. (2015: PMID 25491313) have reported results of a search for muscle phenotypes by RNAi of a large number of *C. elegans* homologs of proteins that comprise the human integrin-adhesome. The authors knocked down, by RNAi in adults, 113 *C. elegans* genes that are homologs of the 151 human integrin-adhesome proteins and assessed the structure of sarcomeres by the localization of GFP::MHC A, and the structure of integrin attachment sites by localization of UNC-95-GFP. Fifty-five (49%) showed defects in thick filaments, and 22 (19.5%) showed defects in attachment structures. Nine of these genes had not previously been found to have one or more of these defects. What is more impressive from this study, however, is that RNAi of 102 of the 113 targets (90%) resulted in defects in mitochondrial structure as assessed by imaging GFP tagged mitochondria for fragmented or disorganized mitochondrial networks. Moreover, the

authors found that the maximum rates of mitochondrial ATP production from purified mitochondria were decreased in either *unc-52ts* or *unc-112ts* mutants. The analysis of mitochondrial defects is an important contribution to the nematode muscle field. The effects of reduced expression or mutation of sarcomeric and attachment proteins on the organization and function of mitochondria is an underappreciated and understudied area. The authors also knocked down 47 genes that encode new attachment site proteins, as described above by Meissner et al. (2011: PMID 21611156). Similarly, 46 of the 47 genes (98%) resulted in defects in mitochondria, and 15 of the 47 (32%) resulted in defects in thick filament organization and/or the attachment structures. Apparently, reduced expression of mitochondrial proteins can result in disorganization of the myofilament lattice: of the 25 proteins determined to be localized to mitochondria by Meissner et al. (2011: PMID 21611156), four (*mdh-2*, R119.3, T09A5.5, T10B11.6) result in disorganization of thick filaments when knocked down by RNAi (Meissner et al., 2009: PMID 19557190).

Using a new method to enrich for antigens of low abundance from an embryo extract, Takeda et al. (2008: PMID 18498356) have isolated 35 monoclonal antibodies that recognize P granules, muscle, the pharynx, and hypodermal cells. Six of these “KT” series antibodies recognize structures in body wall muscle or the basement membrane. Several have novel localization patterns, including KT12 that seems to recognize the polar regions of A-bands, even more extreme than MHC B. It should prove useful to identify the corresponding immunogens.

Thus, through the studies of Meissner et al. (2009 MID 19557190; 2011: PMID 21611156), Etheridge et al. (2015: PMID 25491313), and Takeda et al. (2008: PMID 18498356), we have many new muscle genes/proteins to study. It will be informative to now characterize the phenotypes of loss-of-function mutants, especially null mutants, for these genes that have been so far only identified through RNAi. It will also be important to study their genetic and biochemical interactions with each other and already known components of muscle. For example, protein-protein interactions could be studied by Y2H assays and binding assays with purified components. In addition, using antibodies or tagged proteins, protein complexes could be identified, and the stoichiometries of the proteins involved can be determined by SILAC-based immunoprecipitations and mass spectrometry.

4. Regulation of the assembly and maintenance of the sarcomere by chaperones and proteases

4.1. Chaperones (UNC-45, UNC-23 and HSP-25)

4.1.1. UNC-45—discovery of a conserved myosin head chaperone

Biochemical studies indicate that myosin heads do not fold spontaneously and require additional proteins (Chow et al., 2002: PMID 12110670; Resnicow et al., 2010: PMID 20080549). The conserved protein UNC-45 was the first myosin head chaperone discovered, and it was first revealed from studies of *C. elegans*. The gene was identified by a temperature sensitive allele, *e286*, which displays sarcomere disorganization and reduced numbers of thick filaments (Epstein and Thomson, 1974: PMID 4845659). When grown at the restrictive temperature, *e286* animals show decreased accumulation of MHC B, but not paramyosin or MHC A (Barral et al., 1998: PMID 9832550). Interestingly, the normal differential localization of MHC A to the middle, and MHC B to the polar ends of the thick filaments is lost: in *e286*, both MHC A and B are found throughout the thick filaments.

The UNC-45 protein is 961 residues long and consists of 3 regions: a TPR (tetratricopeptide repeat) region (3 TPR (34 residue long) repeats), a central unique region, and a UCS (UNC-45, CRO1, She4p) domain (Barral et al., 1998: PMID 9832550; Venolia et al., 1999: PMID 10098931). The UCS domain was defined by sequence homology to two fungal proteins that functionally interact with myosin. The *unc-45* temperature sensitive mutations are amino acid substitutions in the UCS domain whereas Pat embryonic lethal mutants carry stop codons upstream of the UCS domain (Venolia and Waterston, 1990: PMID 2245914; Barral et al. 1998 PMID 9832550). The domains of UNC-45 are functionally distinct in vitro and in vivo. The TPR region binds to heat shock protein 90 (Hsp90), and the central region and UCS domain bind to myosin heads (Barral et al., 2002: PMID 11809970). Moreover, UNC-45 can inhibit the thermal aggregation of myosin heads in vitro, suggesting that UNC-45 chaperones the myosin head (Barral et al., 2002: PMID 11809970). In adult body wall muscle antibodies to UNC-45 localize the protein to the polar regions of the A-band, co-localizing with MHC B (Ao and Pilgrim, 2000: PMID 10648570; Gazda et al., 2013: PMID 23332754). It is curious as to why UNC-45

does not colocalize with MHC A, whose myosin heads presumably also require a chaperone.

Clever single molecule experiments using AFM provide nearly direct evidence that UNC-45 promotes the folding of the myosin head (Kaiser et al., 2012: PMID 22824286). A polyprotein consisting of eight tandem copies of an Ig domain from human titin (with known AFM force-displacement profiles) attached to either full length myosin or myosin S1 heads (from rabbit skeletal muscle) was mechanically stretched three consecutive times, separated by relaxation for 10 seconds to allow refolding of the Ig domains. Normally, a set of Ig domains will spontaneously refold, as indicated by observing the Ig domain sawtooth pattern on a force vs. displacement graph for each consecutive stretch. When performed with the myosin-Ig set polyprotein, the sawtooth pattern was absent in the second and third pulls, suggesting that the unfolded myosin head interferes with refolding of the Ig domains. However, when repeated with inclusion of UNC-45 (mouse UNC-45b), the sawtooth pattern was seen in four consecutive stretches, indicating that the Ig domains serve as a “sensor” for myosin head refolding promoted by UNC-45 (Kaiser et al., 2012: PMID 22824286).

The myosin-binding UCS domain alone is sufficient to rescue both lethal *unc-45* null (Pat) mutants, and ts loss-of-function *unc-45* mutants. Removal of the Hsp90-binding TPR domain from portions of UNC-45 that contain the UCS does not affect this rescue (Ni et al. 2011). Titration experiments demonstrate that, on a per mole basis, UCS has greater activity *in vivo* than full-length UNC-45, suggesting that full length UNC-45 is inhibited by either the TPR domain or its interaction with Hsp90. Using purified recombinant proteins it can be shown that Hsp90 and UNC-45 compete for interaction with myosin. Therefore, Hsp90 has an inhibitory role in relation to the activity of UNC-45 in promoting myosin head folding and/or thick filament assembly (Ni et al., 2011: PMID 21914819).

The sole cytosolic Hsp90 in *C. elegans* is DAF-21 and it is 74% and 76% identical to human Hsp90 α and β , respectively (Birnby et al., 2000: PMID 10790386). RNAi knockdown of *daf-21* in a strain expressing GFP::MYO-3 results in abnormally organized A-bands and aggregates of MYO-3 (MHC A) (Gaiser et al., 2011: PMID 21980476). Moreover, both *daf-21* RNAi animals and the loss-of-function mutant *daf-21(p673)* show decreased motility in a thrashing assay (Gaiser et al., 2011: PMID 21980476). Using a traditional transgenic approach in which YFP::DAF-21 is overexpressed, YFP::DAF-21 localized primarily to the I-band. Interestingly, FRAP indicates that because fluorescence recovered very rapidly and completely ($t_{1/2} \sim 1$ sec), the authors conclude that DAF-21 is freely diffusible and only transiently associated with the I-band.

UNC-45 homologs are found in all metazoa (Price et al., 2002: PMID 12356907); *Drosophila* and *C. elegans* have one UNC-45 gene expressed in all cells; vertebrates have two UNC-45 genes, one expressed in striated muscle (UNC-45B) and one expressed in all cells (UNC-45A). *C. elegans* UNC-45 not only chaperones body wall muscle myosins, it also chaperones NMY-2, a non-muscle myosin II (Kachur et al., 2004: PMID 15454571; Kachur et al., 2008: PMID 18190904). Maternally contributed UNC-45 acts with NMY-2 during embryonic polarity establishment, cytokinesis, and germline cellularization (Kachur et al., 2008: PMID 18190904). In early embryos UNC-45 and NMY-2 co-localize at cell boundaries (Kachur et al., 2004: PMID 15454571). A Y2H library screen with UNC-45 revealed interaction with NMY-2 and with HUM-2, a class V myosin (Kachur et al., 2004: PMID 15454571). Therefore, UNC-45 encoded by its single gene, interacts with, and likely chaperones, both conventional (UNC-54, NMY-2) and unconventional (HUM-2) myosins.

Although we do not know how UNC-45 aids the folding of the myosin head, we do have some insight into the complex mechanism by which UNC-45 aids thick filament assembly. It is very likely that UNC-45 regulates the levels of myosins in coordination with degradation of myosins via the ubiquitin proteasome system (Landsverk et al., 2007: PMID 17438072). Both loss-of-function mutants and transgenic overexpression of *unc-45* lead to decreased myosin accumulation, decreased thick filament assembly, and decreased nematode locomotion (Landsverk et al., 2007: PMID 17438072). By using different segments of UNC-45, it was determined that the overexpression phenotype depends on whether UNC-45 contains the UCS domain (Ni et al., 2011: PMID 21914819). A mechanism compatible with these results is that the concentration of soluble complexes of UNC-45 and mis-folded myosin is rate-limiting for accumulation of normally folded myosin and its assembly; too low or too high concentrations of these complexes lead to shifting to unfolded myosin and its ubiquitylation and proteasomal degradation (Landsverk et al., 2007: PMID 17438072; Epstein and Benian, 2012: PMID 23146617).

The first crystal structure of an UNC-45 type molecule was obtained for *Drosophila* UNC-45 (Lee et al., 2011: PMID 21397190). Although present in the crystal, the TPR domain could not be “seen”, exhibiting either disorder or flexibility relative to the central and UCS domains. The overall shape of the protein is a “horseshoe” with the central region making up the short leg. Interestingly, the entire central and UCS domains

consist nearly entirely of 17 armadillo (ARM) repeats, each consisting of 2-3 α -helices. The crystal structure of *C. elegans* UNC-45 (recombinant protein expressed in *E. coli*) shows that UNC-45 forms a linear multimer (Gazda et al., 2013; PMID 23332754). The length of the repeating unit in this multimer (17.0 nm) is similar to the repeating unit in the staggered arrangement of myosin heads in a thick filament (closest distance between adjacent double heads is 14.3 nm). Although staggering of myosin heads on the surface of thick filaments is dictated by the stagger of 98 residues of parallel myosin rods to optimize charge-charge interactions (McLachlan and Karn, 1982; PMID 7202124), UNC-45 multimers may help stabilize this arrangement during thick filament and sarcomere assembly (Figure 8A). UNC-45 multimers may also be recruited to and assemble onto established thick filaments to assist the refolding of damaged myosin heads.

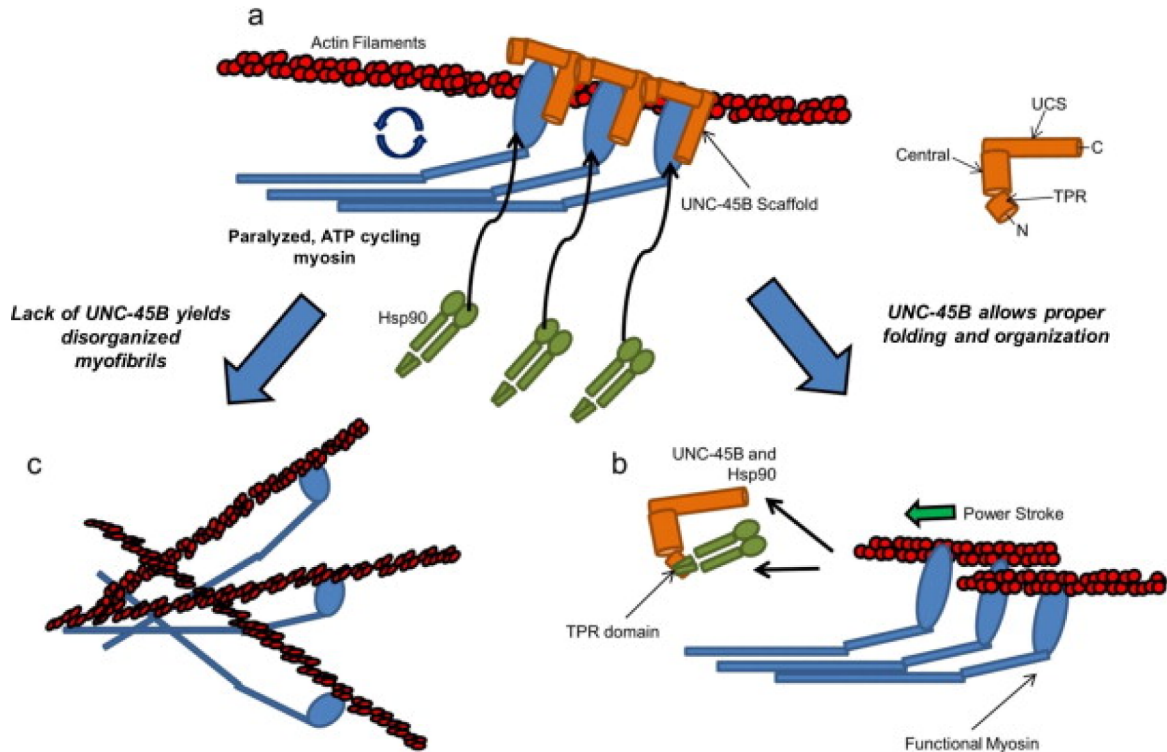


Figure 8. Model for the action of UNC-45 in sarcomere assembly and sarcomere repair. (a) UNC-45 (orange) forms a multimer with periodicity matching the display of myosin heads on the thick filament surface. As thick filaments are forming, or damaged myosin heads are being repaired in mature muscle, the UNC-45 multimer binds to the thick filament allowing hydrolysis of ATP but locking myosin into an actin-bound conformation, without powerstrokes taking place. (b) Addition of Hsp90 results in release of UNC-45 from the thick filament in which myosin heads are properly folded, and powerstrokes are free to occur. (c) The absence of UNC-45 results in the disorganization of the sarcomere, which is then targeted from proteasomal degradation. (Reprinted, with permission, from Nicholls et al. 2014: PMID 25240199)

If UNC-45 promotes the folding of myosin heads and/or maintains the folded state, one would predict that the presence of UNC-45 would enhance the activity of the myosin head. However, surprisingly, Nicholls et al. (2014: PMID 25240199) found the opposite effect. Addition of bacterially expressed mouse UNC-45B to rabbit skeletal muscle myosin or myosin subfragment-1 (S1) inhibited the ability of myosin to move fluorescently labeled actin filaments in a classical actin filament gliding assay. However, UNC-45 did not inhibit myosin ATPase activity, nor did UNC-45B bind to F-actin. Although the TPR domain of UNC-45 can recruit Hsp90, the authors found that Hsp90 on its own did not affect actin gliding, but when Hsp90 was added after the UNC-45-induced halt, Hsp90 reversed it. This Hsp90 reversal of UNC-45 induced halt of myosin motor activity depended on the ATPase activity of Hsp90 as it was inhibited by geldanamycin. Therefore, the authors conclude that UNC-45 inhibits the power stroke but not the hydrolysis of ATP. They go on to further speculate that UNC-45's inhibition of myosin head activity has crucial roles both during formation of sarcomeres and during repair of sarcomeres. That is, while UNC-45 assists the myosin head to attain its native conformation, it prevents powerstrokes that would otherwise be damaging to the assembly. Once the myosin head is properly folded, the inhibited state of the myosin head is relieved when Hsp90 binds to UNC-45 and releases UNC-45 from the myosin head (Figure 8). This model needs to be confirmed by showing that nematode UNC-45 has a similar activity.

4.1.2. UNC-23, a chaperone regulator

Mutations in the *unc-23* gene result in detachment of body wall muscle cells from the hypodermis beginning during mid-larval development (Waterston et al., 1980: PMID 7190524; Plenefisch et al., 2000: PMID 10683173). This detachment only occurs in the front or “head” region of the animal, and results in adults with a thinner head region that is bent. Interestingly, this bent-head phenotype only occurs when *unc-23* mutants are grown on plates; when grown in liquid culture, there is no detachment or bent heads. Nevertheless, when liquid-grown *unc-23* mutants are subjected to mechanical stress by gently rolling them under a coverslip, the muscle cells do detach (Rahmani et al., 2015: PMID 26435886). As worms need to overcome higher surface tension when moving on agar than in liquid, this suggests that the function of UNC-23 is to resist mechanical force in the attachment of muscle cells to hypodermis.

unc-23 encodes potentially 3 isoforms up to 458 residues long (Rahmani et al., 2015: PMID 26435886). At its C-terminus is a 45 residue BAG domain, which UNC-23 shares with human BAG-2, a member of the Bcl-2 associated athanogene (BAG) family of molecular chaperone regulators. In other members of this family, the BAG domain binds to and modulates the activity of the ATPase domain of the heat shock cognate protein 70, Hsc70, thus inhibiting its chaperone activity. A rescuing UNC-23::GFP fusion protein is expressed throughout development and is expressed in both body wall muscle and hypodermis (Rahmani et al., 2015: PMID 26435886). In body wall muscle UNC-23::GFP is localized to dense bodies and M-lines near the sarcolemma, and in hypodermal cells in a pattern similar to intermediate filaments and also in nuclei and nucleoli.

An *unc-23* suppressor screen resulted in isolation of 7 extragenic suppressor strains, two of which are alleles of *hsp-1*, which encodes the nematode ortholog of Hsc70. Both alleles of *hsp-1* are amino acid substitutions in the ATPase domain of the HSP-1 protein. Using the BAG domain of UNC-23 as bait, a screen of a Y2H library yielded multiple clones representing HSP-1, and the minimal region of interaction contained part of the ATPase domain of HSP-1. In support of the genetic and Y2H evidence that UNC-23 and HSP-1 interact, Papsdorf et al. (2014: PMID 25053410) have shown that UNC-23 and HSP-1 interact in vitro, and have also demonstrated that UNC-23 acts as a nucleotide exchange factor. Moreover, Papsdorf et al. (2014: PMID 25053410) show that overexpression of HSP-1 (in transgenic animals expressing *hsp-1p::CFP::HSP-1*) results in a phenotype similar to the bent-head phenotype of *unc-23* loss-of-function mutants. This suggests that the level of the HSP-1 chaperone needs to be tightly regulated to maintain the proper folding of substrates in muscle or hypodermis to maintain the strength of attachment structures. It is known that Hsc70 is also regulated by Hsp40. Interestingly, RNAi knockdown of one of the Hsp40 proteins in *C. elegans*, DNJ-13, suppressed the *unc-23* muscle phenotype (Papsdorf et al., 2014: PMID 25053410). Although UNC-23 is expressed in both muscle and hypodermis, the critical tissue is likely to be the hypodermis; expression of UNC-23 only in muscle was not sufficient to rescue the bent-head phenotype of *unc-23* mutants (Rahmani et al., 2015: PMID 26435886).

Thus, these seminal studies by Rahmani et al. (2015: PMID 26435886) and Papsdorf et al. (2014: PMID 25053410) demonstrate a role for a molecular chaperone (HSP-1) and its regulators, UNC-23(BAG-2) and DNJ-13 (Hsp40), in the maintenance of muscle adhesion complexes so that they function optimally in the transmission of mechanical force generated in muscle, through the hypodermis, and ultimately to the cuticle. It will be interesting to determine which proteins of hypodermal cells, and dense bodies and M-lines in muscle cells, are the substrates of this folding complex—perhaps the folding of only one or a few proteins is critically involved.

4.1.3. HSP-25

Finally, it should be mentioned that HSP-25 was the first molecular chaperone reported to be associated with the sarcomere in *C. elegans* (Ding and Candido, 2000: PMID 10734099). HSP-25 is localized to dense bodies and M-lines (Ding and Candido, 2000). HSP-25 is one of 16 “small heat shock proteins (smHSPs)” in the *C. elegans* proteome (Ding and Candido, 2000: PMID 10734099). smHSPs are found in all kingdoms of life and although they are incapable of catalyzing the refolding of protein substrates, they are able to bind partially unfolded proteins and hold them in a folding-competent state for interaction with other chaperones which can catalyze refolding. The localization of HSP-25 to integrin adhesion sites suggests that HSP-25 may be involved in the maintenance, turnover, or assembly of these structures. Alternatively, the M-lines and dense bodies might represent storage sites from which HSP-25 can exit to assist folding of damaged proteins elsewhere in muscle. Ding and Candido (2000: PMID 10734099) showed that an affinity column of HSP-25 is capable of pulling out DEB-1 and ATN-1 from worm extracts. However, whether these proteins interact directly was not demonstrated. Further, the authors reported that *hsp-25* RNAi resulted in no obvious phenotype (Ding and Candido, 2000: PMID 10734099). Although an analysis of *hsp-25* mutants has not been reported, there is a

nonsense mutation in this gene available in the [Million Mutation Project](#) (MMP) collection (Thompson et al., 2013: PMID 23800452).

4.2. The ubiquitin/proteasome system and calpains

4.2.1. The ubiquitin/proteasome system

The M-line proteins UNC-96 and UNC-98 interact with CSN-5 (Miller et al., 2009: PMID 19535455). Interactions were identified by a Y2H library screen and confirmed by biochemical methods. CSN-5 is a component of the highly conserved “COP9 signalosome complex” that is found in multiple organisms to regulate protein stability, usually through SCF ubiquitin ligases (Cope and Deshaies, 2003: PMID 14505567; Schwechheimer, 2004: PMID 15571808). Anti-CSN-5 antibody co-localizes with paramyosin at A-bands in wild type, and co-localizes with abnormal accumulations of paramyosin found in *unc-98*, *unc-96*, and *unc-15* mutants. RNAi knock down of *csn-5* results in an increase in the level of UNC-98 protein and a slight decrease in the level of UNC-96 protein, suggesting that CSN-5 promotes the degradation of UNC-98 and that CSN-5 stabilizes UNC-96. In *unc-15* and *unc-96* mutants, CSN-5 protein is reduced, implying the existence of feedback regulation from myofibril proteins to CSN-5 protein levels. This implicates for the first time CSN-5 or the COP9 signalosome in myofibrillar organization. These findings are consistent with the ubiquitin proteasome system being required for muscle protein turnover in vertebrate muscle, mediated by the muscle specific ubiquitin ligase Atrogin-1 and the MuRF family (Muscle specific RING Finger proteins) (Bodine et al., 2001: PMID 11679633; Gomes et al., 2001: PMID 11717410).

Moreover, in *C. elegans* muscle, the RING finger protein RNF-5 is localized to dense bodies and regulates the levels of UNC-95 (Broday et al., 2004: PMID 15210732). RNF-5 and UNC-95 interact by Y2H (Didier et al., 2003: PMID 12861019): heat shock induced overexpression of RNF-5 results in a reduction in UNC-95::GFP, and this reduction depends on the presence of an active RING finger domain in RNF-5; in contrast, RNAi mediated knockdown of *rnf-5* results in an increase in UNC-95::GFP (Broday et al., 2004: PMID 15210732).

Both UNC-89 and its vertebrate homolog, obscurin, play important roles in regulating protein turnover in muscle, again, through the ubiquitin/proteasome system. Two segments of UNC-89 (Ig2-Ig3 and 1/3 interkinase-Ig53-Fn2) interact with MEL-26, a substrate recognition protein for cullin 3 (Wilson et al., 2012: PMID 22621901). Cullins, first discovered in *C. elegans* (Bosu and Kipreos, 2008: PMID 18282298), are conserved scaffolds for assembly of the ubiquitin protein degradation machinery, including E3 ubiquitin ligases. By antibody staining, MEL-26 and UNC-89 partially colocalize at sarcomeric M-lines. This was the first time that a component of a cullin complex had been reported in the sarcomere. Loss-of-function (lof) or gain-of-function (gof) mutations of *mel-26* result in disorganization of myosin thick filaments similar to that found in *unc-89* mutants. It had been reported previously that in early *C. elegans* embryos, a target of the CUL-3/MEL-26 complex is the microtubule-severing enzyme katanin (MEI-1) (Furukawa et al., 2003: PMID 14528312; Pintard et al., 2003: PMID 13679921; Xu et al., 2003: PMID 13679922). Lof or gof of *mei-1* also result in disorganization of thick filaments similar to *unc-89* mutants. Genetic data indicated that at least some of the *mel-26* lof phenotype in muscle can be attributed to increased microtubule severing activity of MEI-1. The level of the MEI-1 protein is reduced in an *unc-89* mutant, and MEI-1 is normally degraded by the proteasome. A model proposes that the interaction of UNC-89 with MEL-26 inhibits the activity of the CUL-3/MEL-26 complex from promoting the ubiquitin-mediated degradation of MEI-1. MEI-1 severs microtubules, and this activity is in some way required for thick filament organization in muscle (Wilson et al., 2012: PMID 22621901).

Similarly, Lange and colleagues (2012: PMID 22573887) have reported in their studies on the obscurin knockout mouse that degradation of small ankyrin 1.5 (sAnk1.5) is dependent upon obscurin, and is promoted by a cullin 3 substrate recognition protein, KCTD6. Thus, independent studies point to evolutionarily conserved mechanisms by which UNC-89 or obscurin regulate ubiquitin mediated protein degradation in muscle.

4.2.2. calpains are required for the proper assembly and maintenance of muscle adhesion complexes

Etheridge et al. (2012: PMID 22253611) have reported a fascinating role for integrin adhesion sites in blocking activation of the proteases called calpains. Moreover, calpains were shown to be required for the maintenance of integrin adhesion sites. RNAi in adults for any one of 14 adhesion site proteins (PAT-2, PAT-3,

PAT-4, PAT-6, UNC-52, UNC-97, UNC-112, TLN-1, ZYX-1, UNC-82, ATN-1, DEB-1, CDC-42, and UIG-1) results in decreased levels of cytosolic LacZ, a reporter of muscle protein degradation. Interestingly, RNAi knockdown of one protein, UNC-89, did not result in loss of cytosolic LacZ (UNC-89 may have a role in inhibiting the ubiquitin proteasome system at the M-line (see above). Similar induction of cytosolic LacZ degradation was observed when ts mutants of either *unc-52* or *unc-112* adults were grown at the restrictive temperature. Moreover, the effect was not specific for LacZ; degradation of cytosolic GFP or cytosolic DsRed was also observed in *unc-97(RNAi)* and *unc-112(RNAi)*. Using several chemical inhibitors of the ubiquitin proteasome system or autophagy, and mutants in autophagic pathways or cell death (caspases), the authors found that degradation of cytosolic LacZ could not be blocked. However, they were able to block degradation induced by either *unc-52ts* or *unc-112ts*, by treatment with chemical inhibitors of calpains, or RNAi for any one of five calpain encoding genes (*clp-1*, *clp-4*, *tra-3*, *clp-6*, and *clp-7*). Therefore, they conclude that calpains are the proteases that are activated when integrin attachment complexes are disrupted. Although this study is thorough and rather compelling, one criticism is that it heavily relies on the monitoring of degradation of an overexpressed artificial cytosolic protein. However, the authors did show by quantitative Western blot that an endogenous dense body protein, DEB-1 (vinculin), is also degraded in *unc-112ts* and this degradation can be blocked by a calpain inhibitor. Finally, RNAi against any of the calpain genes resulted in defects in adult muscle, either when RNAi is performed in adults or when RNAi is performed for several generations, including disruption in myofilament lattice array and, at least for *clp-1*, disruption of attachment complexes. Their conclusion is that calpains are required to maintain integrin attachment complexes. This is consistent with the role of calpains in maintaining focal adhesions in vertebrate tissue culture cells (Lebart and Benyamin, 2006: PMID 16884487). A possible mechanism might be that the calpains contribute to the removal of damaged proteins at the attachment complexes.

Loss of proteostasis has emerged as a hallmark of the cellular aging process (Taylor and Dillin, 2011: PMID 21441594). The failure of proteins to fold or to maintain folded states can result in the formation of toxic aggregates and loss of essential cellular functions. Muscle aging, also referred to as sarcopenia, is characterized by the accumulation of misfolded proteins contributing to the loss of skeletal muscle function and mass. In *C. elegans*, progressive locomotory impairment has been described during aging and proposed to be the consequence of a decline in muscle function (Herndon et al., 2002: PMID 12397350). The authors demonstrate that aged muscle shows a progressive decrease in sarcomere organization. In addition, using aggregation-prone PolyQ peptides expressed in muscle cells, Morley et al. (2002: PMID 12122205) demonstrated an age-related increase of protein aggregation and proteotoxicity that correlates with motility decline. These results suggest that maintenance of sarcomere structure and proteostasis, both processes involving molecular chaperones and proteases, are essential for the preservation of correct muscle function. Moreover, because aging as well as the control of proteostasis are cell nonautonomous processes (reviewed in van Oosten-Hawle and Morimoto, 2014: PMID 25030693), molecular chaperones and muscle proteases constitute potential targets to prevent age related-loss of muscle function and potentially an increase in overall healthspan.

5. Roles of giant kinases in regulation of contraction and sarcomere organization

5.1. Introduction

Muscle sarcomeres contain a number of giant polypeptides (>700 kDa), consisting of multiple copies of immunoglobulin (Ig) and fibronectin type 3 (Fn) domains, and one or even two protein kinase domains near their C-termini. These are all related to the largest polypeptide known, titin, which is found in vertebrate striated muscles. Much is currently known about the function of vertebrate titin, including its role in myofibrillar assembly, muscle elasticity, and muscle specific signaling pathways. Mutations in the human titin gene are responsible for a number of myopathies and cardiomyopathies. *C. elegans* muscle contains three such giant protein kinases: twitchin (754,000 Da) located at the outer regions of the A-band, TTN-1 (2.2 MDa) located in the I-band, and UNC-89 (multiple isoforms as large as 900,000 Da) located at the M-line.

In vertebrates, sarcomeres are 2.2-2.5 mm long (distance from Z-disk to Z-disk). However, in many invertebrate muscles, sarcomeres are much longer: in adult *C. elegans* body wall muscle, the sarcomere is about 12 mm long, with thick filaments and A-bands spanning 10 mm. A single polypeptide of vertebrate titin (~3 MDa and 1.2 mm long) spans half a sarcomere, with its C-terminus at the M-line and N-terminus at the Z-disk. However, the dimensions of invertebrate sarcomeres preclude even the possibility of such a polypeptide—it would need to span 6 mm, and have a molecular mass of 15 MDa. Such proteins have not been identified, and not predicted from analysis of genome sequences. Invertebrate titins, such as TTN-1 in *C. elegans* or D-titin in

Drosophila, are ~2 MDa and are restricted to the I-band. One hypothesis is that the function of one titin in vertebrates is served by one continuous polymer of 3 proteins in invertebrates—UNC-89 at the M-line, twitchin in the A-band (multiple molecules), and TTN-1 in the I-band. We already have a hint of such an overlap for twitchin and TTN-1, although each confocal image is not necessarily consistent with this conclusion (Forbes et al., 2010: PMID 20346955). Using conventional confocal microscopy, it has not been determined whether twitchin is localized continuously throughout polar regions of the A-band (e.g., as a polymer), or whether it is located periodically with gaps. Hopefully, super-resolution fluorescence microscopy or immuno-Au EM, combined with epitope-specific antibodies, will resolve these questions.

5.2. Twitchin: the structure of the kinase domain and question of its activation

One of the first protein kinases to have its structure elucidated was that of twitchin kinase (Hu et al., 1994: PMID 8202162). Like the more distantly related myosin light chain kinase, a 60 residue “C-terminal regulatory domain (CRD)”, which lies just C-terminal of the catalytic core of the enzyme, inhibits enzymatic activity (Lei et al., 1994: PMID 8063727). In vitro, using fragments of twitchin kinase, catalytic activity towards a model peptide substrate is low when the CRD is present, and increased when the CRD is missing. The crystal structure of *C. elegans* twitchin kinase (kinase-CRD) revealed that the CRD wedges itself between the two lobes of the catalytic core, and blocks the binding sites for ATP and protein substrate. A similar conformation of the CRD and catalytic core was verified with the crystal structures of *Aplysia* twitchin kinase (Kobe et al., 1996: PMID 9003756), and human titin kinase (Mayans et al., 1998: PMID 9804419).

However, how activation of these protein kinases occurs *in vivo* is unknown. Although calmodulin binds to the CRD of twitchin kinase *in vitro*, it does not lead to significant activation (Lei et al., 1994: PMID 8063727). Nevertheless, it was hypothesized that activation results from small mechanical pulling forces, occurring during normal muscle activity, that are sufficient to remove the CRD from the catalytic pocket and permit binding to substrates. This model was based on steered molecular dynamics (SMD) simulations on human titin kinase (Grater et al., 2005: PMID 15531631), and was in agreement with the observed functional association of titin kinase with certain proteins in a stretch-activated manner (Lange et al., 2005: PMID 15802564). There is also some evidence that stretching force activates twitchin kinase in *Mytilus*: with permeabilized smooth muscles, a 10% stretch results in a 2-fold increase in phosphorylation of a model substrate for molluscan twitchin kinase *in vitro* (Butler and Siegman, 2011: PMID 21286791). Single molecule experiments of titin kinase using atomic force microscopy (AFM) can demonstrate that ATP binds to stretch-induced forms of the kinase (Puchner et al., 2008: PMID 18765796). However, stretch-induced catalysis has not yet been proven for titin kinase or any other giant kinase. Seeking to obtain experimental evidence for the force-induced unfolding of the CRD suggested by the SMD simulations, AFM was used to pull on single molecules of *C. elegans* twitchin kinase (Greene et al., 2008: PMID 18390597). This was the first time that the response of any kinase to pulling force was reported. It revealed that twitchin kinase is significantly resistant to force, unfolding at ~50-80 pN, and surrounded by Ig and Fn3 domains that are more resistant, unfolding at approximately 100 pN. This is what would be expected if the kinase domains of the giant proteins act as force sensors. Moreover, the AFM data demonstrates that the kinase domains unfold in a step-wise manner (rather than all at once for Ig or Fn3 domains), first with the unfolding of the β -sheet-rich smaller lobe, followed by unfolding of the α -helical larger lobe. The sought-after movement of the CRD from the catalytic pocket was not observed, although the noise of the instrument was probably too high.

The crystal structure, *in vitro* kinase assays, and SMDs of a larger segment of *C. elegans* twitchin (Fn-NL-kinase-CRD-Ig), indicate that the regulation of twitchin kinase activity is more complex than previously appreciated (von Castelmur et al., 2012: PMID 22869697). The structure (Figure 9) revealed for the first time that an N-terminal linker (NL), of 45 residues that lies between the Fn and kinase catalytic core, forms a “crown” that rests on the back of the interlobular kinase hinge region, with its remaining chain folded against the N-terminal lobe, sprawling across the β 1- β 2 hairpin (containing the glycine-rich loop in the ATP binding pocket). The NL also makes direct contacts with the catalytic helix aC. Kinase assays reveal that both the CRD and the NL each inhibit catalysis by half, and if both are present, kinase activity is totally inhibited. SMD of this larger structure indicates that it is the NL, and not the CRD, that is mechanically sensitive. In fact, during the SMD, even after the N-terminal lobe has unwound, the CRD remains bound to the folded C-terminal kinase lobe. This, together with the observed catalytic tolerance of twitchin kinase to the CRD, suggests that the CRD might help maintain stabilizing contacts with the kinase domain throughout the catalytic cycle, protecting the active site from mechanical damage (von Castelmur et al., 2012: PMID 22869697). However, whether the CRD is ever removed *in vivo*, and if so, how it is removed remains a mystery.

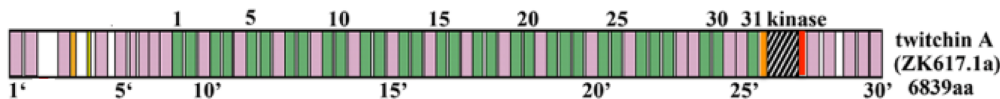
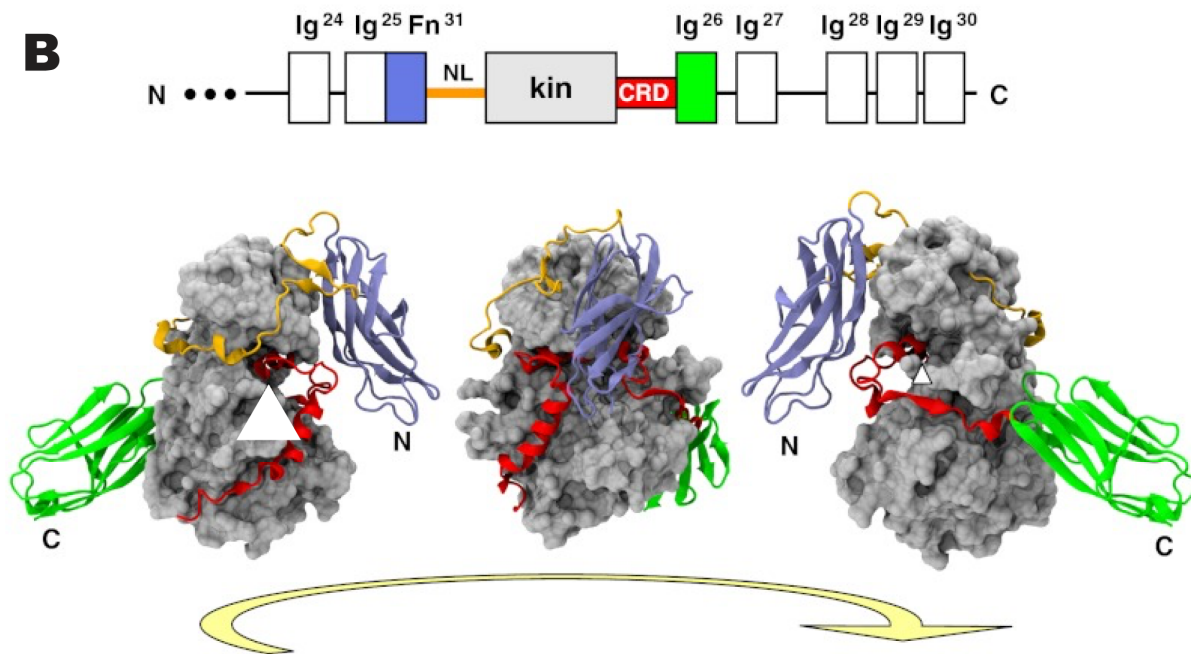
A**B**

Figure 9. Crystal structure of a portion of twitchin containing its protein kinase domain. (A) Schematic representation of domains in the originally described twitchin molecule. Ig domains, violet; Fn3 domains, green; protein kinase domain, as indicated; non-domain regions, clear. (B) On top shows a region of twitchin near its C-terminus, and in color, which portions were included in the new crystal structure. The numbering of domains corresponds to the numbering of domains in (A). NL denotes the N-terminal linker, a 45-residue segment lying between Fn31 and the kinase catalytic core (kin); CRD denotes the “C terminal regulatory domain”, a 60-residue segment that lies between the kinase catalytic core and Ig26. Below shows the crystal structure in three rotated views. A white arrowhead indicates helix α R2 of CRD that blocks the ATP binding site. The CRD wedges itself between the two lobes of the catalytic core (shown in grey space-filling mode), and blocks the binding sites for ATP and protein substrate. The NL forms a “crown” that rests on the back of the interlobe kinase hinge region, with its remaining chain folded against the N-terminal lobe, sprawling across the β 1- β 2 hairpin containing the glycine-rich loop in the ATP binding pocket. The NL also makes direct contacts with the catalytic helix α C. In vitro kinase assays show that both the CRD and the NL each inhibit catalysis by one-half. In steered molecular dynamics (SMD) simulations, it is the NL that first responds to pulling force, whereas the CRD remains bound to the C-terminal kinase lobe. Note that in part B, both in the schematic drawing and crystal structures, the Fn domain is blue and the Ig domain is green (different from Figure 9A and Figure 10). (B, reprinted, with permission, from von Castelmur et al., 2012: PMID 22869697).

A recent report (Matsunaga et al., 2015: PMID 25851606) suggests that the binding to and/or phosphorylation of twitchin’s CRD by MAPKAP kinase 2 is involved in removing the CRD from twitchin’s catalytic pocket. Clones representing a *C. elegans* ortholog of MAPKAP kinase 2 called MAK-1 were isolated upon screening a Y2H library using the twitchin fragment Ig-Fn-NL-kinase-CRD. Minimally, for this interaction to occur, the NL-kinase-CRD of twitchin and residues 81-405 (essentially 58 residues N-terminal of the kinase domain) of MAK-1 are required. By Y2H assays, MAK-1 interacts with twitchin kinase but not comparable regions of UNC-89 or TTN-1. Analysis of a series of twitchin/TTN-1 chimeras indicated that a 140 aa region containing the end of the kinase catalytic core and most of the CRD is crucial for interaction. Using in vitro binding assays with purified recombinant proteins, the CRD was found to be important for binding to MAK-1. The *mak-1* promoter is expressed in body wall muscle, the intestine, and the hypodermis. Antibodies to MAK-1 localize between and around dense bodies, extending into the outer edges of the A-band where there is overlap with twitchin. A likely null allele, *mak-1(ok2987)*, has normal muscle structure but slightly reduced motility in a swimming assay. Exposure of wild type animals to 0.1% nicotine results in paralysis within 30 minutes, but all *unc-22* mutants continue to move. *mak-1(ok2987)* shows partial resistance to nicotine. A *mak-1(ok2987); unc-22 (RNAi)* double mutant shows complete resistance to nicotine. This epistasis suggests that MAK-1 may phosphorylate twitchin kinase. In in vitro kinase assays, active MAK-1 can phosphorylate catalytically dead twitchin kinase. The following model was proposed: the flanking NL and CRD sequences each inhibit twitchin kinase activity by one half; partial activation occurs by mechanical pulling force to remove

the NL from the catalytic pocket; and additional or independent partial activation occurs by the binding and/or phosphorylation of twitchin's CRD by MAK-1. It should be pointed out that physiological substrates for twitchin kinase have not yet been identified.

5.3. TTN-1: a twitchin/titin hybrid in the I-band

In *C. elegans*, the largest polypeptide known is TTN-1 (originally called "CeTitin"), which has a molecular mass of 2.2 MDa. This giant polypeptide was first predicted by analysis of genomic sequence and partial cDNAs (Flaherty et al., 2002: PMID 12381307), and later detected with antibodies (EU143 and 9/10) to two portions of TTN-1 on Western blot (Forbes et al., 2010: PMID 20346955). On [WormBase](#), based on predictions and partial cDNAs, 7 isoforms are listed, generated by alternative 3' ends and alternative splicing. They range in size from ~18,500 residues for isoforms e, f, and g, to 10,578 residues for isoform d, 3,215 residues for isoform c, and ~700 residues for isoforms a and b. On the opposite strand of the largest intron for *ttn-1* (9.5 kb) resides the mutationally defined gene *exp-2*, which encodes a K⁺ channel (Flaherty et al., 2002: PMID 12381307). By immunofluorescence staining, antibodies to TTN-1 localize to the I-band, and may extend into the outer edge of the A-band (Forbes et al., 2010: PMID 20346955). Consistent with this localization, six different 300-residue segments of TTN-1 were shown to variously interact with actin and/or myosin in vitro, using F-actin pelleting assays and myosin ELISAs, respectively (Forbes et al., 2010: PMID 20346955). It should be noted that the first report of TTN-1 localizing between dense bodies (Flaherty et al., 2002: PMID 12381307), in retrospect, was an artifact. The antibody, EU102, had been generated to a portion of TTN-1, but later, surprisingly, was found to only react with KETN-1 (kettin), another poly-Ig domain polypeptide of large size (472 kDa) specific for invertebrates. In transgenic animals, the N-terminal 100 residues of TTN-1 tagged with GFP localizes to dense bodies (Flaherty et al., 2002: PMID 12381307). Therefore, it is likely that single TTN-1 polypeptides have their N-termini embedded at the dense body, and their C-termini extending into the I-band, perhaps into the outer edge of the A-band.

The largest isoform of TTN-1 resembles twitchin in that it contains multiple Ig (56 total) and Fn3 (11 total) domains, and a single protein kinase domain near its C-terminus. In addition, TTN-1 contains five classes of short (14- to 51-residue) repeat motifs arranged mostly as tandem copies: 39- residue repeats forming an ~2400-residue "PEVT region" similar in amino acid composition to PPAK repeats of the PEVK region, the main elastic region of vertebrate titin; 51-residue CEEEI repeats that interrupt the PEVT repeats, similar to the E-rich repeats that interrupt the PPAK repeats in titin's PEVK region; 14-residue repeats making up the 254-residue AAPLE region; 16-residue "BLUE" repeats that make up an ~1500-residue region originally predicted to form a coiled-coil structure; and a 30-residue DispRep repeat present in 15 dispersed copies that punctuate other originally predicted coiled-coil regions. Conformations of synthetic peptides of representative copies of each of the five classes of repeats were studied by circular dichroism (Forbes et al., 2010: PMID 20346955). The data indicate that the PEVT, CEEEI, AAPLE, and DispRep regions are all intrinsically disordered and quite similar to the conformational malleability and elasticity of vertebrate titin PEVK segments. Circular dichroism and modeling studies suggest that the BLUE repeats form long, modular, and unstable α -helical oligomerization domains, suggesting that TTN-1 could perhaps bundle.

Like twitchin kinase, TTN-1 kinase has in vitro kinase activity towards a model peptide derived from vertebrate myosin light chains. Intriguingly, alternative splicing results in two isoforms of the CRD (one is 60 residues, the other is 75 residues), and protein kinase domains with these different-length CRDs have different kinase activities (Flaherty et al., 2002: PMID 12381307). A candidate in vivo substrate for TTN-1 kinase is the dense body UNC-112 interactor UIG-1. The phosphorylation of UIG-1 by TTN-1 may inhibit interaction with UNC-112 (D. Greene, H. Qadotas, and G.M. Benian, unpublished data). Single molecule AFM experiments have revealed that the segment of TTN-1, Fn-kinase-Ig, responds similarly to force as twitchin (Greene et al., 2008: PMID 18390597). The kinase domain of TTN-1 is most similar to the kinase domains of twitchin (54% identical) and less similar to vertebrate titin kinase (39% identical). Interestingly, there is evidence that vertebrate titin kinase is likely to be an inactive pseudokinase (Bogomolovas et al., 2014: PMID 24850911). Therefore, *C. elegans* TTN-1 can be regarded as a "hybrid" between invertebrate twitchin, due to its homologous kinase domain with demonstrable in vitro phosphotransferase activity, and vertebrate titin, due to its multiple tandem repeat regions that are similar to titin PEVK.

Currently, a mutant phenotype for *ttn-1* has not been described. Preliminary RNAi experiments using multiple regions of the coding sequence have failed to reveal anything significant (D.B. Flaherty and G.M. Benian, unpublished data). The [MMP](#) (Thompson et al., 2013: PMID 23800452) lists 374 mutations in *ttn-1*, including 13 nonsense mutations, 3 splicing defects, 2 with deletions in exons, and 2 with insertions leading to frameshifts in exons. Certainly, this issue is ripe for exploration.

5.4. UNC-89, a scaffold for multiple proteins at the M-line

In *C. elegans*, *unc-89* loss-of-function mutants display reduced locomotion, disorganized myofibrils, and lack M-lines (Waterston et al., 1980: PMID 7190524; Benian et al., 1999: PMID 10396143; Small et al., 2004: PMID 15313609). *unc-89* mutants show disorganization of myosin thick filaments by immunostaining of late larvae and adults (Qadota et al., 2008b: PMID 18801371; Wilson et al., 2012: PMID 22621901), although at the L1 larval stage thick filaments are properly organized (Spooner et al., 2012: PMID 22768340). This indicates that UNC-89 is required either for maintenance of sarcomere organization or growth of sarcomeres. *unc-89* is a complex gene: through the use of three promoters and alternative splicing at least eight major polypeptides are generated, ranging in size from 156,000 to 900,000 Da (Benian et al., 1996: PMID 8603916; Small et al., 2004: PMID 15313609; Ferrara et al., 2005: PMID 16453163). The largest of these isoforms, UNC-89-B and UNC-89-F, consist of 53 Ig domains, two Fn3 domains, a triplet of SH3, DH and PH domains near their N-termini, and two protein kinase domains (called PK1 and PK2) near their C termini (Figure 10). Antibodies localize UNC-89 to the M-line (Benian et al., 1996: PMID 8603916; Small et al., 2004: PMID 15313609).

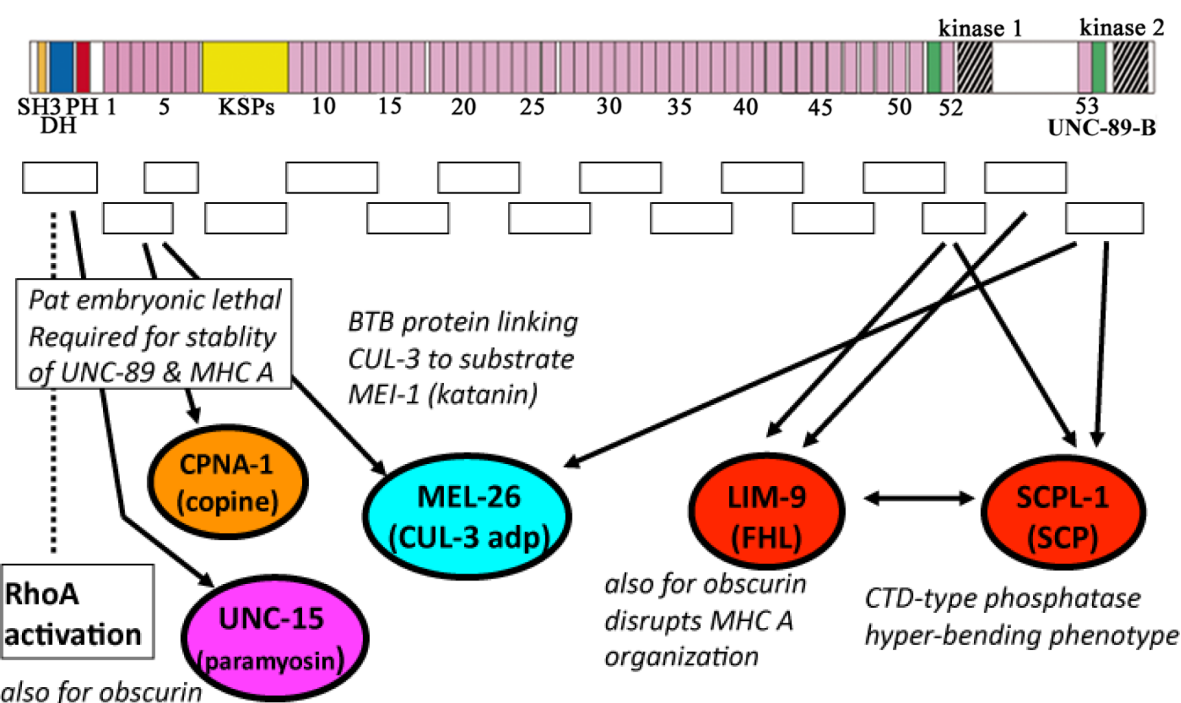


Figure 10. Progress in identifying proteins that interact with the giant protein UNC-89. On top is a schematic representation of domains in the largest UNC-89 isoform, UNC-89-B, which contains 8081 residues. Ig domains, violet; Fn3 domains, green; a 645 residue long region containing multiple copies of the 3 amino acid triplet KSP, yellow; protein kinase domains, SH3, DH, and PH domains, as indicated. Open rectangles beneath this schematic denote segments used for screening a Y2H library. Interactions have been verified by a combination of demonstrating binding in vitro using purified recombinant proteins, co-immunolocalization in muscle, and identifying muscle mutant phenotypes. Interacting proteins identified so far are indicated as ovals with their protein names (including in parentheses the names of the human homolog or nature of the protein) with arrows leading from the segments of UNC-89 that interact with them. Brief descriptions of the type of protein (e.g., CTD-type phosphatase) and/or mutant phenotype of the interacting protein (e.g., Pat embryonic lethal) are indicated.

The human homolog of UNC-89 is obscurin, which was identified five years after UNC-89 was characterized at the molecular level (Bang et al., 2001: PMID 11717165; Young et al., 2001: PMID 11448995). While obscurin contains all the same domains as UNC-89, the SH3, DH, and PH domains are located near the C-terminus rather than near the N-terminus as they are in UNC-89. Although UNC-89 is located only at the M-line, various obscurin isoforms are located at either the M-line, or the Z-disk (Young et al., 2001: PMID 11448995; Bowman et al., 2007: PMID 17382936).

To learn how UNC-89 is localized and performs its functions, the Benian laboratory is systematically identifying its binding partners. The coding sequence for the largest isoform, UNC-89-B, is entirely represented as a set of 17 overlapping segments in Y2H vectors. All 17 have been used to screen both a Y2H bookshelf of 23 known components of the nematode M-line, and a Y2H cDNA library. Published interactions are

summarized in Figure 10. Each of the kinase domains, PK1 and PK2, interact with SCPL-1 (Qadota et al., 2008a; PMID 18337465), a CTD-type protein phosphatase. Previously, CTD phosphatases were known to be involved in the regulation of transcription. The UNC-89 to SCPL interaction suggests a new function for this class of phosphatases in sarcomere specific signaling through giant muscle protein kinases. *scpl-1* mutants show “hyper-bending” during locomotion (Nahabedian et al., 2012; PMID 22126736; see above), and are defective in egg laying muscle function (Qadota et al., 2008a; PMID 18337465). Both the PK1 region and the “interkinase region” each interact with LIM-9 (Xiong et al., 2009; PMID 19244614), the closest worm homolog of the human protein FHL2 (“four and a half LIM domains” protein) (Lecroisey et al., 2013; PMID 23427270). *lim-9(RNAi)* shows aggregates of myosin (Meissner et al., 2009; PMID 19557190). Recently, a similar interaction between vertebrate obscurin and FHL2 has been reported (Hu and Kontrogianni-Konstantopoulos, 2013; PMID 23392350). As noted above, LIM-9 was identified as a binding partner of UNC-97 (PINCH) (Qadota et al., 2007; PMID 17761533), a member of the four protein complex associated with integrin, suggesting a connection between the integrin adhesion complex and UNC-89.

The DH-PH region of UNC-89 activates RHO-1 (RhoA) specifically, and attenuated RNAi for *rho-1* results in disorganization of muscle thick filaments (Qadota et al., 2008b; PMID 18801371). A similar interaction between RhoA and obscurin has also been demonstrated (Ford-Speelman et al., 2009; PMID 19605563). Ig1-3 of UNC-89 interacts with CPNA-1, a copine domain protein with human and mouse homologs, located at both M-lines and dense bodies (Warner et al., 2013; PMID 23283987). As noted above, loss-of-function of *cpna-1* is Pat embryonic lethal (Meissner et al., 2009; PMID 19557190). Although CPNA-1 is not required for initial assembly of UNC-89 and MHC A at the M-line, it is required for retention of these proteins at the M-line, once embryonic muscle contraction begins. It is interesting to note that the N-terminal half of PAT-6 (actopaxin) interacts with CPNA-1. This interaction is supported by genetic data: in embryos, in a *pat-6* null mutant, CPNA-1 is mis-localized; in adults subjected to *pat-6(RNAi)*, CPNA-1 is found in abnormal accumulations or misclocalized (Warner et al., 2013; PMID 23283987). The PAT-6 to CPNA-1 to UNC-89 interactions suggests another way in which UNC-89 is localized to the integrin adhesion complex of the M-line.

Most recently, the SH3 domain of UNC-89 has been reported to interact with paramyosin, the invertebrate-specific protein with significant homology with myosin rods (Qadota et al., 2016; PMID 27009202). The SH3 domain interacts with an 82 amino acid segment (residues 294-376) of the mostly coiled-coil 873 residue-long paramyosin. *unc-89* mutants lacking expression of giant isoforms that contain the SH3 domain (e.g., *su75* and *r452*) show paramyosin aggregates. Overexpression of the SH3 domain results in mis-localization of paramyosin. This interaction is unexpected for two reasons. First, SH3 domains usually interact with proline rich sequences that are absent in coiled-coil proteins like paramyosin. Nevertheless, there are several targets of SH3 domains that have been shown to lack the proline-rich consensus sequence (reviewed in Saksela and Permi, 2012; PMID 22710157). Second, the model for the structure of the nematode thick filament is that it consists of an outer layer of myosins MHC A and B, an intermediate layer of paramyosin, and an inner layer of paramyosin and filagrinins (Deitiker and Epstein, 1993; PMID 8408214; Liu et al., 1998; PMID 9442110). The vertebrate M-line is observed by EM to be a structure in which the shafts of the thick filaments are crosslinked at their surfaces by a series of struts and additional filaments (Knappeis and Carlsen, 1968; PMID 5691974; Luther and Squire, 1978; PMID 731697). Assuming that the nematode M-line has a similar structure, it is difficult to understand how UNC-89 interacts with the thick filament. One possibility is that the myosin surface of the thick filament shaft has small openings that allow penetration of UNC-89’s SH3 domain into the intermediate or core layers that contain paramyosin. Another possibility is that during sarcomere assembly paramyosin and UNC-89 associate before they are incorporated into thick filaments and M-lines. In support of this idea, during embryonic muscle development paramyosin is detected in 420 minute embryos (Epstein et al., 1993; PMID 8349734) during which thick filament precursors are being assembled, and this is the same time at which UNC-89 is first detected (Hresko et al., 1994; PMID 8106548).

At least five isoforms of UNC-89 contain two protein kinase domains of the titin/twitchin family. The importance of the kinase region of UNC-89 is demonstrated by the fact that three mutant alleles of *unc-89*, *tm752*, *ok1116*, and *st79*, eliminate all detectable expression of the kinase-containing isoforms, but retain the non-kinase containing isoforms (Ferrara et al., 2005; PMID 16453163), and show disorganization of the myofilament array by polarized light microscopy. UNC-89 isoforms -B, -F, and -H contain two complete protein kinase domains called PK1 and PK2 (Small et al., 2004; PMID 15313609). In contrast, UNC-89-C and -D, controlled by alternative promoters, begin with partial kinase domains. Homology modeling shows that PK1-C and PK1-D are the large lobes of a protein kinase domain, preceded by a hinge, and homologous N-terminal tails that form similar β -turn- β structures. The functional significance of such partial kinase domains is unknown. Each complete kinase domain found in the other isoforms follows the topology of a typical two-lobed kinase. However, examination of the residues forming an expected ATP binding pocket suggests that PK2 is an

active kinase, but that PK1 is not catalytically active. Using in vitro kinase assays, PK2 can phosphorylate several model peptide substrates, and thus, indeed is an active kinase (T. Ferrara and [G.M. Benian](#), unpublished data).

The general structure of a kinase, an intervening sequence of 450-1100 residues, and a second kinase, is conserved in four proteins: *C. elegans* UNC-89, fly Unc-89 (obscurin), vertebrate obscurin, and SPEGb. Within the intervening or interkinase region, all four proteins have an Ig followed by an Fn3 domain N-terminal of the second kinase, but otherwise there is no significant homology. The interkinase region has low sequence complexity in all four proteins and high proline content in UNC-89, obscurin, and SPEGb (11.8, 13.7 and 13.3%). The interkinase regions are similar in length for UNC-89, obscurin, and SPEGb (905, 955, and 1098 aa), but shorter in fly Unc-89 (457 aa). The low sequence complexity and high proline content is reminiscent of the well-known molecular springs of titin (PEVK, N2B, and N2A). Preliminary experiments using AFM demonstrate that application of force upon the interkinase of UNC-89 results in a smooth and gradual force extension curve consistent with a highly elastic random coil ([A.F. Oberhauser](#) and [G.M. Benian](#), unpublished data).

VAV-1 is a guanine nucleotide exchange factor (GEF) for Rac that regulates the concentration of intracellular Ca^{2+} and rhythmic behaviors such as pharyngeal pumping (Norman et al., 2005: PMID 16213217). *vav-1* is widely expressed, including in the pharynx and body wall muscle. Overexpression of *vav-1* in body wall muscle results in decreased locomotion. Mutagenesis of this strain led to isolation of suppressor mutations that reduce impaired movement; these suppressors are loss-of-function alleles of *egl-19* and *unc-89* (Spooner et al., 2012: PMID 22768340). EGL-19 is an L-type voltage gated Ca^{2+} channel, and isolation of an *egl-19* mutant is consistent with VAV-1 regulating Ca^{2+} signaling. However, isolation of an *unc-89* mutant, *ak155*, was unexpected. This finding is compatible with the previously described role of obscurin as a linking molecule between sarcomere and sarcoplasmic reticulum (SR), through interaction of obscurin with the SR membrane protein small ankyrin 1 and 2 (Bagnato et al., 2003: PMID 12527750; Kontogianni-Konstantopoulos et al., 2003: PMID 12631729). It is also compatible with the disorganization of the SR observed in skeletal muscle in the obscurin knockout mouse (Lange et al., 2009: PMID 19584095).

To obtain more direct evidence that UNC-89 has a role in Ca^{2+} signaling, a gof mutation in *egl-19* that shows a short hyper-contracted body phenotype was used. The double mutant, *unc-89(ak155); egl-19(gof)* was suppressed for the hyper-contracted phenotype (Spooner et al., 2012: PMID 22768340). Both the *vav-1* overexpression and *egl-19(gof)* phenotypes can be suppressed by the canonical *unc-89* allele, *e1460*. Both *ak155* and *e1460* are nonsense mutations lying in the coding sequences for Ig domains 15 and 21, respectively. These mutations are predicted to disrupt the large UNC-89 isoforms, but not the short kinase-containing isoforms, since the short isoforms are controlled by promoters lying downstream of the *ak155* and *e1460* mutation sites. *unc-89(st79)*, which contains a stop codon in the Ig domain lying just N-terminal of the second kinase domain (Ferrara et al., 2005: PMID 16453163) and does not express the small isoforms, cannot suppress *vav-1(gof)* and *egl-19(gof)* (Spooner et al., 2012: PMID 22768340). Similarly, RNAi of the kinase containing isoforms of *unc-89* could not suppress *vav-1(gof)*, while RNAi of the large UNC-89 isoforms could. Therefore, the large Ig-rich isoforms of UNC-89, but not the kinase encoding isoforms of UNC-89, are involved in Ca^{2+} signaling. Also, it was found that *unc-89* acts in the same genetic pathway as *egl-19* and *unc-68*, which encodes the ryanodine receptor (RyR), and both the RyR and the SR calcium ATPase (SERCA), a Ca^{2+} reuptake pump, are mislocalized in *unc-89* mutants lacking the large Ig-rich isoforms (Spooner et al., 2012: PMID 22768340). These data suggest that UNC-89 plays a critical role in Ca^{2+} signaling in the body wall muscle. Indeed, using the Ca^{2+} sensor, yellow cameleon YC3.60, although there are reliable Ca^{2+} transients in *unc-89(ak155)*, the peak amplitudes are reduced and there is a delay in the time required to reach maximal Ca^{2+} concentration, as compared to wild type (Spooner et al., 2012: PMID 22768340).

The functional implications of the different UNC-89 interactions are various: CPNA-1 stabilizes UNC-89 at the M-line in embryonic muscle, the interaction of UNC-89 with UNC-15 (paramyosin) is important for thick filament assembly or stability, and interaction with LIM-9 helps UNC-89 localize to the M-line through LIM-9's interaction with UNC-97 and UNC-97's interaction (via UNC-112, PAT-4 and PAT-6) with integrin. The other interactions seem related to UNC-89's influence on enzymatic activities at the M-line—thus, the DH-PH region of UNC-89 activates RHO-1 (RhoA), UNC-89 is likely to inhibit the activity of the CUL-3/MEL-26 complex from promoting ubiquitin-mediated degradation of MEI-1 and possibly other substrates, the interaction of UNC-89 kinase domains with SCPL-1 may be involved in some type of signaling in which the kinase activates or inhibits the phosphatase (or vice versa), or each has antagonistic activity towards the same unknown substrate(s).

6. New insights into dystrophin function from *C. elegans*

6.1. Structure and localization of the DYS-1 protein

The skeletal muscle isoform of human dystrophin is a 427 kDa (3685 amino acids) sub-sarcolemmal protein. The X-linked dystrophin gene is 2.5Mb, making it one of the largest human genes, occupying about 1% of the X chromosome. Mutations that abrogate dystrophin function lead to Duchenne Muscular Dystrophy (DMD), a severe progressive muscle wasting pathology, affecting about one out of 3500 male births (Hoffman et al., 1987: PMID 3319190; Koenig et al., 1987: PMID 3607877; Emery, 1991: PMID 1822774; Emery, 2002: PMID 11879882). Dystrophin localizes at costamere muscle adhesion complexes and the neuromuscular junction (NMJ) (Rybakova et al., 2000: PMID 10974007; Pilgram et al., 2010: PMID 19899002). The protein binds on its N-terminal end to the actin cytoskeleton, and on the C-terminal end to a large multi-protein complex, the Dystrophin Glycoprotein Complex (DGC), thus forming a bridge between the cytoskeleton and the sarcolemma and extracellular matrix. The DGC is composed of at least 10 proteins: the intracellular proteins α -dystrobrevin and syntrophins, the trans-membrane proteins β -dystroglycan, α -, β -, γ -, δ - sarcoglycans, and sarcospan, and the extra-cellular proteins laminin 2 and α -dystroglycan (reviewed in Blake et al., 2002: PMID 11917091).

The highly conserved dystrophin protein consists of three major domains. In the N-terminus the actinin-like domain is important for actin binding. The C-terminal region contains a cysteine-rich domain as well as WW, EF, hand and ZZ modules, which are important for dystrophin to bind to β -dystroglycan, and a coiled-coil domain which is important for dystrobrevin binding. The rod region is composed of 24 helical spectrin-like repeats which are important for actin binding as well as phospholipid binding in addition to structural integrity.

Dystrophin is thought to play a structural role in ensuring membrane stability and force transduction during muscle contraction. In addition, the DGC provides a scaffold for various signaling and channel proteins, which may implicate dystrophin and the DGC in regulation of signaling processes (Constantin, 2014: PMID 24021238). However, it has not been clearly established yet why muscles degenerate in the absence of dystrophin, and in particular whether the pathology observed in DMD patients is due to a mechanical weakness of the sarcolemma, or if it results from a secondary impairment of proteins displaced because of the absence of dystrophin.

C. elegans has a dystrophin-like protein encoded by the *dys-1* gene. The *dys-1* gene is expressed in pharyngeal, vulval and striated body wall muscles of *C. elegans* (Bessou et al., 1998: PMID 9933302). Sub-cellular analyses using a monoclonal antibody to DYS-1 or a DYS-1::GFP expressing strain showed that DYS-1 localizes in body wall muscles similarly to its vertebrate counterparts—under the sarcolemma of striated body wall muscle, at I bands near the dense bodies, and in muscle arms (the postsynaptic elements of the NMJ in the *C. elegans* muscle) (Dixon and Roy, 2005: PMID 15930100; Brouilly et al., 2015: PMID 26358775).

The *dys-1* gene contains 46 exons spanning 31 Kb. DYS-1 has two distinct isoforms, though the function of the short isoform B is currently unknown and will not be further discussed here. Isoform A is a 3,674-amino acids protein (Figure 11), which shares extensive sequence similarities with its mammalian counterparts, including several similar key motifs: the N-terminal actinin-like domain (20% homology with human dystrophin), the central rod-like domain (10 % of homology with human dystrophin) composed of repetitions of spectrin-like triple helices, the C-terminal region (37% of homology with human dystrophin) containing a WW domain, a cysteine-rich domain, and at the very C-terminal end, a coiled-coil domain. Furthermore, the nematode protein seems to have some functional properties in common with its human counterpart, since a chimeric gene containing 80% of human dystrophin coding sequence is able to partly rescue the phenotype of *dys-1* mutants (Bessou et al., 1998: PMID 9933302).

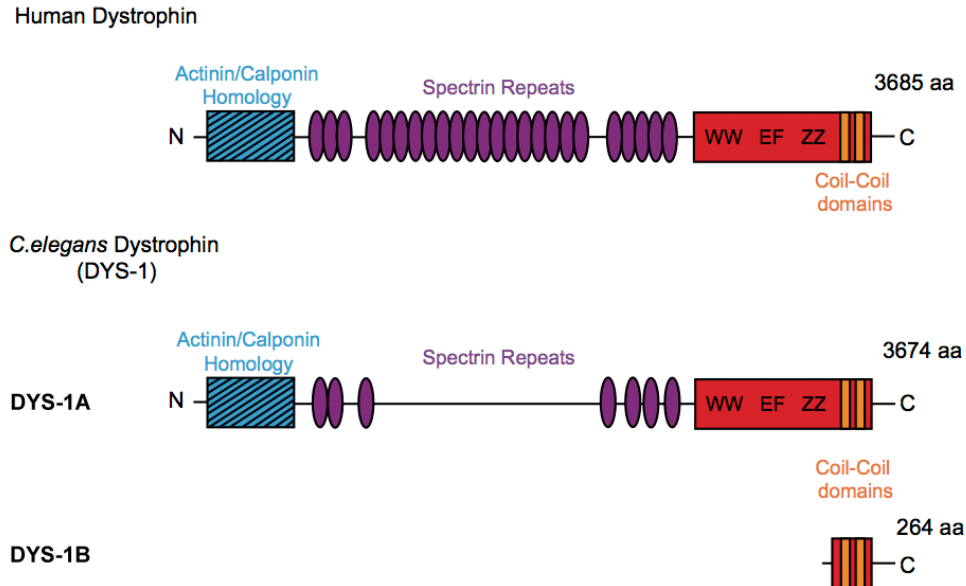


Figure 11. Structure of human and *C. elegans* dystrophin proteins.

The structure of the large muscular isoform of human muscular dystrophin is presented (adapted from Blake et al., 2002: PMID [11917091](#)) along with the two isoforms (A and B) of *C. elegans* DYS-1. The size of human dystrophin and DYS-1 isoform A is approximately analogous. The N-terminal ends of these proteins share 20% homology and correspond to an actinin/calponin like actin binding domain (blue). The C-terminal ends share 37% homology and contain WW, EF Hand, and Zinc Finger (ZZ) motifs as well as a coiled-coil domain (orange). The central rod domain, which shares only 10% homology, contains helical spectrin-like repeats (purple). The distribution and abundance of spectrin repeats varies between species, 24 were found in the sequence of human dystrophin and 7 in DYS-1A. The predicted short isoform DYS-1B corresponds to the last 237 amino acids of isoform A. Figure designed by [M. Baritaud](#).

6.2. The function of DYS-1 and the DGC in cholinergic transmission and calcium homeostasis

dys-1 loss-of-function mutants are viable, undergo slight muscle degeneration (see below), and have a peculiar phenotype consisting of hyperactivity, exaggerated head bending, and a tendency to hyper-contract. Moreover, *dys-1* mutants are hypersensitive to acetylcholine and to the acetylcholine esterase (AchE) inhibitor aldicarb, suggesting that the absence of functional dystrophin up-regulates cholinergic transmission in *C. elegans* (Bessou et al., 1998: PMID 9933302). It was also shown that AchE activity was reduced in *dys-1* mutants (Giugia et al., 1999: PMID 10606735). However, since *dys-1* and AchE mutants have different phenotypes in *C. elegans*, AchE activity modulation alone was not sufficient to explain the *dys-1* mutant phenotype. Evidence for a role of dystrophin in cholinergic transmission came from forward genetic screens aimed at recovering other mutations leading to a *dys-1*-like phenotype. This work led to the identification of several other genes. One of these genes turned out to encode a dystrobrevin ortholog, a protein known to interact with dystrophin in mammals. Two other genes encoded SLO-1, a calcium-dependent BK potassium channel (Wang et al., 2001: PMID 11738032), and DYC-1, a protein homologous to the CAPON adaptor protein (Gieseler et al., 2000: PMID 10996789; Carre-Pierrat et al., 2006: PMID 16527307; Lecroisey et al., 2008: PMID 18094057). Finally, the isolation of mutations in the *snf-6* gene, leading to the same phenotype as mutations in *dys-1*, strongly suggested that increased Ach levels at the NMJ may contribute to the *dys-1* phenotype (Kim et al., 2004: PMID 15318222; Ségalat and Anderson, 2005: PMID 15483645). Indeed, the *snf-6* gene encodes an acetylcholine/choline transporter, which regulates the uptake of acetylcholine at neuromuscular junctions.

In addition to dystrophin (DYS-1) and dystrobrevin (DYB-1), *C. elegans* has other orthologs of vertebrate DGC proteins, such as δ/γ -sarcoglycan (SGN-1), syntrophins (STN-1 and -2), α - and β -sarcoglycans (SGCA-1 and SGCB-1), and dystroglycan (DGN-1). No sarcospan counterpart was found (Grisoni et al., 2002: PMID 12234669; our unpublished results). DYS-1 was shown to interact with DYB-1 and STN-1 suggesting that a DGC may exist in *C. elegans* (Gieseler et al., 1999a: PMID 10369883; Gieseler et al., 1999b: PMID 10561496; Grisoni et al., 2003: PMID 14499607). In addition, mutation or RNAi mediated gene knock down led to a *dys-1* phenotype for some of the DGC ortholog encoding genes: *dyb-1*, *stn-1*, *stn-2*, *sgn-1*, and *sgca-1* (Gieseler et al., 1999a: PMID 10369883; Grisoni et al., 2002: PMID 12234669; Grisoni et al., 2003: PMID

14499607; Zhou et al., 2008: PMID 18791240; our unpublished observations). Mutations in the *dgn-1* gene lead to different phenotypes and the gene is not expressed in muscle (Johnson et al., 2006: PMID 16611689), thus *dgn-1* function is not linked to *dys-1*. DYB-1, STN-1, and STN-2, however, are expressed in neurons and striated body wall muscles where all localize at sarcomeres, close to dense bodies. For *sgn-1*, *sgca-1*, and *sgcb-1* the expression pattern has, to our knowledge, not yet been analysed. Interestingly, STN-1 interacts with SNF-6, and in *dys-1* and *stn-1* mutants SNF-6 localization at NMJ is lost (Kim et al., 2004: PMID 15318222). Together, this strongly suggests a role for DYS-1 and the associated DGC in cholinergic neurotransmission at the NMJ, and this role may in part be responsible for the hyperactivity/hypercontraction phenotype of *dys-1* and DGC mutants (Figure 12).

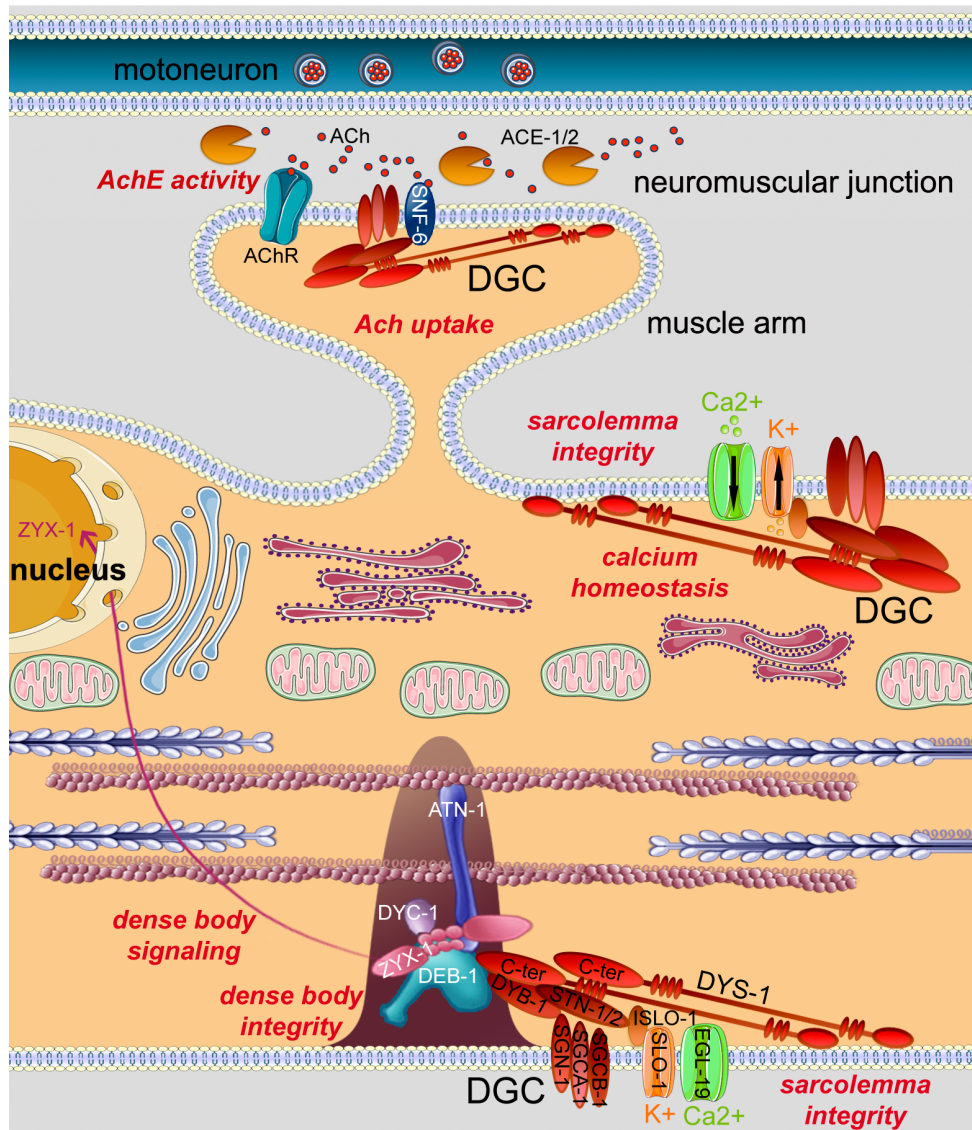


Figure 12. Functions of DYS-1 and associated proteins in muscle

Part of a muscle cell is shown with one dense body anchored to the distal sarcolemma. Actin containing filaments are anchored to the dense body and interact with myosin containing thick filaments. Cellular organelles such as the nucleus, mitochondria, and endoplasmic reticulum with ribosomes are localized in the deeper part of the muscle cell. A muscle arm corresponding to the postsynaptic elements of the neuromuscular junction in the *C. elegans* muscle is represented in close contact with a motoneuron. DYS-1 and the associated Dystrophin Glycoprotein Complex (DGC, represented in red) fulfill different functions in muscle. DYS-1 is involved in maintaining dense body and sarcolemma integrity. DYS-1 localizes under the entire sarcolemma of striated body wall muscle and in muscle arms. Through the interaction of its C-terminal end with the dense body protein DEB-1 (vinculin; blue), DYS-1 links the DGC to the dense body. The LIM-domain protein ZYX-1, which interacts with DEB-1, ATN-1, and DYC-1 may be involved in signaling from the dense body to the nucleus, thus linking DYS-1 and DGC function to dense body signaling. The interaction of ISLO-1 with STN-1 and SLO-1 connects the K⁺ channel, SLO-1, to the DGC. SLO-1 localizes close to the L-type Ca²⁺ channel EGL-19. SLO-1 mediated potassium efflux is thought to negatively regulate the calcium-mediated activation of muscle, thus involving DYS-1 and DGC in the control of calcium homeostasis. At the neuromuscular junction acetylcholine (Ach) binding to its receptor (AchR) leads to muscle excitation. DYS-1 and the DGC are involved in cholinergic transmission by controlling ACE-1/2 acetylcholine esterase (AchE) activity and Acetylcholine (Ach) uptake through the acetylcholine/choline transporter SNF-6, which interacts with STN-1.

In addition, several lines of evidence indicate that disturbed calcium homeostasis may contribute to this phenotype. The identification of *islo-1*, encoding a sub-unit of SLO-1, a voltage-, and calcium-dependent potassium (BK) channel, and the interaction of ISLO-1 with STN-1 and SLO-1 connect SLO-1 to the DGC. Mutations in either *slo-1* or *islo-1* mimic the *dys-1* phenotype. In addition, SLO-1 localizes close to the L-type calcium channel EGL-19, and this localization is lost in either *dys-1* or *islo-1* mutants. It has, therefore, been proposed that loss of DYS-1, and other DGC components, may contribute to increased calcium-mediated responses by disturbing the SLO-1 mediated potassium efflux thought to negatively regulate the calcium-mediated activation of muscle (Kim et al., 2009: PMID 20019812). Along this line, another study using in vivo single-molecule imaging identified altered dynamics of the subunit UNC-36 of the L-type calcium channel EGL-19 in *dys-1* mutants (Zhan et al., 2014: PMID 25232639).

6.3. The function of DYS-1 in dense body and sarcolemma integrity

In *C. elegans* the loss of *dys-1* function only leads to moderate muscle cell death as observed by progressive loss of actin filaments and muscle nuclei (Bessou et al., 1998: PMID 9933302; Oh and Kim, 2013: PMID 24191049). This indicates that the *C. elegans* muscle is more resistant to the loss of dystrophin function than human muscle. However, the amount of muscle cell death (referred hereafter as muscle degeneration) significantly increased when a *dys-1* loss-of-function mutation was combined with a hypomorphic mutation in the *hh-1* gene (Gieseler et al., 2000: PMID 10996789). In addition, muscle degeneration increases in both the *dys-1(cx18)* single mutant and the *dys-1(cx18); hh-1(cc561)* double mutant with higher body bending forces on firm culture medium, supporting the hypothesis of a mechanical role for DYS-1 (Brouilly et al., 2015: PMID 26358775). This result is in agreement with studies performed in dystrophin deficient *mdx* mice that revealed a higher vulnerability and enhanced dystrophic progression in response to exercise (Brussee et al., 1997: PMID 9447605; De Luca et al., 2003: PMID 12490622).

Dystrophin plays an important role in linking the cytoskeleton to the sarcolemma and was thus hypothesized to protect against contraction-induced muscle damage via tension transmission and stabilization of the sarcolemma (Blake et al., 2002: PMID 11917091). In vertebrate skeletal muscle, dystrophin is associated with costameres, which link the sarcomeres to the sarcolemma through an association with Z-disks. The *C. elegans* dense body fulfills the function of both vertebrate Z-disks and costameres and plays a role in transducing the force generated by sarcomeres to the extracellular matrix (Figure 1A and B; Figure 5). In Y2H experiments, DYS-1 interacts with the vinculin ortholog DEB-1, which localizes at the bases of dense bodies (Brouilly et al., 2015: PMID 26358775). This suggests that DYS-1 links the DGC to the dense body. Indeed, different proteins belonging to or associated with the DGC have been localized to dense bodies, including DYC-1, which is not directly associated with the DGC but interacts with the LIM domain protein ZYX-1 (ZYX-1 interacts with ATN-1 and DEB-1), and ZYX-1 was shown to be involved in DYS-1 dependent muscle degeneration (Lecroisey et al., 2008: PMID 18094057; Lecroisey et al., 2013: PMID 23427270; our unpublished results) (Figure 12). Most interestingly, mutations in DGC ortholog encoding genes not only lead to the *dys-1* hyperactivity/hypercontraction phenotype, but also cause muscle degeneration in the sensitized genetic *hh-1(cc561)* background: *snf-6*, *slo-1*, *sgca-1*, *dyb-1*, *stn-1*, or *dyc-1* (Gieseler et al., 1999a: PMID 10369883; Gieseler et al., 2000: PMID 10996789; Grisoni et al., 2003: PMID 14499607; Kim et al., 2004: PMID 15318222; Carre-Pierrat et al., 2006: PMID 16527307; Lecroisey et al., 2008: PMID 18094057; our unpublished results). Along this line it is noteworthy that mutants that exhibit a strong hypercontraction phenotype do not present any muscle degeneration. This is the case for worms with lof mutations in the *unc-105* gene, which encodes a member of the Degenerin protein family in *C. elegans*, involved in mechanical signal transduction and having similarities to the mammalian amiloride-sensitive epithelial sodium channel (ENaC) (Liu et al., 1996: PMID 8662524). The strong hypercontraction of *unc-105* mutants leads to severely impaired movement (Park and Horvitz, 1986 : PMID 3744029) thus preventing muscle degeneration.

The contribution of mechanical forces and movement to DYS-1 dependent muscle degeneration is further supported by a reduction of muscle degeneration in adult *dys-1; hh-1* double mutants when sarcomere contraction is inhibited by mutations in different genes affecting the myofilament lattice (Mariol et al., 2007: PMID 17134897), RNAi mediated knock down of the EGL-19 L-type voltage gated Ca²⁺ channel (Mariol and Ségalat 2001: PMID 11696327), or after forced immobilization by treatment with muscimol, a GABA agonist and anesthetic used to paralyze *C. elegans* (Brouilly et al., 2015: PMID 26358775). Similarly, limb immobilization or treatment with muscle relaxants prevent and reduce the occurrence of muscle degeneration in *mdx* mice (Mokhtarian et al., 1999: PMID 10066706). One possible explanation for this observation is that reduced movement and force production allows for the cell to repair damage at dense bodies and plasma membrane. This hypothesis may also explain why most muscle cells degenerate only after the last (L4) larval

stage. Indeed, in *C. elegans*, the cuticle is remade at the end of each of the four larval stages during episodes of physiological lethargic periods (lethargus) (Raizen et al., 2008: PMID 18185515). Interestingly, the composition and dynamics of the dense bodies change during this quiescent period (Zaidel-Bar et al., 2010: PMID 20385102), and some dense body proteins are differentially expressed during lethargus (Turek and Bringmann, 2014: PMID 25409030). In dystrophin-deficient muscle, these periods of quiescence may be used to repair cell damage and the dystrophic phenotype would be consequently delayed and visible only in adulthood when such phases are absent. Alternatively, adult tissues may in general have reduced ability to repair cell damage compared to larvae.

An ultra-structural analysis performed on muscle cells during development, from L1 larvae to 3-days post-L4 *dys-1(cx18); hlh-1(cc561)* mutants allowed for the observation of the subcellular events occurring during muscle degeneration and to determine their chronology in the degenerative process (Brouilly et al., 2015: PMID 26358775). The small size of *C. elegans* makes possible the use of High Pressure Freezing on the whole organism thus reducing fixation artifacts. In addition, *C. elegans* muscles do not contain satellite cells and are thus not able to regenerate after damage. This model is, therefore, best suited for such a time course study of the subcellular degenerative process. Contrary to degenerative muscle tissues in vertebrates, which present a high degree of spatio-temporal heterogeneity, macrophage infiltration and fibrosis, and uncertain sectioning, using *C. elegans* reduces heterogeneity and allows a quantitative time-course analysis of muscle degeneration at the ultra-structural level. In this study, the first defects were observed at the very beginning of larval development (L1) with a disorganization of the sarcomeric bundles, presenting an irregular shape when compared to wild type. From the L2 stage, dense body sections of both *dys-1(cx18)* single and *dys-1(cx18); hlh-1(cc561)* double mutants were smaller than wild-type. Thus the irregular shape of the sarcomeric bundles could result from organization defects of dense bodies lacking DYS-1. In addition, smaller dense bodies were observed in *dys-1(cx18); hlh-1(cc561)* mutants at the L3 larval stage and their fragmentation or their detachment from the sarcolemma was frequent (Brouilly et al., 2015: PMID 26358775; http://www.inmg.fr/en/gieseler/wormbook_gieseler.php). This may explain the disrupted actin network phenotype observed under light microscopy in phalloidin-rhodamine and LifeAct staining experiments. These revealed accumulation of actin in coils and at the tips of the cell, which is probably a consequence of the tension exerted by the excitation/relaxation cycles on dense bodies weakened by the absence of DYS-1, fragmented and detached from the sarcolemma (Gieseler et al., 2000: PMID 10996789). These observations are in agreement with a role for DYS-1 in the maintenance of dense body anchorage and integrity (Figure 12).

A role for DYS-1 in the maintenance of sarcolemma integrity is suggested by plasma membrane interruptions and a significant increase of single- and double membrane vesicles in *dys-1; hlh-1* mutants that were observed by ultra-structural analysis starting from the L3 larval stage. The single membrane vesicles were often located at sub-sarcolemmal regions, suggesting a possible link with plasma membrane repair mechanisms. These mechanisms often involve endo/exocytosis flux in plasma membrane healing or budding (Brouilly et al., 2015: PMID 26358775).

The disruption of dense body and sarcolemma integrity occurs early in development of *dys-1; hlh-1* mutants. In addition to the above-mentioned defects at the neuromuscular junction and the control of ion channel activity, these defects are likely to increase the disruption of cellular homeostasis and to trigger downstream cellular responses. High calcium concentrations were previously observed in muscle of DMD patients and *mdx* mice (Turner et al., 1988: PMID 3173492). A calcium overload is also a possible origin for mitochondria dysfunction and mitochondria dynamics, which were observed during muscle degeneration in *C. elegans* and the zebrafish (Giacomotto et al., 2013: PMID 23804750). Another consequence of the loss of sarcolemma integrity could be the disturbance of protein homeostasis. Indeed, an acceleration of age-dependent protein aggregation was observed in *dys-1* mutant muscle cells (Oh and Kim, 2013: PMID 24191049). An accumulation of double-membrane vesicles observed in *dys-1; hlh-1* mutants starting from the L3 stage could be reminiscent of the activation of autophagy, which participates in the degradation of protein aggregates. Autophagy could further be implicated in the degradation of disrupted muscle filaments and dense bodies, mitochondria as well as ribosomes, and endoplasmic reticulum that were identified within these vesicles (Brouilly et al., 2015: PMID 26358775; our unpublished results).

Most interestingly, ultra-structural analysis of skeletal muscle biopsies from young DMD patients revealed similar defects to those described in *C. elegans dys-1; hlh-1* mutants, such as disruption of Z-disks and sarcomeric bundles, loss of plasma membrane integrity, accumulation of vesicles near the sarcolemma and in internal regions, and abnormal morphology of mitochondria and endoplasmic reticulum (Brouilly et al., 2015: PMID 26358775). This result emphasizes the suitability of the *C. elegans* model to unravel mechanisms leading to muscle degeneration diseases in humans. It is likely that in human patients, as in *C. elegans*, the loss of

dystrophin leads to defects in Z-disc and costamere organization, the submembrane cytoskeleton, thus affecting sarcomere attachment to the sarcolemma and membrane integrity. This together with impaired function of NMJ and ion channels could then trigger downstream responses such as membrane repair and protein degradation, which may however not be sufficient to repair cellular damages and to prevent cell death.

Finally, it has to be pointed out that dystrophin-dependent muscle degeneration shares some subcellular features of age-dependent muscle decline, also known as sarcopenia. While sarcopenia has not yet been studied in *C. elegans*, loss of sarcomere integrity, accumulation of autophagosomes and protein aggregates, and disturbed mitochondrial dynamics and functions have been observed in muscles of aged nematodes that likely contribute to the progressive loss of motility and muscle strength (Herndon et al., 2002: PMID 12397350; Morley et al., 2002: PMID 12122205; Yu et al., 2012: PMID 23114011; Regmi et al., 2014: PMID 24642473; C. Scholtes and [K. Gieseler](#), unpublished results). Sarcopenia is a long-lasting partially reversible process, which is often qualified as physiologic muscle degeneration in contrast to pathologic muscle degeneration occurring in some neuromuscular disorders such as muscular dystrophies. Pathologic muscle degeneration progresses fast and irreversibly leads to premature muscle cell death. Thus, dystrophin-dependent muscle degeneration may in some aspects be considered as accelerated muscle aging in which additional cellular processes occur that lead to progressive cell death. The precise mechanisms involved in pathologic muscle cell death still need to be clarified (reviewed in Carmelli et al., 2015: PMID 26017731).

6.4. How does the *hlh-1(cc561)* mutation contribute to muscle degeneration?

Mice lacking both dystrophin and the myogenic factor MyoD display severe myopathy, compared with *mdx* mice (Megeney et al., 1996 : PMID 8675005). This increased severity of muscle degeneration in *MyoD*; *mdx* double-mutants is thought to be caused by a reduction of muscle regeneration from satellite cells, which requires MyoD function. *C. elegans* muscle differ from mammalian muscle in that they do not contain satellite cells. Therefore, damaged muscle cells are not replaced in *C. elegans*. Nevertheless, the *hlh-1(cc561)* allele of the *C. elegans* MyoD ortholog potentializes muscle degeneration of *dys-1/dystrophin* loss-of function mutations.

The *hlh-1(cc561)* allele is partially thermosensitive and produces a truncated protein, which contains the N-terminal region of HLH-1 including the bHLH domain. At permissive temperature (15 °C), about 60% of eggs have normal development and reach adulthood. Young animals move well and have normal body shape, but contain extra sex muscles (Harfe et al., 1998: PMID 9609831). At the restrictive temperature (25 °C), severe defects in motility and body shape were observed, with most animals dying as newly hatched larvae (Harfe et al., 1998: PMID 9609831). The phenotypic effects seen in *hlh-1(cc561)* animals are likely due to insufficiency rather than novel effects of this truncated protein since the mutant phenotype can be rescued by extra-copies of *hlh-1(cc561)* (Harfe et al., 1998: PMID 9609831).

Transgenic animals carrying the GFP sequence fused to the endogenous *hlh-1* wild-type or *cc561* allele (lines generated by the CRISPR technology), grown at 15 °C, exhibited a GFP signal in all body wall muscle nuclei in larvae and adults. However, the signal was much weaker in *hlh-1(cc561)::gfp* animals than in *hlh-1(wt)::gfp* (E. Martin and [K. Gieseler](#), unpublished results). This observation suggests that the truncated protein is correctly addressed to the nucleus but is less stable than the wild-type form, even at 15 °C.

An ultra-structural analysis performed by transmission electron microscopy at larval stages (L1 to L4) and in young adults revealed that *hlh-1(cc561)* mutants grown at the permissive temperature have a globally normal body wall muscle structure (Brouilly et al., 2015: PMID 26358775). However, when combined with a loss-of-function allele of *dys-1*, the *hlh-1(cc561)* allele leads, at the permissive temperature for *hlh-1(cc561)*, to a strong progressive muscle degeneration phenotype starting at the L4 and paralysis of adult worms at 3 days post-L4 (Gieseler et al., 2000: PMID 10996789; Brouilly et al., 2015: PMID 26358775; see above). This phenotype can also be rescued by extra-copies of *hlh-1(wt)* or *hlh-1(cc561)* (our unpublished results), suggesting that the enhancement of muscle degeneration is due to insufficient function of the HLH-1(cc561) protein.

Transcriptomic data obtained on *hlh-1(cc561)* L4 larvae grown at permissive temperature revealed altered expression of numerous genes that encode proteins involved in lysosomal function, protein turnover and metabolism, or sarcomere and DGC organization ([A. Rea-Boutros](#), [A.R. Reedy](#), and [K. Gieseler](#), unpublished results). This observation suggests that HLH-1 contributes post-embryonically to cellular homeostasis, sarcomeric protein turnover, and muscle maintenance. While the perturbation of these processes is not sufficient to induce a mutant phenotype in *hlh-1(cc561)* single mutants, it likely sensitized body wall muscle to other

perturbations, thus contributing to the severe muscle degeneration phenotype observed in *dys-1(cx18); hlh-1(cc561)* double mutants. This hypothesis is further supported by the above mentioned muscle degeneration phenotype observed when the *hlh-1(cc561)* allele is combined with loss-of-function mutations in either *snf-6*, *slo-1*, *sgca-1*, *dyb-1*, *stm-1*, or *dyc-11* (Gieseler et al., 1999a: PMID 10369883; Gieseler et al., 2000: PMID 10996789; Grisoni et al., 2003: PMID 14499607; Kim et al., 2004: PMID 15318222; Carre-Pierrat et al., 2006: PMID 16527307; Lecroisey et al., 2008: PMID 18094057; our unpublished results). These mutations all lead to a *dys-1*-like hyperactivity/hypercontraction phenotype, which is likely to be associated with increased cholinergic transmission and/or disturbed calcium homeostasis. Finally, *hlh-1(cc561)* mutants also exhibit increased sensitivity of post-embryonic and adult muscle to impaired proteostasis ([A.R. Reedy](#) and [K. Gieseler](#), unpublished results), and reduced resistance of muscle during aging (M. Cortes and [K. Gieseler](#), unpublished results).

Altogether, this indicates that in *C. elegans* HLH-1 may contribute to the repair of cellular damages and prevent cell death. Further research will be required to decipher in detail the role of the myogenic HLH-1 transcription factor in differentiated muscle cells.

7. Conclusion

Sarcomere assembly and/or maintenance in *C. elegans* involves at least several hundred different proteins, most of which are conserved in all animals. However, exactly how each of them is involved in assembly and maintenance and how they work together is still largely unknown. Outstanding questions include: how do thick and thin filaments attain fixed and uniform lengths, what determines and maintains the exact spacing and patterning of muscle attachment structures, what determines whether a dense body or an M-line is formed when each begins with the same base proteins, what determines the height and width of dense bodies and M-lines, how are protein components of sarcomeres and other cellular structures repaired and replaced during the stress of muscle activity, what are the essential mechanisms by which loss of dystrophin results in muscle degeneration, what are the targets of the MRFs, what are the full set of pathways that the muscle cell uses to sense its activity, and why are there so many different components of attachment structures that seem not to be functionally redundant? Functional analysis using forward and reverse genetics, cell biology, and biochemistry, especially on the many new components of muscle identified in the last 10-15 years, holds much promise for addressing these and other questions.

8. Table1 and Table 2

Table 1. Notable discoveries about muscle from *C. elegans* research

Protein	Contribution	References
UNC-54	Cloning, sequencing, and analysis of the first complete myosin heavy chain, UNC-54; model for parallel assembly of myosin rods in the thick filament	Epstein et al. 1974: PMID 4453018 ; McLachlan and Karn, 1982: PMID 7202124; Dibb et al. 1985: PMID 4020869
DEB-1, UNC-52, PAT-3, etc.	Discovery that perlecan, integrin, and its associated proteins are critical for sarcomere assembly	Barstead and Waterston, 1991: PMID 1907975; Rogalski et al. 1993: PMID 8393416; Williams and Waterston, 1994: PMID 8106547; Hresko et al. 1994: PMID 8106548; Gettner et al., 1995: PMID 7744961; Hobert et al., 1999: PMID 9885243; Rogalski et al. 2000: PMID 10893272; Mackinnon et al. 2002: PMID 12015115; Lin et al. 2003: PMID 12781130
UNC-45	The first myosin head chaperone, UNC-45	Epstein and Thomson, 1974: PMID 4845659; Venolia and Waterston, 1990: PMID 2245914; Barral et al. 1998: PMID 9832550; Barral et al. 2002: PMID 11809970

Protein	Contribution	References
UNC-22/twitchin	The first complete sequence of a giant titin-like protein twitchin; the first intracellular protein to join the Ig superfamily	Moerman et al. 1986: PMID 3010313; Moerman et al. 1988: PMID 2833427; Benian et al. 1989: PMID 2812002; Benian et al. 1993: PMID 8397135
UNC-22/twitchin	The first crystal structure of a protein kinase domain from a titin family member, that of twitchin kinase, and structural basis of autoinhibition	Hu et al. 1994: PMID 8202162; von Castelmur et al. 2012: PMID 22869697
UNC-89	Function and domain organization of the first obscurin family member, UNC-89	Waterston et al. 1980: PMID 7190524; Benian et al. 1996: PMID 8603916; Small et al. 2004: PMID 15313609
UNC-112	First recognition that kindlins have a role in integrin adhesion complexes by cloning and mutational analysis of UNC-112	Rogalski et al. 2000: PMID 10893272
UNC-60	First recognition that actin regulatory proteins are crucial for sarcomere assembly or maintenance by the cloning, mutational, and biochemical analysis of UNC-60 (ADF/cofilin)	Waterston et al. 1980: PMID 7190524; McKim et al. 1994: PMID 8107682; Ono et al. 1999: PMID 10225951
HSP-1, UNC-23	First recognition that a molecular chaperone, HSP-1 (Hsc70), and its regulators (including UNC-23 (BAG-2)) are required to maintain muscle adhesion complexes in the face of mechanical stress	Waterston et al. 1980: PMID 7190524; Plenefisch et al. 2000: PMID 10683173; Papsdorf et al. 2014: PMID 25053410; Rahmani et al. 2015: PMID 26435886
DYS-1	First ultrastructural chronology of dystrophin-dependent muscle degeneration	Brouilly et al. 2015: PMID 26358775

Table 2. Proteins that function in muscle assembly, maintenance or function*

Protein	Human homolog/ortholog	Location	Interacting partners	Phenotype of mutants	Key references
ALP-1	cypher/ZASP/oracle	dense body (deeper part), nucleus (muscle and hypodermis)	ZYX-1, ATN-1?	normal thrashing assay; reduced maximal bending; low penetrance F-actin aggregates enhanced by <i>atn-1/+</i> or <i>ketn-1</i> (RNAi)	McKeown et al. 2006: PMID 16278882; Han and Beckerle 2009: PMID 19261811
ATN-1	α -actinin	dense body (deeper part)	DEB-1, ZYX-1, ALP-1?	short and broad dense bodies; F-actin aggregates; reduced maximum bending	Barstead et al. 1991: PMID 1756579 ; Moulder et al. 2010: PMID 20850453
CPNA-1	CPNE5	M-line, dense body	PAT-6, UNC-89, LIM-9, UNC-96, SCPL-1	Pat, at 2 fold stage UNC-89 and MYO-3 form accumulations	Warner et al. 2013: PMID 23283987
CSN-5	CSN5	A-band	UNC-96, UNC-98	RNAi increases steady state level of UNC-98	Miller et al. 2009: PMID 19535455
CYK-1	formin	dense body		narrow muscle cells, fewer striations per cell	Mi-Mi et al. 2012: PMID 22753896
DAF-21	Hsp90	transiently at and diffusible from I-band	UNC-45, UNC-54?	reduced motility in liquid; aggregates of GFP::MYO-3 outside myofilament lattice	Gaiser et al. 2011: PMID 21980476
DEB-1	vinculin	dense body (base)	TLN-1, UIG-1, DYS-1, PXL-1, ZYX-1, ATN-1	Pat	Barstead and Waterston 1989: PMID 2498337; Barstead and Waterston 1991: PMID 1907975

Protein	Human homolog/ortholog	Location	Interacting partners	Phenotype of mutants	Key references
DIM-1		around and between dense bodies	UNC-112, UIG-1	slight disorganization of myofilament lattice; reduced maximum bending; suppresses <i>unc-112</i>	Rogalski et al. 2003: PMID 12663531
DYB-1	dystrobrevin	close to dense bodies	DYS-1, STN-1	hyperactive, hypercontracted, headbending, muscle degeneration in combination with <i>hlh-1(cc561)</i>	Gieseler et al. 1999a: PMID 10369883; Gieseler et al. 1999b: PMID 10561496
DYC-1	capon	close to dense bodies	ZYX-1	hyperactive, hypercontracted, headbending, muscle degeneration in combination with <i>hlh-1(cc561)</i>	Gieseler et al. 2000: PMID 10996789; Lecroisey et al. 2008: PMID 18094057
DYS-1	dystrophin	I-band, dense body, sarcolemma	DYS-1, DYB-1, DEB-1	hyperactive, hypercontracted, headbending, muscle degeneration in combination with <i>hlh-1(cc561)</i>	Bessou et al. 1998: PMID 9933302; Brouilly et al. 2015: PMID 26358775
FHOD-1	formin	around and between dense bodies		narrow muscle cells, fewer striations per cell	Mi-Mi et al. 2012: PMID 22753896
α -filagenin		A-band (center; thick filament cores)	UNC-15?, MYO-3?, UNC-54?	unknown	Liu et al. 2000: PMID 11058087
b-filagenin		A-band (polar and center; thick filament cores)	UNC-15?, MYO-3?, UNC-54?	unknown	Liu et al. 1998: PMID 9442110
g-filagenin		A-band (polar regions; thick filament cores)	UNC-15?, MYO-3?, UNC-54?	unknown	Liu et al. 2000: PMID 11058087
FRG-1	FRG1	dense body, nucleus (nucleoli)	F-actin	overexpression: disruption of some muscle cell-cell junctions and absence of some muscle cells	Liu et al. 2010: PMID 20215405
HLH-1	MyoD	nuclei		L1 arrest, paralysis	Krause et al. 1990: PMID 2175254
HND-1		nuclei?		intragenic deletion is embryonic lethal; point mutation is Unc and small fraction are Pat	Baugh et al. 2005: PMID 15892873
HSP-25	abcrystallin	M-line, dense body	DEB-1?, ATN-1?	not fully characterized	Ding and Candido 2000: PMID 10734099
KETN-1 (kettin)		between dense bodies	F-actin, ATN-1?	by RNAi, F-actin aggregates enhanced by tetramisole-induced hypercontraction and by <i>atn-1</i>	Ono et al. 2006: PMID 16597697

Protein	Human homolog/ortholog	Location	Interacting partners	Phenotype of mutants	Key references
LIM-8		M-line, around and between dense bodies	UNC-97, UNC-95, PXL-1, ZYX-1, UNC-96, MYO-3, MEL-26	normal; mildly disorganized MYO-3 in <i>pxl-1</i> ; <i>lim-8</i> double	Qadota et al. 2007: PMID 17761533; Warner et al. 2011: PMID 21633109
LIM-9	FHL-2	M-line, around and between dense bodies	UNC-97, UNC-89, ZYX-1, UNC-96, SCPL-1	mildly disorganized MYO-3	Qadota et al. 2007: PMID 17761533; Meissner et al. 2009: PMID 19557190
MAK-1	MAPKAP2	around and between dense bodies	UNC-22	partially resistant to nicotine; <i>unc-22</i> is epistatic to <i>mak-1</i> in nicotine resistance	Matsunaga et al. 2015: PMID 25851606
MEL-26		M-line, I-band	CUL-3, MEI-1, UNC-89	disorganized MYO-3	Wilson et al. 2012: PMID 22621901
MYO-3 (MHC A)	myosin heavy chain	A-band (center)	UNC-98, UNC-96, LIM-8, UNC-15?, UNC-54?, UNC-45?	Pat, severe, very few or no thick filaments	Miller et al. 1983: PMID 6352051; Miller et al. 1986: PMID 2422655; Ardizzi and Epstein 1987: PMID 3320053; Waterston 1989: PMID 2583106
PAL-1		nuclei of C and D blastomeres in embryos		embryonic lethal	Hunter and Kenyon 1996 PMID: 8861906; Bowerman et al. 1997 PMID: 9367437; Baugh et al. 2005 PMID 15892873
PAT-2	integrin α	M-line, dense body (cell membrane)	PAT-3?	Pat; in Pat embryos actin and myosin not polarized	Williams and Waterston 1994: PMID 8106547
PAT-3	integrin β	M-line, dense body (cell membrane)	UNC-112, PAT-2?	Pat; in Pat embryos actin and myosin not polarized	Gettner et al. 1995: PMID 7744961
PAT-4	integrin linked kinase	M-line, dense body (base)	UNC-112, PAT-6, UNC-97	Pat; in Pat embryos actin and myosin are polarized, but no thick or thin filaments	Mackinnon et al. 2002: PMID 12015115
PAT-6	actopaxin(α -parvin)	M-line, dense body (base)	PAT-4, CPNA-1	Pat; in Pat embryos actin and myosin are polarized, but no thick or thin filaments	Lin et al. 2003: PMID 12781130
PAT-9		nucleus		Pat	Liu et al. 2012: PMID 22616817
PFN-3	profilin	dense body (deeper part)	F-actin?	slightly slower thrashing assay; reduced maximal bending; null--normal I-bands; F-actin aggregates in <i>pfn-3</i> ; <i>unc-94</i> (RNAi)	Polet et al. 2006: PMID 16317718; Yamashiro et al. 2008: PMID 18984629
PKN-1	protein kinase N	M-line, dense body	RHO-1, CED-10, MIG-2	loopy Unc	Qadota et al. 2011: PMID 21277858
PXL-1	paxillin	M-line, dense body	UNC-95, UIG-1, DEB-1, UNC-96, LIM-8	normal; mildly disorganized MYO-3 in <i>pxl-1</i> ; <i>lim-8</i> double	Warner et al. 2011: PMID 21633109

Protein	Human homolog/ortholog	Location	Interacting partners	Phenotype of mutants	Key references
RNF-5		dense body (base)	UNC-95	dense bodies (stained with anti-DEB-1) not organized in straight rows; overexpression leads to reduced UNC-95; RNAi leads to increased UNC-95	Didier et al. 2003: PMID 12861019; Broday et al. 2004: PMID 15210732
SCPL-1		M-line, I-band	UNC-89, CPNA-1, LIM-9, ZYX-1	increased maximal bending	Qadota et al. 2008a: PMID 18337465 ; Nahabedian et al. 2012: PMID 22126736
SGCA-1				muscle degeneration in combination with <i>hlh-1(cc561)</i>	K. Gieseler, unpublished results
SGCB-1					K. Gieseler, unpublished results
SGN-1				hyperactive, hypercontracted, headbending	Grisoni et al. 2002: PMID 12234669
STN-1		close to dense bodies	DYS-1, DYB-1, SNF-6	hyperactive, hypercontracted, headbending	Grisoni et al. 2003: PMID 14499607; Kim et al. 2004: PMID 15318222
STN-2		close to dense bodies	SAX-7	hyperactive, hypercontracted, headbending	Zhou et al. 2008: PMID 18791240
TTN-1		I-band	UIG-1	unknown	Flaherty et al. 2002: PMID 12381307; Forbes et al. 2010: PMID 20346955
UIG-1		dense body	UNC-112, CDC-42, DIM-1, TTN-1, TLN-1, DEB-1, PXL-1, UNC-95, ZYX-1	disorganized myofilament lattice	Hikita et al. 2005: PMID 16055082
UNC-15 (paramyosin)		A-band	UNC-54?, MYO-3?, UNC-96, UNC-98, UNC-89	Unc, limp paralyzed, myofilament lattice very disorganized, shorter hollow thick filaments	Waterston et al. 1977: PMID 564970; MacKenzie and Epstein 1980: PMID 7193096 ; Kagawa et al. 1989: PMID 2754728
UNC-22 (twitchin)		A-band (polar regions)	MAK-1	Unc, twitching; resistant to nicotine	Moerman et al. 1988: PMID 2833427; Benian et al. 1989: PMID 2812002 ; Hu et al. 1994: PMID 8202162
UNC-23	BAG-2	M-line, dense body (base), hypodermal cell (nucleus, Ifs)	HSP-1	Unc, bent, detachment of muscle cells in "head" region	Rahmani et al. 2015: PMID 26435886

Protein	Human homolog/ortholog	Location	Interacting partners	Phenotype of mutants	Key references
UNC-35 (TLN-1)	talin	dense body, (M-line)	PAT-3?, DEB-1?, F-actin?	Unc, not fully characterized; requires <i>pat-3</i> but not <i>deb-1</i> for localization	Moulder et al. 1996: PMID 8856663 ; Etheridge et al. 2012: PMID 22253611
UNC-45	UNC-45	A-band (polar regions)	NMY-2, HUM-2, DAF-21, UNC-54?	Pat, Unc; ts allele: reduced number of thick filaments	Venolia and Waterston 1990: PMID 2245914; Barral et al. 1998: PMID 9832550; Ao and Pilgrim, 2000: PMID 10648570; Barral et al. 2002: PMID 11809970; Kachur et al. 2004: PMID 15454571
UNC-52	perlecan	M-line, dense body (ECM)	PAT-2?, PAT-3?	Unc, Pat; in Pat embryos actin and myosin not polarized	Rogalski et al. 1993: PMID 8393416; Rogalski et al. 1995: PMID 7535716
UNC-54 (MHC B)	myosin heavy chain	A-band (polar regions)	UNC-22?, UNC-15?, MYO-3?, UNC-45?	Unc, limp paralyzed, myofilament lattice very disorganized, reduced numbers of thick filaments	Epstein et al. 1974: PMID 4453018; Miller et al. 1983: PMID 6352051; Karn et al. 1983: PMID 6576334; Dibb et al. 1985: 4020869 PMID ; Ardizzi and Epstein 1987: PMID 3320053
UNC-82		M-line		Unc, mislocalization of thick filament/M-line proteins during embryonic elongation	Hoppe et al. 2010: PMID 19901071
UNC-89	obscurin	M-line (full depth)	RHO-1, UNC-15, CPNA-1, MEL-26, LIM-9, SCPL-1	Unc, missing M-line	Benian et al. 1996: PMID 8603916; Small et al. 2004: PMID 15313609
UNC-95		M-line, dense body, (nucleus?)	RNF-5, UNC-97, PXL-1, LIM-8, UIG-1	Unc, shorter or broken dense bodies and M-lines	Broday et al. 2004: PMID 15210732
UNC-96		M-line, (dense body?)	LIM-9, UNC-98, CPNA-1, PXL-1, LIM-8, MYO-3, CSN-5, UNC-15	Unc, accumulations of UNC-15, UNC-98, CSN-5	Mercer et al. 2006: PMID 16790495
UNC-97	PINCH	M-line, dense body (base), nucleus	PAT-4, UNC-95, LIM-8, LIM-9, UNC-98	Unc, Pat; in Pat embryos actin and myosin are polarized, but no thick or thin filaments	Hobert et al. 1999: PMID 9885243; Norman et al. 2007: PMID 17662976
UNC-98		M-line, nucleus, (dense body?)	UNC-97, UNC-96, MYO-3, UNC-15, CSN-5	Unc, accumulations of UNC-15, UNC-96, CSN-5	Mercer et al. 2003: PMID 12808046; Miller et al. 2006: PMID 17158957
UNC-112	kindlin	M-line, dense body (base)	PAT-3, PAT-4, UIG-1, DIM-1	Unc, Pat; in Pat embryos actin and myosin not polarized	Rogalski et al. 2000: PMID 10893272; Qadota et al. 2012: PMID 22761445

Protein	Human homolog/ortholog	Location	Interacting partners	Phenotype of mutants	Key references
UNC-120	serum response factor	nuclei?		intragenic deletion is embryonic lethal; ts allele at 20-25 shows progressive paralysis and reduced numbers of A and I bands and small fraction Pat	Baugh et al. 2005: PMID 15892873; Fukushige et al. 2006: PMID 17142668
ZYX-1	zyxin	M-line, dense body (middle), nucleus	LIM-9, LIM-8, SCPL-1, UIG-1, ALP-1, DYC-1, DEB-1, ATN-1	reduced maximal bending; suppresses muscle degeneration in <i>dys-1; hlh-1</i>	Lecroisey et al. 2008: PMID 18094057; Lecroisey et al. 2013: PMID 23427270

*: actin regulatory proteins not included; please see Ono 2014: PMID 25125169

? interactions inferred from what is known about vertebrate orthologs and/or genetic

9. Acknowledgements

The authors also thank Claire Lecroisey, Nicolas Brouilly and Mathieu Baritaud for designing Figures 2, 5, and 11, respectively, and Nicole Mounier for helpful comments and suggestions. The authors gratefully acknowledge the very helpful suggestions for improving the manuscript from the reviewers (Don Moerman, and Michael Krause), and the editors, Michel Labouesse and Jane Mendel. K.G. acknowledges grant support from the Claude Bernard University Lyon1 and the CNRS , the Association Française contre les Myopathies and the French Agence Nationale de la Recherche. G.M.B. acknowledges grant support from the NIH (AR064307) and the Human Frontier Science Program (RGP0044/2012).

10. References

- Ahringer J. (1997). Maternal control of a zygotic patterning gene in *Caenorhabditis elegans*. *Development* *124*, 3865-3869.
- Albertson, D.G. (1985). Mapping muscle protein genes by in situ hybridization using biotin-labeled probes. *EMBO J.* *4*, 2493-2498.
- Ao, W., and Pilgrim, D. (2000). *Caenorhabditis elegans* UNC-45 is a component of muscle thick filaments and colocalizes with myosin heavy chain B, but not myosin heavy chain A. *J. Cell Biol.* *148*, 375-384.
- Ardizzi, J.P., and Epstein, H.F. (1987). Immunochemical localization of myosin heavy chain isoforms and paramyosin in developmentally and structurally diverse muscle cell types of the nematode *Caenorhabditis elegans*. *J. Cell Biol.* *105*, 2763-2770.
- Bagnato, P., Barone, V., Giacomello, E., Rossi, D., and Sorrentino, V. (2003). Binding of an ankyrin-1 isoform to obscurin suggests a molecular link between the sarcoplasmic reticulum and myofibrils in striated muscles. *J. Cell Biol.* *160*, 245-253.
- Bang, M.L., Centner, T., Fornoff, F., Geach, A.J., Gotthardt, M., McNabb, M., Witt, C.C., Labeit, D., Gregorio, C.C., Granzier, H., and Labeit, S. (2001). The complete gene sequence of titin, expression of an unusual approximately 700-kDa titin isoform, and its interaction with obscurin identify a novel Z-line to I-band linking system. *Circ. Res.* *89*, 1065-1072.
- Barral, J.M., Bauer, C.C., Ortiz, I., and Epstein, H.F. (1998). *Unc-45* mutations in *Caenorhabditis elegans* implicate a CRO1/She4p-like domain in myosin assembly. *J. Cell Biol.* *143*, 1215-1225.
- Barral, J.M., Hutagalung, A.H., Brinker, A., Hartl, F.U., and Epstein, H.F. (2002). Role of the myosin assembly protein UNC-45 as a molecular chaperone for myosin. *Science* *295*, 669-671.

Barstead, R.J., and Waterston, R.H. (1989). The basal component of the nematode dense body is vinculin. *J. Biol. Chem.* 264, 10177-10185.

Barstead, R.J., Kleiman, L., and Waterston, R.H. (1991). Cloning, sequencing and mapping of an a-actinin gene from the nematode *C. elegans*. *Cell Motil. Cytoskeleton* 20, 69-78.

Barstead, R.J., and Waterston, R.H. (1991). Vinculin is essential for muscle function in the nematode. *J. Cell Biol.* 114, 715-724.

Baugh L.R., Wen J.C., Hill A.A., Slonim D.K., Brown E.L., and Hunter C.P. (2005). Synthetic lethal analysis of *Caenorhabditis elegans* posterior embryonic patterning genes identifies conserved genetic interactions. *Genome Biol.* 6, R45.

Baugh, L.R., and Hunter, C.P. (2006). MyoD, modularity, and myogenesis: conservation of regulators and redundancy in *C. elegans*. *Genes Dev.* 20, 3342-3346.

Benian, G.M., Kiff, J.E., Neckelmann, N., Moerman, D.G., and Waterston, R.H. (1989). Sequence of an unusually large protein implicated in regulation of myosin activity in *C. elegans*. *Nature* 342, 45-50.

Benian, G.M., L'Hernault S.W., and Morris, M.E. (1993). Additional sequence complexity in the muscle gene, *unc-22*, and its encoded protein, twitchin, of *Caenorhabditis elegans*. *Genetics* 134, 1097-1104.

Benian, G.M., Tinley, T.L., Tang, X., and Borodovsky, M. (1996). The *Caenorhabditis elegans* gene *unc-89*, required for muscle M-line assembly, encodes a giant modular protein composed of Ig and signal transduction domains. *J. Cell Biol.* 132, 835-848.

Benian, G.M., Ayme-Southgate, A., and Tinley, T.L. (1999). The genetics and molecular biology of the titin/connectin-like proteins of invertebrates. *Rev. Physiol. Biochem. Pharmacol.* 138, 235-268.

Bessou, C., Giugia, J.B., Franks, C.J., Holden-Dye, L., and Ségalat, L. (1998). Mutations in the *Caenorhabditis elegans* dystrophin-like gene *dys-1* lead to hyperactivity and suggest a link with cholinergic transmission. *Neurogenetics* 2, 61-72.

Blake, D.J., Weir, A., Newey, S.E., and Davies, K.E. (2002). Function and genetics of dystrophin and dystrophin-related proteins in muscle. *Physiol. Rev.* 82, 291-329.

Bodine, S.C., Latres, E., Baumhueter, S., Lai, V.K., Nunez, L., Clarke, B.A., Poueymirou, W.T., Panaro, F.J., Na, E., Dharmarajan, K., et al. (2001). Identification of ubiquitin ligases required for skeletal muscle atrophy. *Science* 294, 1704-1708.

Bogomolovas, J., Gasch, A., Simkovic, F., Rigden, D.J., Labeit, S., and Mayans, O. (2014). Titin kinase is an inactive pseudokinase scaffold that supports MuRF1 recruitment to the sarcomeric M-line. *Open Biol.* 4, 140041.

Bosu, D.R., and Kipreos, E.T. (2008). Cullin-RING ubiquitin ligases: global regulation and activation cycles. *Cell Div.* 3, doi:10.1186/1747-1028-3-7

Bowerman B., Eaton B.A., and Priess J.R. (1992). *skn-1*, a maternally expressed gene required to specify the fate of ventral blastomeres in the early *C. elegans* embryo. *Cell* 68, 1061-1075.

Bowerman B., Ingram M.K., Hunter C.P. (1997). The maternal par genes and the segregation of cell fate specification activities in early *Caenorhabditis elegans* embryos. *Development* 124, 3815-3826.

Bowman, A.L., Kontogianni-Konstantopoulos, A., Hirsch, S.S., Geisler, S.B., Gonzalez-Serratos, H., Russell, M.W., and Bloch, R.J. (2007). Different obscurin isoforms localize to distinct sites at sarcomeres. *FEBS Lett.* 581, 1549-54.

Brenner, S. (1974). The genetics of *Caenorhabditis elegans*. *Genetics* 77, 71-94.

- Broday, L., Kolotuev, I., Didier, C., Bhoumik, A., Podbilewicz, B., and Ronai, Z. (2004). The LIM domain protein UNC-95 is required for the assembly of muscle attachment structures and is regulated by the RING finger protein RNF-5 in *C. elegans*. *J. Cell Biol.* *165*, 857-867.
- Brussee, V., Tardif, F., and Tremblay, J.P. (1997). Muscle fibers of mdx mice are more vulnerable to exercise than those of normal mice. *Neuromuscul. Disord.* *7*, 487-492.
- Brouilly, N., Lecroisey, C., Martin, E., Pierson, L., Mariol, M.-C., Qadota, H., Labouesse, M., Streichenberger, N., Mounier, N., and Gieseler, K. (2015). Ultra-structural time-course study in the *C. elegans* model for Duchenne muscular dystrophy highlights a crucial role for sarcomere-anchoring structures and sarcolemma integrity in the earliest steps of the muscle degeneration process. *Hum. Mol. Genet.* *24*, 6428-6445.
- Brown, A.E., Yemini, E.I., Grundy, L.J., Jucikas, T., and Schafer, W.R. (2013). A dictionary of behavioral motifs reveals clusters of genes affecting *Caenorhabditis elegans* locomotion. *Proc. Natl. Acad. Sci. U. S. A.* *110*, 791-796.
- Burkeen, A.K. Maday, S.L., Rybicka, K.K., Sulcove, J.A., Ward, J., Huang, M.M., Barstead, R., Franzini-Armstrong, C., and Allen, T.S. (2004). Disruption of *Caenorhabditis elegans* muscle structure and function caused by mutation of troponin I. *Biophys. J.* *86*, 991-1001.
- Butler, T.M. and Siegman, M.J. (2011). A force-activated kinase in a catch smooth muscle. *J. Muscle Res. Cell Motil.* *31*, 349-358.
- Carmeli, E., Aizenbud, D., and Rom, O. (2015). How do skeletal muscles die? An overview. *Adv. Exp. Med. Biol.* *14*, 99-111.
- Carre-Pierrat, M., Grisoni, K., Gieseler, K., Mariol, M.-C., Martin, E., Jospin, M., Allard, B., and Ségalat, L. (2006). The SLO-1 BK channel of *Caenorhabditis elegans* is critical for muscle function and is involved in dystrophin-dependent muscle dystrophy. *J. Mol. Biol.* *358*, 387-395.
- Chen L., Krause M., Draper B., Weintraub H., and Fire A. (1992). Body-wall muscle formation in *Caenorhabditis elegans* embryos that lack the MyoD homolog *hh-1*. *Science* *256*, 240-243.
- Chen L., Krause M., Sepanski M., and Fire A. (1994). The *Caenorhabditis elegans* MYOD homologue HLH-1 is essential for proper muscle function and complete morphogenesis. *Development* *120*, 1631-1641.
- Chow, D., Srikantham, R., Chen, Y., and Winkelmann, D.A. (2002). Folding of the striated muscle myosin motor domain. *J. Biol. Chem.* *277*, 36799-36807.
- Constantin, B. (2014). Dystrophin complex functions as a scaffold for signalling proteins. *Biochim. Biophys. Acta* *1838*, 635-642.
- Cope, G.A., and Deshaies, R.J. (2003). COP9 signalosome: multifunctional regulator of SCF and other cullin-based ubiquitin ligases. *Cell* *114*, 663-671.
- Corsi A.K., Kostas S.A., Fire A., and Krause M. (2000). *Caenorhabditis elegans* twist plays an essential role in non-striated muscle development. *Development* *127*, 2041-2051.
- Cox, E.A., and Hardin, J. (2004). Sticky worms: adhesion complexes in *C. elegans*. *J. Cell Sci.* *117*, 1885-1897.
- Deitiker, P.R., and Epstein, H.F. (1993). Thick filament substructures in *C. elegans*: evidence for two populations of paramyosin. *J. Cell Biol.* *123*, 303-311.
- De Luca, A., Pierno, S., Liantonio, A., Cetrone, M., Camerino, C., Fraysse, B., Mirabella, M., Servidei, S., Ruegg, U.T., and Conte Camerino, D. (2003). Enhanced dystrophic progression in mdx mice by exercise and beneficial effects of taurine and insulin-like growth factor-1. *J. Pharmacol. Exp. Ther.* *304*, 453-463.
- Dey, C.S., Deitiker, P.R., and Epstein, H.F. (1992). Assembly-dependent phosphorylation of myosin and paramyosin of native thick filaments in *Caenorhabditis elegans*. *Biochem. Biophys. Res. Commun.* *186*, 1528-1532.

Dibb, N.J., Brown, D.M., Karn, J., Moerman, D.G., Bolten, S.L., and Waterston, R.H. (1985). Sequence analysis of mutations that affect the synthesis, assembly and enzymatic activity of the *unc-54* myosin heavy chain of *Caenorhabditis elegans*. *J. Mol. Biol.* 183, 543-551.

Dichoso D., Brodigan T., Chwoe K.Y., Lee J.S., Llacer R., Park M., Corsi A.K., Kostas S.A., Fire A., Ahnn J., and Krause M. (2000). The MADS-Box factor CeMEF2 is not essential for *Caenorhabditis elegans* myogenesis and development. *Dev. Biol.* 223, 431-440.

Didier, C., Broday, L., Bhoumik, A., Israeli, S., Takahashi, S., Nakayama, K., Thomas, S.M., Turner, C.E., Henderson, S., Sabe, H., and Ronai, Z. (2003). RNF5, a RING finger protein that regulates cell motility by targeting paxillin ubiquitination and altered localization. *Mol. Cell. Biol.* 23, 5331-5345.

Ding, L., and Candido, E.P. (2000). HSP25, a small heat shock protein associated with dense bodies and M-lines of body wall muscle in *Caenorhabditis elegans*. *J. Biol. Chem.* 275, 9510-9517.

Dixon, S.J., and Roy, P.J. (2005). Muscle arm development in *Caenorhabditis elegans*. *Development* 132, 3079-3092.

Edgar L.G., Carr S., Wang H., and Wood W.B. (2001). Zygotic expression of the caudal homolog *pal-1* is required for posterior patterning in *Caenorhabditis elegans* embryogenesis. *Dev. Biol.* 229, 71-88.

Emery, A.E. (1991). Population frequencies of inherited neuromuscular diseases--a world survey. *Neuromuscul. Disord.* 1, 19-29.

Emery, A.E. (2002). The muscular dystrophies. *Lancet* 359, 687-695.

Epstein, H.F., and Thomson, J.N. (1974). Temperature-sensitive mutation affecting myofilament assembly in *Caenorhabditis elegans*. *Nature* 250, 579-580.

Epstein, H.F., Waterston, R.H., and Brenner, S. (1974). A mutant affecting the heavy chain of myosin in *Caenorhabditis elegans*. *J. Mol. Biol.* 90, 291-300.

Epstein, H.F., Casey, D.L., and Ortiz, I. (1993). Myosin and paramyosin of *Caenorhabditis elegans* embryos assemble into nascent structures distinct from thick filaments and multi-filament assemblages. *J. Cell Biol.* 122, 845-858.

Epstein, H.F., Lu, G.Y., Deitiker, P.R., Ortiz, I., and Schmid, M.F. (1995). Preliminary three-dimensional model for nematode thick filament core. *J. Struct. Biol.* 115, 163-174.

Epstein, H.F., and Benian, G.M. (2012). Paradigm shifts in cardiovascular research from *Caenorhabditis elegans* muscle. *Trends Cardiovasc. Med.* 22, 201-209.

Ervasti, J.M. (2003). Costameres: the Achilles' heel of Herculean muscle. *J. Biol. Chem.* 278, 13591-13594.

Etheridge, T., Oczypok, E.A., Lehmann, S., Fields, B.D., Shephard, F., Jacobson, L.A., and Scewczyk, N.J. (2012). Calpains mediate integrin attachment complex maintenance of adult muscle in *Caenorhabditis elegans*. *PLoS Genet.* 8, e1002471.

Etheridge, T., Rahman, M., Gaffney, C.J., Shaw, D., Shephard, F., Magudia, J., Solomon, D.E., Milne, T., Blawdziewicz, J., Constantin-Teodosiu, D., et al. (2015). The integrin-adhesome is required to maintain muscle structure, mitochondrial ATP production, and movement forces in *Caenorhabditis elegans*. *FASEB J.* 29, 1235-1246.

Ferrara, T.M., Flaherty, D.B., and Benian, G.M. (2005). Titin/connectin-related proteins in *C. elegans*: a review and new findings. *J. Muscle Res. Cell Motil.* 26, 435-447.

Flaherty, D.B., Gernert, K.M., Shmeleva, N., Tang, X., Mercer, K.B., Borodovsky, M., and Benian, G. M. (2002). Titins in *C. elegans* with unusual features: coiled-coil domains, novel regulation of kinase activity and two new possible elastic regions. *J. Mol. Biol.* 323, 533-549.

Forbes, J.G., Flaherty, D.B., Ma, K., Qadota, H., Benian, G.M., and Wang, K. (2010). Extensive and modular intrinsically disordered segments in *C. elegans* TTN-1 and implications in filament binding, elasticity and oblique striation. *J. Mol. Biol.* *398*, 672-689.

Ford-Speelman, D.L., Roche, J.A., Bowman, A.L., and Bloch, R.J. (2009). The rho-guanine nucleotide exchange domain of obscurin activates rhoA signaling in skeletal muscle. *Mol. Biol. Cell* *20*, 3905-3917.

Francis, G.R., and Waterston, R.H. (1985). Muscle organization in *Caenorhabditis elegans*: localization of proteins implicated in thin filament attachment and I-band organization. *J. Cell Biol.* *101*, 1532-1549.

Francis, R., and Waterston, R.H. (1991). Muscle cell attachment in *Caenorhabditis elegans*. *J. Cell Biol.* *114*, 465-479.

Fukuda, K., Gupta, S., Chen, K., Wu, C., and Qin, J. (2009). The pseudoactive site of ILK is essential for its binding to α -Parvin and localization to focal adhesions. *Mol. Cell* *36*, 819-830.

Fukushige T. and Krause M. (2005). The myogenic potency of HLH-1 reveals wide-spread developmental plasticity in early *C. elegans* embryos. *Development* *132*, 1795-1805.

Fukushige T., Brodigan T.M., Schriefer L.A., Waterston R.H., and Krause M. (2006). Defining the transcriptional redundancy of early bodywall muscle development in *C. elegans*: evidence for a unified theory of animal muscle development. *Genes Dev.* *20*, 3395-3406.

Funabara, D., Hamamoto, C., Yamamoto, K., Inoue, A., Ueda, M., Osawa, R., Kanoh, S., Hartshorne, D.J., Suzuki, S., and Watabe, S. (2007). Unphosphorylated twitchin forms a complex with actin and myosin that may contribute to tension maintenance in catch. *J. Exp. Biol.* *210*, 4399-4410.

Furukawa, M., He, Y.J., Borchers, C., and Xiong, Y. (2003). Targeting of protein ubiquitination by BTB-cullin 3-Roc1 ubiquitin ligases. *Nat. Cell Biol.* *5*, 1001-1007.

Gaiser, A.M., Kaiser, C.J.O., Haslbeck, V., and Richter, K. (2011). Downregulation of the Hsp90 system causes defects in muscle cells of *Caenorhabditis elegans*. *PLoS One* *6*, e25485.

Gautel M. (2008). The sarcomere and the nucleus: functional links to hypertrophy, atrophy and sarcopenia. *Adv. Exp. Med. Biol.* *642*, 176-191.

Gazda, L., Pokrzywa, W., Hellerschmied, D., Lowe, T., Forne, I., Mueller-Planitz, F., Hoppe, T., and Clausen, T. (2013). The myosin chaperone UNC-45 is organized in tandem modules to support myofilament formation in *C. elegans*. *Cell* *152*, 183-195.

Gettner, S.N., Kenyon, C., and Reichardt, L.F. (1995). Characterization of β pat-3 heterodimers, a family of essential integrin receptors in *C. elegans*. *J. Cell Biol.* *129*, 1127-1141.

Ghosh, S.R., and Hope, I.A. (2010). Determination of the mobility of novel and established *Caenorhabditis elegans* sarcomeric proteins in vivo. *Eur. J. Cell Biol.* *89*, 437-448.

Giacomotto, J., Brouilly, N., Walter, L., Mariol, M.-C., Berger, J., Ségalat, L., Becker, T.S., Currie, P.D., and Gieseler, K. (2013). Chemical genetics unveils a key role of mitochondrial dynamics, cytochrome c release and IP3R activity in muscular dystrophy. *Hum. Mol. Genet.* *22*, 4562-4578.

Gieseler, K., Bessou, C., and Ségalat, L. (1999a). Dystrobrevin- and dystrophin-like mutants display similar phenotypes in the nematode *Caenorhabditis elegans*. *Neurogenetics* *2*, 87-90.

Gieseler, K., Abdel-Dayem, M., and Ségalat, L. (1999b). In vitro interactions of *Caenorhabditis elegans* dystrophin with dystrobrevin and syntrophin. *FEBS Lett.* *461*, 59-62.

Gieseler, K., Grisoni, K., and Ségalat, L. (2000). Genetic suppression of phenotypes arising from mutations in dystrophin-related genes in *Caenorhabditis elegans*. *Curr. Biol.* *10*, 1092-1097.

Giugia, J., Gieseler, K., Arpagaus, M., and Ségalat, L. (1999). Mutations in the dystrophin-like *dys-1* gene of *Caenorhabditis elegans* result in reduced acetylcholinesterase activity. FEBS Lett. 463, 270–272.

Gomes, M.D., Lecker, S.H., Jagoe, R.T., Navon, A., and Goldberg, A.L. (2001). Atrogin-1, a muscle-specific F-box protein highly expressed during muscle atrophy. Proc. Natl. Acad. Sci. U. S. A. 98, 14440–14445.

Grater, F., Shen, J., Jiang, H., Gautel, M., and Grubmuller, H. (2005). Mechanically induced titin kinase activation studied by force-probe molecular dynamics simulations. Biophys. J. 88, 790–804.

Greene, D.N., Garcia, T., Sutton, R.B., Gernert, K.M., Benian, G.M., and Oberhauser, A.F. (2008). Single-molecule force spectroscopy reveals a stepwise unfolding of *Caenorhabditis elegans* giant protein kinase domains. Biophys. J. 95, 1360–1370.

Grisoni, K., Martin, E., Gieseler, K., Mariol, M.-C., and Ségalat, L. (2002). Genetic evidence for a dystrophin-glycoprotein complex (DGC) in *Caenorhabditis elegans*. Gene 294, 77–86.

Grisoni, K., Gieseler, K., Mariol, M.C., Martin, E., Carre-Pierrat, M., Moulder, G., Barstead, R., and Ségalat, L. (2003). The *stn-1* syntrophin gene of *C. elegans* is functionally related to dystrophin and dystrobrevin. J. Mol. Biol. 332, 1037–1046.

Han, H.F., and Beckerle, M.C. (2009). The ALP-Enigma protein ALP-1 functions in actin filament organization to promote muscle structural integrity in *Caenorhabditis elegans*. Mol. Biol. Cell 20, 2361–2370.

Harfe, B.D., Branda, C.S., Krause, M., Stern, M.J., and Fire, A. (1998). MyoD and the specification of muscle and non-muscle fates during postembryonic development of the *C. elegans* mesoderm. Development 125, 2479–2488.

Harfe B.D., Vaz Gomes A., Kenyon C., Liu J., Krause M., and Fire A. (1998). Analysis of a *Caenorhabditis elegans* Twist homolog identifies conserved and divergent aspects of mesodermal patterning. Genes Dev. 12, 2623–2635.

Herndon, L. A., Schmeissner, P. J., Dudaronek, J. M., Brown, P. A., Listner, K. M., Sakano, Y., Paupard, M.C., Hall, D.H., and Driscoll, M. (2002). Stochastic and genetic factors influence tissue-specific decline in ageing *C. elegans*. Nature 419, 808–814.

Hikita, T., Qadota, H., Tsuboi, D., Taya, S., Moerman, D.G., and Kaibuchi, K. (2005). Identification of a novel Cdc42 GEF that is localized to the PAT-3-mediated adhesive structure. Biochem. Biophys. Res. Commun. 335, 139–145.

Hobert, O., Moerman, D.G., Clark, K.A., Beckerle, M.C., and Ruvkun, G. (1999). A conserved LIM protein that affects muscular adherens junction integrity and mechanosensory function in *Caenorhabditis elegans*. J. Cell Biol. 144, 45–57.

Hoffman, E.P., Brown, R.H., Jr, and Kunkel, L.M. (1987). Dystrophin: the protein product of the Duchenne muscular dystrophy locus. Cell 51, 919–928.

Hoppe, P.E., Chau, J., Flanagan, K.A., Reedy, A.R., and Schriefer, L.A. (2010). *Caenorhabditis elegans unc-82* encodes a serine-threonine kinase important for myosin filament organization in muscle during growth. Genetics 184, 79–90.

Hresko, M.C., Williams, B.D., and Waterston, R.H. (1994). Assembly of body wall muscle and muscle cell attachment structures in *Caenorhabditis elegans*. J. Cell Biol. 124, 491–506.

Hu S.H., Parker, M.W., Lei, J.Y., Wilce, M.C., Benian, G.M., and Kemp, B.E. (1994). Insights into autoregulation from the crystal structure of twitchin kinase. Nature 369, 581–584.

Hu, L.Y., and Kontogianni-Konstantopoulos, A. (2013). The kinase domains of obscurin interact with intercellular adhesion proteins. FASEB J. 27, 2001–2012.

Hunter C.P. and Kenyon C. (1996). Spatial and temporal controls target *pal-1* blastomere-specification activity to a single blastomere lineage in *C. elegans* embryos. *Cell.* *87*, 217-226.

Husson, S.J. et al. Keeping track of worm trackers (September 10, 2012), *WormBook*, ed. The *C. elegans* Research Community, WormBook, doi/10.1895/wormbook.1.156.1, <http://www.wormbook.org>.

Hwang, H., Barnes, D.E., Matsunaga, Y., Benian, G.M., Ono, S., and Lu, H. (2016). Muscle contraction phenotypic analysis enabled by optogenetics reveals functional relationships of sarcomere components in *Caenorhabditis elegans*. *Sci. Rep.* *6*, 19900. doi: 10.1038/srep19900.

Johari, S., Nock, V., Alkaisi, M.M., and Wang, W. (2013). On-chip analysis of *C. elegans* muscular forces and locomotion patterns in microstructured environments. *Lab Chip* *13*, 1699-1707.

Johnson, R.P., Kang, S.H., and Kramer, J.M. (2006). *C. elegans* dystroglycan DGN-1 functions in epithelia and neurons, but not muscle, and independently of dystrophin. *Development* *133*, 1911-1921.

Kachur, T., Ao, W., Berger, J., and Pilgrim, D. (2004). Maternal UNC-45 is involved in cytokinesis and colocalizes with non-muscle myosin in the early *Caenorhabditis elegans* embryo. *J. Cell Sci.* *117*, 5313-5321.

Kachur, T.M., Audhya, A., and Pilgrim, D.B. (2008). UNC-45 is required for NMY-2 contractile function in early embryonic polarity establishment and germline cellularization in *C. elegans*. *Dev. Biol.* *314*, 287-299.

Kagawa, H., Gengyo, K., McLachlan, A.D., Brenner, S., and Karn, J. (1989). Paramyosin gene (*unc-15*) of *Caenorhabditis elegans*. Molecular cloning, nucleotide sequence and models for thick filament structure. *J. Mol. Biol.* *207*, 311-333.

Kaiser, C.M., Bujalowski, P.J., Ma, L., Anderson, J., Epstein, H.F., and Oberhauser, A.F. (2012). Tracking UNC-45 chaperone-myosin interaction with a titin mechanical reporter. *Biophys. J.* *102*, 2212- 2219.

Karn, J., Brenner, S., and Barnett, L. (1983). Protein structural domains in the *Caenorhabditis elegans unc-54* myosin heavy chain gene are not separated by introns. *Proc. Natl. Acad. Sci. U. S. A.* *80*, 4253-4257.

Kim, H., Rogers, M.J., Richmond, J.E., and McIntire, S.L. (2004). SNF-6 is an acetylcholine transporter interacting with the dystrophin complex in *Caenorhabditis elegans*. *Nature* *430*, 891-896.

Kim, H., Pierce-Shimomura, J.T., Oh, H.J., Johnson, B.E., Goodman, M.B., and McIntire, S.L. (2009). The dystrophin complex controls BK channel localization and muscle activity in *Caenorhabditis elegans*. *PLoS Genet.* *5*, e1000780. doi: 10.1371/journal.pgen.1000780.

Knappeis, G.G., and Carlsen, F. (1968). The ultrastructure of the M line in skeletal muscle. *J. Cell Biol.* *38*, 202-211.

Kobe, B., Heierhorst, J., Feil, S.C., Parker, M.W., Benian, G.M., Weiss, K.R., and Kemp, B.E. (1996). Giant protein kinases: domain interactions and structural basis of autoregulation. *EMBO J.* *15*, 6810-6821.

Koenig, M., Hoffman, E.P., Bertelson, C.J., Monaco, A.P., Feener, C., and Kunkel, L.M. (1987). Complete cloning of the Duchenne muscular dystrophy (DMD) cDNA and preliminary genomic organization of the DMD gene in normal and affected individuals. *Cell* *50*, 509-517.

Kontogianni-Konstantopoulos, A., Jones, E.M., Van Rossum, D.B., and Bloch, R.J. (2003). Obscurin is a ligand for small ankyrin 1 in skeletal muscle. *Mol. Biol. Cell* *14*, 1138-1148.

Koren, Y., Sznitman, R., Arratia, P.E., Caris, C., Krajacic, P., Brown, A.E.X., and Sznitman, J. (2015). Model-independent phenotyping of *C. elegans* locomotion using scale-invariant feature transform. *PLoS One* *10*, e0122326. doi: 10.1371/journal.pone.0122326.

Krajacic, P., Shen, X., Purohit, P.K., Arratia, P., and Lamitina, T. (2012). Biomechanical profiling of *Caenorhabditis elegans* motility. *Genetics* *191*, 1015-1021.

Krause M., Fire A., Harrison S.W., Priess J, and Weintraub H. (1990). CeMyoD accumulation defines the body wall muscle cell fate during *C. elegans* embryogenesis. *Cell* 63, 907-919.

Krause M., Harrison S.W., Xu S.Q., Chen L., and Fire A. (1994). Elements regulating cell- and stage-specific expression of the *C. elegans* MyoD family homolog *hlh-1*. *Dev. Biol.* 166, 133-148.

Krause, M. (1995). MyoD and myogenesis in *C. elegans*. *Bioessays* 17, 219-228.

Kuo, W.-J., Sie, Y.-S., and Chuang, H.-S. (2014). Characterizations of kinetic power and propulsion of the nematode *Caenorhabditis elegans* based on a micro-particle image velocimetry system. *Biomicrofluidics* 8, 024116. doi: 10.1063/1.4872061.

Landsverk, M.L., Li, S., Hutagalung, A.H., Najafov, A., Hoppe, T., Barral, J.M., and Epstein, H.F. (2007). The UNC-45 chaperone mediates sarcomere assembly through myosin degradation in *Caenorhabditis elegans*. *J. Cell Biol.* 177, 205-210.

Lange, S., Xiang, F., Yakovenko, A., Vihola, A., Hackman, P., Rostkova, E., Kristensen, J., Brandmeier, B., Franzen, G., Hedberg, B, et al. (2005). The kinase domain of titin controls muscle gene expression and protein turnover. *Science* 308, 1599-1603.

Lange, S., Ouyang, K., Meyer, G., Cui, L., Cheng, H., Lieber, R.L., and Chen, J. (2009). Obscurin determines the architecture of the longitudinal sarcoplasmic reticulum. *J. Cell Sci.* 122, 2640-2650.

Lange, S., Perera, S., Teh, P., and Chen, J. (2012). Obscurin and KCTD6 regulate cullin-dependent small ankyrin-1 (sAnk1.5) protein turnover. *Mol. Biol. Cell* 23, 2490-2504.

Lebart, M.C., and Benyamin, Y. (2006). Calpain involvement in the remodeling of cytoskeletal anchorage complexes. *FEBS J.* 273, 3415-3426.

Lecroisey, C. (2010). Caractérisation moléculaire et cellulaire de la dégénérescence musculaire dépendante de la dystrophine chez le nématode *Caenorhabditis elegans*. Thesis manuscript, University Lyon 1.

Lecroisey, C., Martin, E., Mariol, M.-C., Granger, L., Schwab, Y., Labouesse, M., Ségalat, L., and Gieseler, K. (2008). DYC-1, a protein functionally linked to dystrophin in *Caenorhabditis elegans* is associated with the dense body, where it interacts with the muscle LIM domain protein ZYX-1. *Mol. Biol. Cell* 19, 785-796.

Lecroisey, C., Brouilly, N., Qadota, H., Mariol, M.-C., Rochette, N.C., Martin, E., Benian, G.M., Ségalat, L., Mounier, N., and Gieseler, K. (2013). ZYX-1, the unique zyxin protein of *Caenorhabditis elegans*, is involved in dystrophin-dependent muscle degeneration. *Mol. Biol. Cell* 24, 1232-1249.

Lee, C.F., Hauenstein, A.V., Fleming, J.K., Gasper, W.C., Engelke, V., Sankaran, B., Bernstein, S.I., and Huxford, T. (2011). X-ray crystal structure of the UCS domain-containing UNC-45 myosin chaperone from *Drosophila melanogaster*. *Structure* 19, 397-408.

Lei, J., Tang, X., Chambers, T.C., Pohl, J., and Benian, G.M. (1994). Protein kinase domain of twitchin has protein kinase activity and an autoinhibitory region. *J. Biol. Chem.* 269, 21078-21085.

Lei H., Fukushige T., Niu W., Sarov M., Reinke V., and Krause M. (2010). A widespread distribution of genomic CeMyoD binding sites revealed and cross validated by ChIP-Chip and ChIP-Seq techniques. *PLoS One* 5, e15898. doi: 10.1371/journal.pone.0015898.

Lei H., Liu J., Fukushige T., Fire A., and Krause M. (2009). Caudal-like PAL-1 directly activates the bodywall muscle module regulator *hlh-1* in *C. elegans* to initiate the embryonic muscle gene regulatory network. *Development* 136, 1241-1249.

Lin, X., Qadota, H., Moerman, D.G. and Williams, B.D. (2003). *C. elegans* PAT-6/Actopaxin plays a critical role in the assembly of integrin adhesion complexes in vivo. *Curr. Biol.* 13, 922-932.

Liu F, Bauer CC, Ortiz I, Cook RG, Schmid MF, and Epstein HF (1998). β -filagenin, a newly identified protein coassembling with myosin and paramyosin in *Caenorhabditis elegans*. *J. Cell Biol.* 140, 347-353.

Liu, F., Ortiz, I., Hutagalung, A., Bauer, C.C., Cook, R.G., and Epstein, H.F. (2000). Differential assembly of α - and γ -filagrinins into thick filaments in *Caenorhabditis elegans*. *J. Cell Sci.* *113*, 4001-4012.

Liu J, Schrank B, and Waterston RH (1996). Interaction between a putative mechanosensory membrane channel and a collagen. *Science* *273*, 361-364.

Liu, Q., Jones, T.I., Bachmann, R.A., Meghpara, M., Rogowshi, L., Williams, B.D., and Jones, P.L. (2012). *C. elegans* PAT-9 is a nuclear zinc finger protein critical for the assembly of muscle attachments. *Cell Biosci.* *2*, 18. doi: 10.1186/2045-3701-2-18.

Liu, Q., Jones, T.I., Tang, V.W., Brieher, W.M., and Jones, P.L. (2010). Facioscapulohumeral muscular dystrophy region gene-1 (FRG-1) is an actin-bundling protein associated with muscle-attachment sites. *J. Cell Sci.* *123*, 1116-1123.

Luther, P., and Squire, J. (1978). Three-dimensional structure of the vertebrate muscle M-region. *J. Mol. Biol.* *125*, 313-324.

Mackenzie, J.M., and Epstein, H.F. (1980). Paramyosin is necessary for determination of nematode thick filament length *in vivo*. *Cell* *22*, 747-755.

Mackinnon, A.C., Qadota, H., Norman, K.R., Moerman, D.G., and Williams, B.D. (2002). *C. elegans* PAT-4 / ILK functions as an adaptor protein within integrin adhesion complexes. *Curr. Biol.* *12*, 787-797.

Mariol, MC., Martin, E., Chambonnier L. and Ségalat L. (2007). Dystrophin-dependent muscle degeneration requires a fully functional contractile machinery to occur in *C. elegans*. *Neuromuscul. Disord.* *17*, 56-60.

Mariol, MC., and Ségalat, L. (2001). Muscular degeneration in the absence of dystrophin is a calcium-dependent process. *Curr Biol.* *11*, 1691-1694.

Maruyama, I.N., Miller, D.M., and Brenner S. (1989). Myosin heavy chain gene amplification as a suppressor mutation in *Caenorhabditis elegans*. *Mol. Gen. Genet.* *219*, 113-118.

Mathies, L.D., Henderson, S.T., and Kimble, J. (2003). The *C. elegans* Hand gene controls embryogenesis and early gonadogenesis. *Development* *130*, 2881-2892.

Matsunaga, Y., Qadota, H., Furukawa, M., Choe, H.H., and Benian, G.M. (2015). Twitchin kinase interacts with MAPKAP kinase 2 in *Caenorhabditis elegans* striated muscle. *Mol. Biol. Cell* *26*, 2096-2111.

Mayans, O., van der Ven, P.F., Wilm, M., Mues, A., Young, P., Furst, D.O., Wilmanns, M., and Gautel M. (1998). Structural basis for activation of the titin kinase domain during myofibrillogenesis. *Nature* *395*, 863-869.

McDonald, K.A., Lakonishok, M., and Horwitz, A.F. (1995). α_v and α_3 integrin subunits are associated with myofibrils during myofibrillogenesis. *J. Cell Sci.* *108*, 2573-2581.

McKeown, C.R., Han, H.F., and Beckerle, M.C. (2006). Molecular characterization of the *Caenorhabditis elegans* ALP/Enigma gene *alp-1*. *Dev. Dyn.* *235*, 530-538.

McKim, K.S., Matheson, C., Marra, M.A., Wakarchuk, M.F., and Baillie, D.L. (1994). The *Caenorhabditis elegans unc-60* gene encodes proteins homologous to a family of actin-binding proteins. *Mol. Gen. Genet.* *242*, 346-357.

McLachlan, A.D., and Karn, J. (1982). Periodic charge distributions in the myosin rod amino acid sequence match cross-bridge spacings in muscle. *Nature* *299*, 226-231.

Megeney L., Kablar B., Garrett K., Anderson J., Rudnicki M. (1996)..MyoD is required for myogenic stem cell function in adult skeletal muscle. *Genes Dev.* *10*, 1173-1183.

Meissner, B., Warner, A., Wong, K., Dube, N., Lorch, A., McKay, S.J., Khattra, J., Rogalski, T., Somasiri, A., Chaudhry, I., et al. (2009). An integrated strategy to study muscle development and myofilament structure in *C. elegans*. PLoS Genet. 5, e1000537.

Meissner, B., Rogalski, T., Viveiros, R., Warner, A., Plastino, L., Lorch, A., Granger, L., Ségalat, L., and Moerman, D.G. (2011). Determining the sub-cellular localization of proteins within *Caenorhabditis elegans* body wall muscle. PLoS One 6, e19937.

Mercer, K.B., Flaherty, D.B., Miller, R.K., Qadota, H., Tinley, T.L., Moerman, D.G., and Benian, G.M. (2003). *C. elegans* UNC-98, a C2H2 Zn finger protein, is a novel partner of UNC-97/PINCH in muscle adhesion complexes. Mol. Biol. Cell 14, 2492-2507.

Mercer, K.B., Miller, R.K., Tinley, T.L., Sheth, S., Qadota, H., and Benian, G.M. (2006). *Caenorhabditis elegans* UNC-96 is a new component of M-lines that interacts with UNC-98 and paramyosin and is required in adult muscle for assembly and/or maintenance of thick filaments. Mol. Biol. Cell 17, 3832-3847.

Miller, D.M. 3rd, Ortiz, I., Berliner, G.C., and Epstein, H.F. (1983). Differential localization of two myosins within nematode thick filaments. Cell 34, 477-490.

Miller, D.M. 3rd, Stockdale, F.E., and Karn, J. (1986). Immunological identification of the genes encoding the four myosin heavy chain isoforms of *Caenorhabditis elegans*. Proc. Natl. Acad. Sci. U. S. A. 83, 2305-2309.

Miller, R.K., Qadota, H., Landsverk, M.L., Mercer, K.B., Epstein, H.F., and Benian, G.M. (2006). UNC-98 links an integrin-associated complex to thick filaments in *Caenorhabditis elegans* muscle. J. Cell Biol. 175, 853-859.

Miller, R.K., Qadota, H., Mercer, K.B., Gernert, K.M., and Benian, G.M. (2008). UNC-98 and UNC-96 interact with paramyosin to promote its incorporation into thick filaments of *Caenorhabditis elegans*. Mol. Biol. Cell 19, 1529-1539.

Miller, R.K., Qadota, H., Stark, T.J., Mercer, K.B., Wortham, T.S., Anyanful, A., and Benian, G.M. (2009). CSN-5, a component of the COP9 signalosome complex, regulates the levels of UNC-96 and UNC-98, two components of M-lines in *Caenorhabditis elegans* muscle. Mol. Biol. Cell 20, 3608-3616.

Mi-Mi, L., Votra, S.B., Kemphues, K., Bretscher, A., and Pruyne, D. (2012). Z-line formins promote contractile lattice growth and maintenance in striated muscles of *C. elegans*. J. Cell Biol. 198, 87-102.

Moerman, D. G., Plurad, S., Waterston, R. H., and Baillie, D. L. (1982). Mutations in the *unc-54* myosin heavy chain gene of *Caenorhabditis elegans* that alter contractility but not muscle structure. Cell 29, 773-781.

Moerman, D.G., Benian, G.M., and Waterston, R.H. (1986). Molecular cloning of the muscle gene unc-22 in *Caenorhabditis elegans* by Tc1 transposon tagging. Proc. Natl. Acad. Sci. U. S. A. 83, 2579-2583.

Moerman, D.G., Benian, G.M., Barstead, R.J., Schriefer, L.A., and Waterston, R.H. (1988). Identification and intracellular localization of the *unc-22* gene product of *Caenorhabditis elegans*. Genes Dev. 2, 93-105.

Moerman, D.G., and Fire, A. (1997). Muscle Structure, Function and Development. In *C. elegans* II, D. L. Riddle, T. Blumenthal, B. J. Meyer, and J. R. Priess, eds. (Plainview, NY: Cold Spring Harbor Laboratory Press), pp. 417-470.

Moerman, D. G. and Williams, B. D. Sarcomere assembly in *C. elegans* muscle (January 16, 2006), WormBook, ed. The *C. elegans* Research Community, WormBook, doi/10.1895/wormbook.1.81.1, <http://www.wormbook.org>.

Mokhtarian, A., Lefaucheur, J.P., Even, P.C., and Sebille, A. (1999). Hindlimb immobilization applied to 21-day-old mdx mice prevents the occurrence of muscle degeneration. J. Appl. Physiol. 86, 924-931.

Morley, J.F., Brignull, H.R., Weyers, J.J., and Morimoto, R.I. (2002). The threshold for polyglutamine-expansion protein aggregation and cellular toxicity is dynamic and influenced by aging in *Caenorhabditis elegans*. Proc. Natl. Acad. Sci. U. S. A. 99, 10417-10422.

Moulder, G.L., Huang, M.M., Waterston, R.H., and Barstead, R.J. (1996). Talin requires β -integrin, but not vinculin, for its assembly into focal adhesion-like structures in the nematode *C. elegans*. Mol. Biol. Cell 7, 1181-1193.

Moulder, G.L., Cremona, G.H., Duerr, J., Stirman, J.N., Fields, S.D., Martin, W., Qadota, H., Benian, G.M., Lu, H., and Barstead, R.J. (2010). α -actinin is required for proper assembly of Z-disk/focal adhesion-like structures and for efficient locomotion in *C. elegans*. J. Mol. Biol. 403, 516-528.

Mullen, G.P., Rogalski, T.M., Bush, J.A., Gorji, P.R., and Moerman, D.G. (1999). Complex patterns of alternative splicing mediate the spatial and temporal distribution of perlecan/UNC-52 in *Caenorhabditis elegans*. Mol. Biol. Cell 10, 3205-3221.

Muller, S.A., Haner, M., Ortiz, I., Aebi, U., and Epstein, H.F. (2001). STEM analysis of *Caenorhabditis elegans* muscle thick filaments: evidence for microdifferentiated substructures. J. Mol. Biol. 305, 1035-1044.

Nahabedian, J.F., Qadota, H., Stirman, J.N., Lu, H., and Benian, G.M. (2012). Bending amplitude—a new quantitative assay of *C. elegans* locomotion: identification of phenotypes for mutants in genes encoding muscle focal adhesion components. Methods 56, 95-102.

Ni, W., Hutagalung, A.H., Li, S., and Epstein, H.F. (2011). The myosin-binding UCS domain but not the Hsp90-binding TPR domain of the UNC-45 chaperone is essential for function in *Caenorhabditis elegans*. J. Cell Sci. 124, 3164-3173.

Nicholls, P., Bujalowski, P.J., Epstein, H.F., Boehning, D.F., Barral, J.M., and Oberhauser, A.F. (2014). Chaperone-mediated reversible inhibition of the sarcomeric myosin power stroke. FEBS Lett. 588, 3977-3981.

Norman, K.R., Fazzio, R.T., Mellem, J.E., Espelt, M.V., Strange, K., Beckerle, M.C., and Maricq, A.V. (2005). The Rho/Rac-family guanine nucleotide exchange factor VAV-1 regulates rhythmic behaviors in *C. elegans*. Cell 123, 119-132.

Norman, K.R., Cordes, S., Qadota, H., Rahmani, P., and Moerman, D.G. (2007). UNC-97/PINCH is involved in the assembly of integrin cell adhesion complexes in *Caenorhabditis elegans* body wall muscle. Dev. Biol. 309, 45-55.

Oh, K.H., and Kim, H. (2013). Reduced IGF signaling prevents muscle cell death in a *Caenorhabditis elegans* model of muscular dystrophy. Proc. Natl. Acad. Sci. U. S. A. 110, 19024-19029.

Ono S., Baillie D.L., and Benian, G.M. (1999). UNC-60B, an ADF/cofilin family protein, is required for proper assembly of actin into myofibrils in *Caenorhabditis elegans* body wall muscle. J. Cell Biol. 145, 591-502.

Ono, K., Yu, R., Mohri, K., and Ono, S. (2006). *Caenorhabditis elegans* kettin, a large immunoglobulin-like repeat protein, binds to filamentous actin and provides mechanical stability to the contractile apparatuses in body wall muscle. Mol. Biol. Cell 17, 2722-2734.

Ono, S. (2014). Regulation of structure and function of sarcomeric actin filaments in striated muscle of the nematode *Caenorhabditis elegans*. Anat. Rec. 297, 1548-1559.

Papsdorf, K., Sacherl, J., and Richter, K. (2014). The balanced regulation of Hsc70 by DNJ-13 and UNC-23 is required for muscle functionality. J. Biol. Chem. 289, 25250-25261.

Park, E.C., and Horvitz, H.R. (1986). *C. elegans unc-105* mutations affect muscle and are suppressed by other mutations that affect muscle. Genetics 113, 853-867.

Perry, S.V. (1999). Troponin I: inhibitor or facilitator. Mol. Cell. Biochem. 190, 9-32.

Pilgram, G.S., Potikanond, S., Baines, R.A., Fradkin, L.G., and Noordermeer, J.N. (2010). The roles of the dystrophin-associated glycoprotein complex at the synapse. Mol. Neurobiol. 41, 1-21.

Pintard, L., Willis, J.H., Willems, A., Johnson, J.-L. F., Srayko, M., Kurz, T., Glaser, S., Mains, P.E., Tyers, M., Bowerman, B., and Peter, M. (2003). The BTB protein MEL-26 is a substrate-specific adaptor of the CUL-3 ubiquitin ligase. *Nature* *425*, 311-316.

Plenefisch, J.D., Zhu, X., and Hedgecock, E.M. (2000). Fragile skeletal muscle attachments in dystrophic mutants of *Caenorhabditis elegans*: isolation and characterization of the *mua* genes. *Development* *127*, 1197-1207.

Polet, D., Lambrechts, A., Ono, K., Mah, A., Peelman, F., Vandekerckhove, J., Baillie, D.L., Ampe, C., and Ono, S. (2006). *Caenorhabditis elegans* expresses three functional profilins in a tissue-specific manner. *Cell Motil. Cytoskeleton* *63*, 14-28.

Price, M.G., Landsverk, M.L., Barral, J.M., and Epstein, H.F. (2002). Two mammalian UNC-45 isoforms are related to distinct cytoskeletal and muscle-specific function. *J. Cell Sci.* *115*, 4013-4023.

Probst, W.C., Cropper, E.C., Heierhorst, J., Hooper, S.L., Jaffe, H., Vilim, F., Beushausen, S., Kupfermann, I., and Weiss, K.R. (1994). cAMP-dependent phosphorylation of Aplysia twitchin may mediate modulation of muscle contractions by neuropeptide cotransmitters. *Proc. Natl. Acad. Sci. U. S. A.* *91*, 8487-8491.

Puchner, E.M., Alexandrovich, A., Kho, A.L., Hensen, U., Schäfer, L.V., Brandmeier, B., Gräter, F., Grubmüller, H., Gaub, H.E., and Gautel, M. (2008). Mechanoenzymatics of titin kinase. *Proc. Natl. Acad. Sci. U. S. A.* *105*, 13385-13390.

Qadota, H., Mercer, K.B., Miller, R.K., Kaibuchi, K., and Benian, G.M. (2007). Two LIM domain proteins and UNC-96 link UNC-97/pinch to myosin thick filaments in *Caenorhabditis elegans* muscle. *Mol. Biol. Cell* *18*, 4317-4326.

Qadota, H., McGaha, L.A., Mercer, K.B., Stark, T.J., Ferrara, T.M. and Benian, G.M. (2008a). A novel protein phosphatase is a binding partner for the protein kinase domains of UNC-89 (Obscurin) in *Caenorhabditis elegans*. *Mol. Biol. Cell* *19*, 2424-2432.

Qadota, H., Blangy, A., Xiong, G. and Benian, G.M. (2008b). The DH-PH region of the giant protein UNC-89 activates RHO-1 GTPase in *Caenorhabditis elegans* body wall muscle. *J. Mol. Biol.* *383*, 747-752.

Qadota, H., and Benian, G.M. (2010). Molecular structure of sarcomere-to-membrane attachment at M-lines in *C. elegans* muscle. *J. Biomed. Biotechnol.* *2010*, 864749.

Qadota, H., Miyauchi, T., Nahabedian, J.F., Stirman, J.N., Lu, H., Amano, M., Benian, G.M., and Kaibuchi, K. (2011). PKN-1, a homologue of mammalian PKN, is involved in the regulation of muscle contraction and force transmission in *C. elegans*. *J. Mol. Biol.* *407*, 222-231.

Qadota, H., Moerman, D.G., and Benian, G.M. (2012). A molecular mechanism for the requirement of PAT-4 (integrin-linked kinase (ILK)) for the localization of UNC-112 (kindlin) to integrin adhesion sites. *J. Biol. Chem.* *287*, 28537-28551.

Qadota, H., Luo, Y., Matsunaga, Y., Park, A.S., Gernert, K.M., and Benian, G.M. (2014). Suppressor mutations suggest a surface on PAT-4 (integrin linked kinase) that interacts with UNC-112 (kindlin). *J. Biol. Chem.* *289*, 14252-14262.

Qadota, H., and Benian, G.M. (2014). An approach for exploring interaction between two proteins in vivo. *Fron. Physiol.* *5*, 162.

Qadota, H., Mayans, O., Matsunaga, Y., McMurry, J.L., Wilson, K.J., Kwon, G.E., Stanford, R., Deehan, K., Tinley, T.L., Ngwa, M.M., and Benian, G.M. (2016). The SH3 domain of UNC-89 (obscurin) interacts with paramyosin, a coiled-coil protein, in *C. elegans* muscle. *Mol. Biol. Cell* *27*, 1606-1620.

Rabets, Y., Backholm, M., Dalnoki-Veress, K., and Ryu, W.S. (2014). Direct measurements of drag forces in *C. elegans* crawling locomotion. *Biophys. J.* *107*, 1980-1987.

Rahmani, P., Rogalski, T., and Moerman, D.G. (2015). The *C. elegans* UNC-23 protein, a member of the BCL-2-associated athanogene (BAG) family of chaperone regulators, interacts with SHP-1 to regulate cell attachment and maintain hydermal integrity. *Worm* 4, e1023496.

Raizen, D.M., Zimmerman, J.E., Maycock, M.H., Ta, U.D., You, Y., Sundaram, M.V., and Pack, A.I. (2008). Lethargus is a *Caenorhabditis elegans* sleep-like state. *Nature* 451, 569–572.

Regmi, SG., Rolland, SG. and Conradt, B. (2014). Age-dependent changes in mitochondrial morphology and volume are not predictors of lifespan. *Aging* 6, 118-130.

Resnicow, D.I., Deacon, J.C., Warrick, H.M., Spudich, J.A., and Leinwand, L.A. (2010). Functional diversity among a family of human skeletal muscle myosin motors. *Proc. Natl. Acad. Sci. U. S. A.* 107, 1053-1058.

Restif, C., Ibáñez-Ventoso, C., Vora, M.M., Guo, S., Metaxas, D., and Driscoll, M. (2014). CeleST: Computer vision software for quantitative analysis of *C. elegans* swim behavior reveals novel features of locomotion. *PLoS Comput. Biol.* 10, e1003702

Riddle, D.L., and Brenner, S. (1978). Indirect suppression in *C. elegans*. *Genetics* 89, 299-314.

Rogalski, T.M., Williams, B.D., Mullen, G.P., and Moerman, D.G. (1993). Products of the *unc-52* gene in *Caenorhabditis elegans* are homologous to the core protein of the mammalian basement membrane heparan sulfate proteoglycan. *Genes Dev.* 7, 1471-1484.

Rogalski, T.M., Mullen, G.P., Gilbert, M.M., Williams, B.D., and Moerman, D.G. (2000). The UNC-112 gene in *C. elegans* encodes a novel component of cell-matrix adhesion structures required for integrin localization in the muscle cell membrane. *J. Cell Biol.* 150, 253-264.

Rogalski, T.M., Gilchrist, E.J., Mullen, G.P., and Moerman, D.G. (1995). Mutations in the *unc-52* gene responsible for body wall muscle defects in adult *Caenorhabditis elegans* are located in alternatively spliced exons. *Genetics* 139, 159-169.

Rogalski, T.M., Gilbert, M.M., Devenport, D., Norman, K.R., and Moerman, D.G. (2003). DIM-1, a novel immunoglobulin superfamily protein in *Caenorhabditis elegans*, is necessary for maintaining bodywall muscle integrity. *Genetics* 163, 905-915.

Rybakova, I.N., Patel, J.R., and Ervasti, J.M. (2000). The dystrophin complex forms a mechanically strong link between the sarcolemma and costameric actin. *J. Cell Biol.* 150, 1209–1214.

Saksela, K., and Permi, P. (2012). SH3 domain ligand binding: What's the consensus and where's the specificity? *FEBS Lett.* 586, 2609-2614.

Samarel, A.M. (2005). Costameres, focal adhesions, and cardiomyocyte mechanotransduction. *Am. J. Physiol. Heart Circ. Physiol.* 289, H2291-H2301.

Schachat, F., Garcea, R.L., and Epstein, H.F. (1978). Myosins exist as homodimers of heavy chains: demonstration with specific antibody purified by nematode mutant myosin affinity chromatography. *Cell* 15, 405-411.

Schrieber, L.A., and Waterston, R.H. (1989). Phosphorylation of the N-terminal region of *Caenorhabditis elegans* paramyosin. *J. Mol. Biol.* 207, 451-454.

Schwechheimer, C. (2004). The COP9 signalosome (CSN): an evolutionary conserved proteolysis regulator in eukaryotic development. *Biochem. Biophys. Acta* 1695, 45-54.

Ségalat, L., and Anderson, J.E. (2005). Duchenne muscular dystrophy: Stalled at the junction? *Eur. J. Hum. Genet.* 13, 4–5.

Shen, X.N., Sznitman, J., Krajacic, P., Lamitina, T., and Arratia, P.E. (2012). Undulatory locomotion of *Caenorhabditis elegans* on wet surfaces. *Biophys. J.* 102, 2772-2781.

Siegman, M.J., Funabara, D., Kinoshita, S., Watabe, S., Hartshorne, D.J., and Butler, T.M. (1998). Phosphorylation of a twitchin-related protein controls catch and calcium sensitivity of force production in invertebrate smooth muscle. Proc. Natl. Acad. Sci. U. S. A. *95*, 5383-5388.

Small, T.M., Gernert, K.M., Flaherty, D.B., Mercer, K.B., Borodovsky, M., and Benian, G.M. (2004). Three new isoforms of *C. elegans* UNC-89 containing MLCK-like protein kinase domains. J. Mol. Biol. *342*, 91-108.

Spooner, P.M., Bonner, J., Maricq, A.V., Benian, G.M., and Norman, K.R. (2012). Large isoforms of UNC-89 (obscurin) are required for muscle cell architecture and optimal calcium release in *Caenorhabditis elegans*. PLoS One *7*, e40182.

Swierczek, N.A., Giles, A.C., Rankin, C.H., and Kerr, R.A. (2011). High-throughput behavioral analysis in *C. elegans*. Nat. Methods *8*, 592-598.

Takeda, K., Watanabe, C., Qadota, H., Hanazawa, M., and Sugimoto, A. (2008). Efficient production of monoclonal antibodies recognizing specific structures in *Caenorhabditis elegans* embryos using an antigen subtraction method. Genes Cells *13*, 653-665.

Taylor, R.C. and Dillin, A. (2011). Aging as an event of proteostasis collapse. Cold Spring Harb. Perspect. Biol. *3*, a004440

Thompson, O., Edgley, M., Strasbourger, P., Flibotte, S., Ewing, B., Adair, R., Au, V., Chaudhry, I., Fernando, L., Hutter, H., et al. (2013). The million mutation project: a new approach to genetics in *Caenorhabditis elegans*. Genome Res. *23*, 1749-1762.

Turek, M., and Bringmann, H. (2014). Gene expression changes of *Caenorhabditis elegans* larvae during molting and sleep-like lethargus. PloS One *9*, e113269.

Turner, P.R., Westwood, T., Regen, C.M., and Steinhardt, R.A. (1988). Increased protein degradation results from elevated free calcium levels found in muscle from mdx mice. Nature *335*, 735-738.

van Oosten-Hawle, P. and Morimoto, R.I. (2014) Organismal proteostasis: role of cell-nonautonomous regulation and transcellular chaperone signaling. Genes and Dev. *28*, 1533-1543.

Varkuti, B.H., Yang, Z., Kintses, B., Erdelyi, P., Bardos-Nagy, I., Kovacs, A.L., Hari, P., Kellermayer, M., Vellai, T., and Malnasi-Csizmadia, A. (2012). A novel actin binding site of myosin required for effective muscle contraction. Nat. Struct. Mol. Biol. *19*, 299-307.

Venolia, L., and Waterston, R.H. (1990). The *unc-45* gene of *Caenorhabditis elegans* is an essential muscle-affecting gene with maternal expression. Genetics *126*, 345-353.

Venolia, L., Ao, W., Kim, S., Kim, C., and Pilgrim, D. (1999). *unc-45* gene of *Caenorhabditis elegans* encodes a muscle-specific tetratricopeptide repeat-containing protein. Cell Motil. Cytoskeleton *42*, 163-177.

von Castelmur, E., Strümpfer, J., Franke, B., Bogomolovas, J., Barbieri, S., Qadota, H., Konarev, P.V., Svergun, D.I., Labeit, S., Benian, G.M., et al. (2012). Identification of an N-terminal inhibitory extension as the primary mechanosensory regulator of twitchin kinase. Proc. Natl. Acad. Sci. U. S. A. *109*, 13608-13613.

Wang, Z.W., Saifee, O., Nonet, M.L. and Salkoff, L. (2001). SLO-1 potassium channels control quantal content of neurotransmitter release at the *C. elegans* neuromuscular junction. Neuron *32*, 867-81.

Warner, A., Qadota, H., Benian, G.M., Vogl, A.W., and Moerman, D.G. (2011). The *C. elegans* paxillin orthologue, PXL-1, is required for pharyngeal muscle contraction and for viability. Mol. Biol. Cell *22*, 2551-2563.

Warner, A., Xiong, G., Qadota, H., Rogalski, T., Vogl, A.W., Moerman, D.G., and Benian, G.M. (2013). CPNA-1, a copine domain protein, is located at integrin adhesion sites and is required for myofilament stability in *C. elegans*. Mol. Biol. Cell *24*, 601-616.

- Waterston, R.H., Fishpool, R.M., and Brenner, S. (1977). Mutants affecting paramyosin in *Caenorhabditis elegans*. *J. Mol. Biol.* *117*, 679-697.
- Waterston, R.H., Thomson, J.N., and Brenner, S. (1980). Mutants with altered muscle structure in *C. elegans*. *Dev. Biol.* *77*, 271-302.
- Waterston, R.H. (1988). Muscle. In The Nematode *Caenorhabditis elegans*, W.B. Wood, ed. (Plainview, NY: Cold Spring Harbor Laboratory Press) pp. 281-335.
- Waterston, R.H. (1989). The minor myosin heavy chain, MHC A, of *Caenorhabditis elegans* is necessary for the initiation of thick filament assembly. *EMBO J.* *8*, 3429-3436.
- Williams, B.D., and Waterston, R.H. (1994). Genes critical for muscle development and function in *Caenorhabditis elegans* identified through lethal mutations. *J. Cell Biol.* *124*, 475-490.
- Wilson, K.J., Qadota, H., Mains, P.E., and Benian, G.M. (2012). UNC-89 (obscurin) binds to MEL-26, a BTB domain protein, and affects the function of MEI-1 (catanin) in striated muscle of *C. elegans*. *Mol. Biol. Cell* *23*, 2623-2634.
- Xu, L., Wei, Y., Reboul, J., Vaglio, P., Shin, T.H., Vidal, M., Elledge, S.J., and Harper, J.W. (2003). BTB proteins are substrate-specific adaptors in an SCF-like modular ubiquitin ligase containing CUL-3. *Nature* *425*, 316-321.
- Xiong, G., Qadota, H., Mercer, K.B., McGaha, L.A., Oberhauser, A.F., and Benian, G.M. (2009). A LIM-9 (FHL)/SCPL-1 (SCP) complex interacts with the C-terminal protein kinase regions of UNC-89 (obscurin) in *C. elegans* muscle. *J. Mol. Biol.* *386*, 976-988.
- Yamashiro, S., Cox, E.A., Baillie, D.L., Hardin, J.D., and Ono, S. (2008). Sarcomeric actin organization is synergistically promoted by tropomodulin, ADF/cofilin, AIP1 and profilin in *C. elegans*. *J. Cell Sci.* *121*, 3867-3877.
- Young, P., Ehler, E., and Gautel, M. (2001). Obscurin, a giant sarcomeric Rho guanine nucleotide exchange factor protein involved in sarcomere assembly. *J. Cell Biol.* *154*, 123-136.
- Yu, X., Ma, J., Lin, F., Zhao, W., Fu, X., and Zhao, Z.J. (2012). Myotubularin family phosphatase ceMTM3 is required for muscle maintenance by preventing excessive autophagy in *Caenorhabditis elegans*. *BMC Cell Biol.* *13*, 28.
- Yuan, L., Fairchild, M.J., Perkins, A.D., and Tanentzapf, G. (2010). Analysis of integrin turnover in fly myotendinous junctions. *J. Cell Sci.* *123*, 939-946.
- Zaidel-Bar, R., and Geiger, B. (2010). The switchable integrin adhesome. *J. Cell Sci.* *123*, 1385-1388.
- Zaidel-Bar, R., Miller, S., Kaminsky, R., and Broday, L. (2010). Molting-specific downregulation of *C. elegans* body-wall muscle attachment sites: the role of RNF-5 E3 ligase. *Biochem. Biophys. Res. Commun.* *395*, 509-514.
- Zengel, J.M., and Epstein, H.F. (1980). Identification of genetic elements associated with muscle structure in the nematode *Caenorhabditis elegans*. *Cell Motil.* *1*, 73-97.
- Zhan, H., Stanciauskas, R., Stigloher, C., Dizon, K.K., Jospin, M., Bessereau, J.-L., and Pinaud, F. (2014). In vivo single-molecule imaging identifies altered dynamics of calcium channels in dystrophin-mutant *C. elegans*. *Nat. Commun.* *5*, 4974.
- Zhou, S., Opperman, K., Wang, X., and Chen, L. (2008). *unc-44* ankyrin and *stn-2* γ -syntrophin regulate *sax-7* L1CAM function in maintaining neuronal positioning in *Caenorhabditis elegans*. *Genetics* *180*, 1429-1443.